Cloning of murine alphaIIbbeta3 integrin and its use in the gene therapy of melanoma cells

Russell, Alan James

Award date:
1996

Awarding institution:
University of Bath

Cloning of Murine αIIbβ3 Integrin and its use in the Gene Therapy of Melanoma Cells

submitted by Alan James Russell

for the degree of PhD.

of the University of Bath

1996

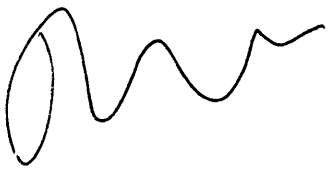

ProQuest LLC
789 East Eisenhower Parkway
P.O. Box 1346
Ann Arbor, MI 48106-1346

Summary

The integrin family of cell surface glycoproteins function as both adhesion and signal transduction molecules mediating cell-cell interactions, adherence to components of the extracellular matrix and providing an essential link between cells and their environment. Expression of specific integrin heterodimers, particularly those of the β3 integrin family (αvβ3 or αIIbβ3) has been closely associated with proliferation, invasion, metastatasis and angiogenesis of many tumour types, particularly malignant melanoma.

Initial studies were aimed at cloning the murine β3 (and to a lesser extent αIIb) integrin subunits from the amelanotic murine melanoma cell line, B16a with the aim of using these in subsequent gene therapy procedures. RT PCR of B16a cDNA was used to obtain two DNA fragments (of 709bp for the αIIb subunit and 657bp for the β3 subunit), identified as belonging to the correct murine integrins. Screening of a λZAP II cDNA libraries with these fragments (labelled with ^{32}P) isolated two library clones, although no homology to integrin subunits was seen. Further studies concentrated upon the gene therapy of the β3 integrin subunit using a human β3 cDNA and an inactive mutant β3 cDNA (obtained from Dr J.C. Loftus, Scripps Research Institute).

Three antisense constructs of the human β3 cDNA (of varying size, from 0.5-3.9kb) were cloned into the expression vector pcDNA3. These vectors were transfected by electroporation into B16a cells and the human melanoma cell line A375. No significant reduction of integrin expression was noted in either cell line

over a period of transient gene expression (24-72 hours). Further studies of G418 antibiotic stable polyclonal populations of B16a cells demonstrated that surface levels of β3 could be reduced as detected by fluorescence assisted cell sorting (FACS). The size of transfected antisense fragments was potentially significant to the degree of this antisense effect, although total amounts of β3 integrin in these cells appear unchanged when examined by Western blotting. Treatment of B16a cells by FACS or by transfection of antisense integrin constructs had dramatic effects upon tumour cell proliferation, with a greater inhibition of growth arising from transfection of larger antisense fragments.

Other studies examined the potential of using transfected mutant human β3 cDNA to competitively inhibit expression of active β3 heterodimers in B16a cells. No inhibition of β3 was visible due to problems associated with efficiency of expression of integrin subunits after transfection, and after selection of stable transfectants with G418.

Dedication

In the memory of Mr Richard W. Farr,
who I know would have
loved to have seen this work,
and to Mr Paul Lawrence who still can.

Acknowledgements

Much thanks must go to Dr. Colin W. Pouton for his continued optimism and input, even in the roughest periods of the last 3 and a lot years. Additional praise must also go to Dr. Steve Moss for his realistic, level headed influence upon this work.

I am particularly grateful for the considerable advice and aid that has been supplied by both Dr. Stuart Watts and Dr David Hayes of Wellcome plc. Other invaluable people in the progression of this work have been Dr. John Marshall of the ICRF for many enlightening and informative chats, Helen Cox of Sheffield University for advice on plaque screening and Dr. Graham Smith for invaluable FACS help. My thanks also go out to Dr. Anthony Smith, Dr. Adrian Lowe and Dr. Iian Lamont for rapidly expanding my knowledge of molecular biology and making it all seem a little bit more possible. Thanks also go to Dr. Melanie Whelham and Ms Heather Bone for helping with the immunoprecipitation.

Many thanks go to the EPSRC and Wellcome plc for funding this project, and to Prof. D. J. Davies for providing the research facilities.

This last bit has to go out to all the special people who have put up with me over the best and worst times. In no particular order I have to give mucho praise to Mum, Dad, Sarah and Scott, Bruvver (wherever he is at the moment), my Nan, Paddy, Luke, Nicky and Lucy, Ay Oop, The Fluffies, The Lush, Rustic, The Captain Bobs' lot, Joss, Big E and Stan, Gween, Nigel the teaman (and Roy), Julia and Elsie, Pazza, both Gazzas, Max, The Stick, All the Lawrences, Boneo, Rod and The Lardy Boys. I have to save the biggest hand for the 2:29 crew who deserve a big pat on the back - especially Plopps, "Auntie" Rach, Paully, Big Boy, Heenous, Dave, Reeky and The Moose Man. Last laughs go to the wonderful Miss Thomas.

I Love You All

Table of contents.

Tables

Figures

Abbreviations

AMPS	ammonium persulphate
ATP	adenosine triphosphate
BSA	bovine serum albumin
Ci	Curie
cDNA	complimentary deoxyribonucleic acid
cm	centimetre(s)
CMV	cytomegalovirus
Da	daltons
ddH_2O	double distilled water
DEPC	diethyl pyrocarbonate
DMSO	dimethyl sulphoxide
DNA	deoxyribonucleic acid
DTT	dithiothreitol
ECM	extracellular matrix
EDTA	ethylene diamine tetra-acetic acid
ERK	extracellular signal-regulated kinase
F	Farad
FACS	fluorescence activated cell sorting
FITC	fluorescein isothiocyanate
FCS	foetal calf serum
G418	geneticin
g	gramme(s)
g	acceleration due to gravity ($9.81 ms^{-2}$)
Ig	immunoglobulin
JNK	Jun kinase
IPTG	isopropyl β-D-thiogalactopyranoside
L1-CAM	neural cell adhesion molecule
l	litre(s)
LB	Luria broth
M	mole(s) per litre
mAb	monoclonal antibody
mol	moles
MEM	Eagles' minimal essential media
mRNA	messenger ribonucleic acid
MTT	1-[4,5-dimethylthiazol-2-yl]-3,5-diphenylformazan

μ	micro
MAdCAM-1	mucosal addressin cell adhesion molecule 1
mg	milligram(s)
ml	millilitre(s)
mm	millimetre(s)
nm	nanometre(s)
OD	optical density
p	pico
P	passage
PCR	polymerase chain reaction
PE	phycoerythrin
pfu	plaque forming units
RNA	ribonucleic acid
rpm	revolutions per minute
RSV	Rous sarcoma virus
RT PCR	reverse transcription polymerase chain reaction
SDS	sodium dodecyl sulphate
SDS-PAGE	sodium dodecyl sulphate-polyacrylamide gel electrophoresis
TEMED	N,N,N,'N'-Tetramethylethylene diamine.
Tris	tris (hydroxymethyl) aminomethane
UVR	Ultraviolet radiation
VCAM-1	vascular cell adhesion molecule 1
V	volt(s)
v/v	volume by volume
w/v	weight by volume
X-gal	5-bromo-4-chloro-3-indoyl-β-D-galactopyranoside

Chapter 1: INTRODUCTION

Cell adhesion events are essential to any biological process involving communication between a cell and its environment. These events are mediated by a number of recently characterised groups of adhesion molecules, spanning the cell membrane. They act as both molecules for cell anchorage and as signal transducers, connecting an extracellular environment to structural cytoskeletal components and signalling pathways that allow cells to respond to both external and internal stimuli. Such events can be diverse, ranging from growth and differentiation of tissue to migratory pathways such as inflammation, haemostasis and wound repair (Hynes, 1992)

Specific events are mediated by a number of significantly different adhesion molecule families. They include the integrins, immunoglobulin (Ig) superfamily, cadherins, selectins, CD44-related molecules and transmembrane proteoglycans. Each family consists of several members and have a specific role in the maintenance or formation of cellular contacts between other cells or to connective proteins of the extracellular matrix (ECM).

The role of these adhesion molecules in tumour cells has been the source of much interest over the past ten years. Tumour invasion and metastasis is a complex multistep process involving proliferation of the primary tumour, invasion of a basement matrix and release of neoplastic cells from the primary tumour into either the lymphatics or blood vessels (Nicolson, 1988; Hart *et al.*, 1989). Arrest of these cells in metastatic sites requires specific interactions with the endothelium and underlying subendothelial matrix before adhesion, invasion and subsequent

proliferation occurs. Most (if not all) of these steps involve cell-cell and cell-matrix interactions so it can be clearly seen that molecules controlling these interactions bear great significance.

Members of the integrin family of cell adhesion molecules consist of non-covalently associated glycoprotein heterodimers and appear to play a significant role in the mediation of the metastatic cascade (Hynes, 1992). As both adhesion molecules and signal transduction receptors, they have a significant impact upon substrate independent growth and proliferation of transformed cells, influencing oncogenesis, proliferation, invasion, metastasis and angiogenesis of secondary tumours (Juliano and Varner, 1993). This is of particular significance in malignant melanoma where invasion and metastatic spread of tumours have a large impact upon patient prognosis (Kramer *et al.* 1991).

In this study we have concentrated on using members of the integrin family of adhesion molecules as a target for gene therapy, particularly those present on the surface of metastatic melanoma cells. A number of gene therapy techniques have been used here in an attempt to reduce expression of specific integrin molecules on the surface of both human and murine melanoma cells and subsequently change the metastatic phenotype of transformed cells.

1.1 Malignant Melanoma

Malignant melanoma is a particularly virulent form of skin cancer which arises from the transformation of normal skin melanocytes to a malignant phenotype. Epidermal melanocytes are neural-crest derived cells which migrate to the basal layer of the epidermis early in embryonic development. Their role in the epidermis is to

closely interact with surrounding keratinocytes, forming a functional structure defined as the epidermal-melanin unit (Weiss and Greep, 1977). Melanocytes transfer melanin pigment granules through dendritic processes to these keratinocytes and help to protect the skin from environmental ultraviolet light damage (Yaar and Gilcrest, 1991). Malignant transformation of these cells appears to reinstate neural-crest cell migratory behaviour and facilitates substrate independent growth leading to highly invasive cells with a well developed ability to migrate to secondary sites in the body (Jimbow *et al.* 1991).

1.1.1. Aetiology

The likelihood of melanoma developing in an individual depends greatly upon skin type, age and exposure to environmental risk factors (Clark *et al.,* 1969). Melanoma occurs predominantly in fair skinned people, with a reducing risk with increasing natural skin colour, although a dark complexion is not a total defence against development of melanoma. Other important predisposing factors in melanoma are the presence of large numbers of moles (melanocytic nevi), freckling and family history of melanoma (Holly *et al.,* 1987; Greene *et al.,* 1985). Melanocytic nevi represent markers of melanoma risk rather than true precursors as at least 70% of melanomas arise in normal skin (Clark *et al.,* 1969).

The effect of age upon melanoma incidence is difficult to separate from factors arising from exposure to environmental factors. Older age is generally the time that clinically significant melanomas appear although evidence suggests that exposure to environmental risk factors at a young age significantly increases risk of development of melanoma in later years (Marks, 1988).

The major environmental risk factor of melanoma (and all other skin cancers) is exposure to sunlight, predominantly in the UVR wavelengths (290-320nm). However, unlike other types of skin cancer, length of exposure does not seem to have a direct relationship to melanoma risk.

1.1.2. Incidence

Although malignant melanoma comprises only 5% of all skin cancers, more than 3/4 of all deaths from skin cancer are due to malignant melanoma (Rigel, 1992). Greater information exists for the incidence of malignant melanoma in the United States where there are approximately 32 000 new cases each year and approximately 6500 Americans die each year from the disease. Incidence of malignant melanoma in the US has increased more than 12-fold over the last 50 years from 1 in 1500 in 1935 to 1 in 250 in 1991. Projections of current figures predict that the lifetime risk for developing malignant melanoma by the year 2000 will be 1 in 75 (Balch et al., 1985b).

1.1.3. Mortality associated with malignant melanoma

Prognosis of melanoma depends on a number of factors, however the primary prognostic variable is the stage of disease, represented by the data shown in table 1.1.

Table 1.1 Effect of stage of malignant melanoma upon patient survival

Stage	Description	Survival
I	localised primary cutaneous malignant melanomas	40%-100% over five years
II	Palpable regional lymph nodes and histological evidence of tumour	30% over five years
III	Distant metastases	Survival 5-16 months

Data taken from Balch *et al.*,(1985a).

Many factors have a prognostic significance, particularly in stage I of malignant melanoma. These include age, where older patients are possibly less able to mount an effective immune response to tumour cells (Thorn *et al.*, 1987; Cohen *et al.*, 1987). Sex of patients has a significance with survival greater amongst females (Shaw *et al.*, 1980). Location of the primary tumour is also significant, as patients with tumours on the extremities (excluding hands and feet) tend to survive longer than other lesions (Thorn *et al.*, 1989) although this phenomenon is not always predictable.

Morphological and histological factors are very important in the prognosis of malignant melanoma. Bleeding, ulcerated and nodular tumours indicate a potentially worse prognosis. The single best determinant of tumour prognosis is its thickness, and thus essentially, degree of invasion (Clark *et al.*, 1969, Breslow 1970). It can be measured as the maximal vertical dimension of the tumour from the top of the granular cell layer to the deepest invasive tumour cell with an ocular micrometer. Mortality associated with tumour thickness is represented by table 1.2.

Table 1.2 Effect of primary tumour depth upon type I malignant melanoma survival.

Tumour depth (mm)	Five year survival
<0.76	96%
0.76-1.49	87%
1.5-2.49	75%
2.5-3.99	66%
>4	47%

Data taken from Balch *et al.*, (1985b)

Tumour thickness characterisation forms the basis of therapeutic decisions, which include surgical resection, lymph node dissection and use of adjuvant chemotherapy. Surgical excision is an effective curative treatment approach for thin (<0.8mm) but less effective for thick (>1.7mm) tumours (Goldman *et al.,* 1986) due to its link with invasion and dissemination. In some cases, tumour depth does not represent an accurate prognostic tool although these cases are isolated to a few individuals.

1.2. The integrin family of cell adhesion molecules

Integrins are non-covalently linked heterodimers of transmembrane glycoproteins consisting of two fairly similar components, termed α and β subunits (Hynes, 1992). Currently the family consists of 16 known α units and 9 known β units which are distinct in terms of processing and surface expression (O'Toole *et al.,* 1989). The range of potential α and β subunit pairs is controlled, however, with α units forming specific heterodimers with distinct β units. However, some integrin β subunits (β1 β2 and β3) can form heterodimers with a range of α units, giving a total of 20 currently identified integrin heterodimers, each with a different spectrum of ligand specificities (Hynes *et al.*, 1992; table 1.3).

A range of integrin heterodimers are constitutively expressed on the surface of all mammalian cells (except mature erythrocytes; Hemler, 1990). They can mediate adhesion contacts to both proteins of the extracellular matrix (ECM, Giancotti *et al.,* 1985, Pytela *et al.,* 1985; Ginsberg *et al.,* 1983) and to other cells through members of the immunoglobulin superfamily (Marlin and Springer, 1987) or through bridging soluble ligands (in the case of platelet coagulation, Plow *et al.*, 1986). Adhesive

contacts are divalent cation dependent (Gailit and Ruoslahti, 1988), and affinity of these integrins can be modulated through conformational changes between "active" and "resting" states to alter ligand binding properties (Shattil *et al.,* 1985). Ligand binding to integrin heterodimers will additionally result in rearrangement of the cell cytoskeleton through contacts with the cytoplasmic portion of the integrin and triggering of secondary signalling pathways (reviewed by Clark and Brugge, 1995). Therefore, integrins can more accurately be described as dynamic surface receptors rather than purely adhesion molecules.

1.2.1. Structure of integrin subunits

Electron microscope images of integrin heterodimers have indicated the presence of a 10-15nm extracellular globular "head" comprising both α and β subunits with two "stalks" extending into the phospholipid membrane bilayer. These terminate in short cytoplasmic domains of ~40-70 amino acid residues (Carrell *et al.*, 1985; Nermut *et al.*, 1988; Weisel *et al.*, 1992).

Integrin β subunits are generally ~1000 amino acid residues long (90-110kd) with a similar basic morphology to the α subunit. The N-terminal 40-50kd "head" portion of the subunit is tightly folded with internal disulphide bonds, while the transmembrane "stalk" of all β subunits consist of characteristic four-fold repeats of a cysteine rich segment, believed to be internally disulphide bonded (Calvete *et al.,* 1991). All β subunit cytoplasmic domains consist of relatively short sequences of ~40-60 amino acids, with the exception of β4 which has a ~1000 residue tail (Suzuki and Naitoh, 1990) and appears directly interact with cytoskeletal components directly. Primary sequences within this region generally carry great homology between both

species, and different β-subunits. Cytoplasmic domains of β integrin subunits interact with components of the cytoskeleton and are essential for activity of many secondary signalling pathways (reviewed by Sastry and Horwitz, 1993 and described in section 1.3.2.).

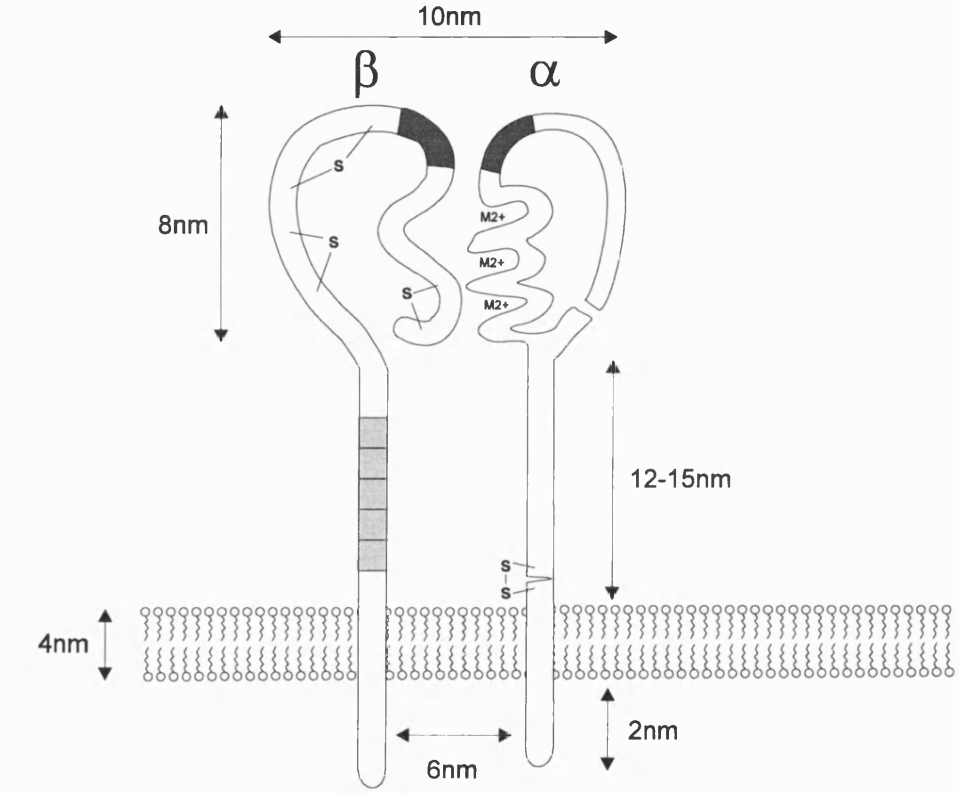

Fig 1.1 Typical structure of an integrin heterodimer, as expressed on the cell membrane. The dark shaded area marks the relative position of sites important to ligand binding for each subunit. The light shaded area on the β subunit shows the position of the characteristic cysteine-rich repeats. Sites marked with an 'S' illustrate the presence of disulphide bonded areas in the β subunit globular head, while the disulphide bonded area in the α subunit indicates the position of the posttranslational cleavage site (if present). Areas of the α subunit marked with M2+ indicate sites of interaction with divalent cations, or EF-hand-like loops. For clarity, the position of the ~190 residue I-domain (N-terminal of the EF hand repeats) has been omitted, although, when present is significant to both ligand and divalent cation binding. This diagram is not shown to scale. (Illustration modified from that presented by Hynes, 1992).

Table 1.3 The integrin receptor family and recognised ligands

Integrin Subunits		Ligands and Counter Receptors	Recognition sequence or domain
β1*	α1	Collagen I, IV, laminin	DGEA (collagen)
	α2	Collagen I, IV, laminin	RGD (?)
	α3*	Collagen I, IV, laminin, fibronectin, epiligrin	Domain 1 & 4 (VCAM-1), EILDV RGD
	α4	VCAM-1, fibronectin	RGD
	α5	Fibronectin	RGD
	α6*	Laminin	YIGSR
	α7*	Laminin	YIGSR
	α8	?	?
	α9	?	?
	αv	Vitronectin, fibronectin	RGD (fibronectin)
β2	αL	ICAM-1, ICAM-2, ICAM-3	Domain 1 (ICAM-1)
	αM	iC3b, ICAM-1, fibronectin, vWF, factor X	Domain 3 (ICAM-1)
	αX	Fibronectin, iC3b	GPRP (fibrinogen)
β3*	αIIb	Fibrinogen, fibronectin, vWF, thrombospondin	RGD, KQADGV (fibrinogen)
	αv	Fibrinogen, fibronectin, vWF, vitronectin, L1-CAM, CD31 (PECAM-1)	RGD, domains 1&2 (CD31)
β4	α6	?	
β5	αv	Laminin (?), basement membrane protein	RGD
		thrombospondin, osteopontin, collagen,	
β6	αv	(?)	
β7	α4	fibronectin, Vitronectin, MAdCAM-1, VCAM-1	RGD
β8	αE	Fibronectin (?)	RGD
	αv	VCAM-1, fibronectin, MAdCAM-1	EILDV (fibronectin)
β9		?	

* indicates the identification of alternatively spliced integrin subunits

Integrin α subunits are approximately 1000 residues long (120-180kd) and comprise a similar N-terminal extracellular globular "head" which is not internally bonded but contains a seven-fold repeat of a homologous segment, termed the EF-hand-like repeats. The last 3 or 4 of these repeats are believed to contribute to divalent cation binding (Gulino *et al.*, 1992) (actual number of sites depends on specific subunits). Some α subunits (αM, αL, αX, α1 and α2) have an additional ~190 residue amino acid sequence, inserted before the last five homologous repeats of the N-terminus, termed the I (insert) domain and are also closely implicated in ligand and divalent cation binding (Michishita *et al.,* 1993). Divalent cations are essential to receptor function, and the nature of the cation has a significant impact upon both affinity and ligand specificity (Smith and Cheresh, 1991), particularly in integrins carrying an I domain (Lee et al., 1995a; Lee et al., 1995b) (see section 1.2.3). Some α subunits are posttranslationally cleaved to give a 25-30kd transmembrane and cytoplasmic domain disulphide-bonded to a larger extracellular chain. The cytoplasmic domain of α subunits are of similar size to β subunits (15-77 residues) and bear significant homology between species. However, homology between different subunits is low (up to 60%). The role of α cytoplasmic domains in cell signalling is less clear although they do have a well defined role in the regulation of ligand specificity (LaFlamme *et al.,* 1994; Kassner *et al.,* 1994).

An additional level of complexity is present in the structure of integrins in that many subunits are present in an alternatively spliced form (indicated on table 1.3). The activity of these alternatively spliced integrins is similar to their "parent" molecules. Reasons for the existence of these alternate forms is currently unknown

but probably serves to add versatility to individual receptor function (discussed in Hynes, 1992).

1.2.2 Integrin ligands

Integrins have been identified as receptors for components of the extracellular matrix (ECM)(Ginsberg *et al.,* 1983), cell surface Ig superfamily receptors including the intercellular adhesion molecules ICAM-1 and ICAM-2 and vascular adhesion molecules VCAM-1 (Marlin and Springer, 1987), micro-organisms such as the adenovirus (Wickham *et al.,* 1993), certain gram positive bacteria (mediating endocytosis, Vannhieu *et al.,* 1996) and the spirochete responsible for lymes disease *Borrelia burgdorferi* (Coburn *et al.,* 1993), certain plasma proteins (deposited at sites of injury in haemostasis e.g. fibrinogen), complement activation (iC3b) and integral membrane proteins, such as MAdcCAM-1 (Berlin *et al.* 1993).

Integrins mediate interactions with components of the insoluble extracellular matrix or surface proteins on other cells to form links with intracellular elements involved in bidirectional signalling events. The extracellular matrix consists of a complex multiplicity of proteins and glycoproteins including fibronectin Mosher, 1993), fibrinogen (which in soluble form can also mediate cell-cell aggregation), von Willebrands' factor (vWF) (Ruggeri,1993), laminin, vitronectin, collagens and thrombospondin. These molecules form specialised matrices on the surfaces of cells, with composition depending on cell-type and location. Matrices can either be derived from cells or by deposition from soluble, plasma derived molecules.

Examination of receptor recognition sites of ligands or counterreceptors almost always identifies the presence of an acidic residue as a key component. Ligands may often have multiple integrin receptors and conversely, an integrin may bind many

different ligands (Reviewed by Hynes, 1992). This redundancy is illustrated in Table 1.3 which additionally indicates active residues involved in ligand binding function. In some ECM proteins, such as fibronectin and vitronectin, these active residues can be assigned to short linear sequences such as Arg-Gly-Asp (RGD; Pierschbacher and Ruoslahti 1984) and can be recognised by integrins containing cleaved α-subunits without I-domains. Other active residues include Lys-Gln-Ala-Gly-Asp-Val (KQAGDV; D'Souza *et al.* 1991) in fibrinogen, Asp-Gly-Glu-Ala (DGEA) in type I collagen (Staatz *et al.*, 1991) and Tyr-Ile-Gly-Ser-Arg (YIGSR) in laminin (Graf *et al.*, 1987). Strong evidence exists to suggest that other ligand domains also contribute to integrin binding: Analysis of tertiary structures in a variety of RGD containing ligands has shown that active peptides are located in highly flexible loop structures containing β turns (Leahy *et al.*, 1992, Main *et al.*, 1992) and that this may allow protein ligands to contribute secondary sites (Obara *et al.*, 1988).

1.2.3. Ligand binding to integrin heterodimers

Studies using ligand binding to fragments of N-terminal integrin subunits, generated through proteolysis (Lam, 1992) or recombinant truncations (Wippler *et al.*, 1994) have identified that both α and β subunits are capable of binding ligand. However, high affinity ligand recognition requires a heterodimer of both α and β subunits (Fitzgerald and Phillips, 1985) and therefore elements of both subunits.

Binding studies using ligand-mimetic peptides (O'Toole *et al.*, 1989), chemical cross-linking (D'Souza *et al.*, 1988), site-directed mutagenesis (Loftus *et al.*, 1990) and monoclonal antibodies (D'Souza *et al.*, 1994) have revealed potential ligand binding and recognition sites in the N-terminal extracellular domains of both integrin subunits. Ligand binding function of β integrin subunits has been mapped to a highly

conserved ~62 residue region of the subunit such as D109-E171 in human integrin β3 subunits (Smith and Cheresh, 1988; D'Souza *et al.,* 1988). Substitution of key, conserved residues within this region (at D119 of β1, β2, β3 and β6) result in a total loss of ligand binding (Loftus *et al.,* 1990). A second site within this same conserved region has also been identified as important for ligand binding (Bajt *et al.,* 1992; Lanza *et al.,* 1992).

Positions of critical ligand recognition sites with α subunits are less easy to classify and depend on the presence of an I-domain. The I-domain of α integrin subunits is closely implicated with ligand recognition and is structurally related in secondary structure to the conserved region of β subunits (Bajt and Loftus, 1994; Lee *et al.,* 1995a). Mutation of the I-domain results in a similar blockage of ligand binding function (Michishita *et al.,* 1993). Identification of recognition sites in α subunits without I-domains (such as αIIb and αv) has only recently become more clear, and requires a combination of two regions, an N-terminal region and the first two EF hand divalent cation repeats (Loftus *et al.,* 1996).

It must be noted that the ligand specificity of many integrins is variable between cell lines (Kirchôfer *et al.,* 1990) and even within the same cell lineage (Elices and Hemler, 1989). Additionally, level of expression of integrins does not necessarily equate with ligand binding or functional activity, as this may depend on activity status (Masumoto and Hemler, 1993).

1.3. Integrin mediated transmembrane signalling

Large amounts of information has recently been gathered concerning the role that integrins take in mediation of a number of biological phenomena. Integrin ligand recognition and receptor occupancy can not only influence a number of signalling pathways, termed "outside in" signalling, but affinity of integrins for ligand can be rapidly changed through interaction with cytoplasmic cell elements, termed "inside out" signalling (as termed by Hynes, 1992).

1.3.1. Modulation of integrin affinity: inside out signalling

Modulation of integrin affinity is an important phenomenon in many integrin mediated biological systems. Platelet aggregation and inflammatory cells such as leukocytes and neutrophils require rapid, reversible "activation" of cell adhesion in order for the transition from suspension to adhesion to occur (Peerschke *et al.,* 1980; Dustin and Springer, 1989). Many (if not all) integrins can exist in different conformational states which influence ligand affinity and recognition. The platelet integrin, αIIbβ3 for example, can exist in two affinity conformations: "unstimulated", where resting platelets will attach to surface-bound fibrinogen and a "stimulated" conformation allowing affinity for soluble fibrinogen in the vasculature. This change in ligand affinity arises from conformational changes in the extracellular domain of the integrin heterodimer (Sims *et al.,* 1991).

Ligand binding to integrins and changes in integrin affinity are closely associated with the displacement of divalent cations, such as calcium. These divalent cations bind to specific active sites present on both α and β subunits (Smith *et al.,* 1994; D'Souza, 1994). The actual location of these domains is unclear as they appear to be coordinated from domains aligned through complex tertiary structural

relationships which also link ligand binding domains. Recent crystal structure elucidation has however closely linked α integrin I domains and structurally related domains in the ligand binding region of β integrin subunits (Lee *et al.,* 1995a).

Specific divalent cations (such as Mn^{2+}) have been shown to enhance the adhesive property of many integrins (Smith *et al.,* 1994; Crowe *et al.,* 1994). It has been suggested that occupancy of cation binding sites with calcium stabilises the "resting" (or low affinity) conformation of the ligand binding site and that increases in ligand affinity caused by Mn^{2+} is thought to be due to antagonism of calcium binding to specific domains (Lee *et al.,* 1995b; Pelletier *et al.,* 1996). An "active" conformation of integrins can be induced by binding of ligands or ligand mimetics (such as RGD for αIIbβ3) and subsequent displacement of divalent cations (Du *et al.,* 1991).

Both α and β integrin cytoplasmic domains play a crucial role in this modulation of affinity, with deletion or mutation within this region affecting ligand affinity (Loftus *et al.,* 1990; Michishita *et al.,* 1993). However, their role in integrin affinity modulation remains difficult to characterise due to apparent variation of integrin activity in different cell types as a result of active cellular signals (Kirchôfer *et al.,* 1990; Masumoto and Hemler, 1993; Elices and Hemler, 1989). A conserved GFFKR motif, present within α integrin cytoplasmic domain, proximal to the cell membrane has been found to closely control the low affinity state of integrins. Deletion studies of this motif result in a constitutively high affinity integrin, independent of cell type or metabolic inhibitors (O'Toole, 1994). It has been suggested that this domain acts as an activating "hinge", inducing long range conformational changes of the ligand binding site. Homology of the remaining

cytoplasmic portion of α integrin subunits is low, indicating the potential for a wide divergence in the variety of interacting cellular elements (reviewed by Sastry and Horwitz, 1993).

The β cytoplasmic domain also has a critical role in affecting ligand affinity. Mutation within the cytoplasmic domain of the β3 integrin subunit Ser^{752} to Pro results in an apparent activation defect (Chen *et al.,* 1992a) of αIIbβ3 indicating that β integrin subunits are necessary for maintenance of a high affinity state. Furthermore, introduction of isolated β subunit cytoplasmic domains into cells lowers ligand binding affinity (Chen *et al.,* 1994b), suggesting that affinity modulation by β integrin cytoplasmic domains is dependent upon beta subunit contacts with cytoplasmic signaling pathways.

Phosphorylation events at integrin cytoplasmic domains have been extensively studied as a source for this activation stimulus (particularly in platelets - reviewed by Shattil and Brugge, 1991). However, the link between phosphorylation and integrin activation seems unclear. For example, phosphorylation of neutrophil β2 has been documented, but many agonists can activate αMβ2 in neutrophils without phosphorylation (Merill *et al.,* 1990; Buyon *et al.,* 1990) and mutation of the phosphorylation site does not block activation (Hibbs *et al.,* 1991). Therefore, no general cytoplasmic pathway can be isolated as specific for increases in integrin affinity. Recent important evidence however has implicated the GTP-binding protein, R-ras (in its activated form), as a potential cytoplasmic modulator of integrin activation (Zhang *et al.,* 1996). The exact mechanism for this activation remains to be elucidated.

1.3.2. Signal transduction through integrins: Outside In Signalling

As transmembrane receptors, integrins represent a primary link between the extracellular environment, cytoskeletal organisation and secondary signalling pathways. The molecules involved in these pathways, and their links with signal transduction through integrins have only recently begun to be identified and the role of integrins in many signalling pathways has yet to be deduced.

Integrins will bind to extracellular matrix proteins and other ligands to form clusters of receptors at sites of close cell-substratum contact. These are termed "focal contacts" and are commonly defined as a tight (10-15nm) clustering of specialised structures to a surface providing a link between the extracellular environment, actin cytoskeleton and signalling pathways (Chen and Singer, 1982). *In vivo* these classic contacts can rarely be seen, due to the irregular nature of the ECM and exist more as "ECM contacts" clustering around streaks or fibrils of the ECM. Integrin clustering and ligand ligation result in the accumulation of receptor bound kinases and the tyrosine phosphorylation of a variety of proteins resulting in the initiation of signal transduction cascades in a distinct hierarchy of interactions (Miyamoto *et al.,* 1995a; Miyamoto *et al.,* 1995b), as displayed in table 1.5. These studies have shown that many of the molecules identified as associating with integrin cytoplasmic domains are only weakly bound. Additionally, the actual stimulus initiating signalling is still unclear.

Table 1.4 represents a current snapshot of identified integrin mediated pathways, many of which link up with classic transduction pathways such as growth factors and cytokines.

Phosphorylation of proteins resulting from integrin occupancy/clustering occurs predominantly in the size range 110-130kDa (Kornberg *et al.*, 1991) and involves the integrin β subunit. One of the primary proteins phosphorylated by many β integrins is focal adhesion kinase (pp125FAK or FAK) which can autophosphorylate in response to clustering of intact integrins or even chimeras of β1, β3 and β5 (but not alternatively spliced β3) integrin cytoplasmic domains (Lukashev *et al.*, 1994; Akiyama *et al.*, 1994).

Table 1.4. Signal transduction pathways mediated through integrins

Signal transduction	Comments	Reference
Calcium influx / mobilisation	through certain αv integrins, linked to IAP	Schwartz *et al.*, 1993
Hydrogen influx		Schwartz & Lechene 1992
FAK tyrosine phosphorylation	Induced by a variety of ECM ligands	Schaller et al., 1992
ILK tyrosine phosphorylation		Hannigan *et al.*, 1996
Insulin induced proliferation	Association of phosphorylated IRS-1 to αvβ3	Vouri & Ruoslahti 1994
Activation of Src and related tyrosine kinases		Schlaepfer *et al.*, 1994
Growth regulation	via β6 cytoplasmic domain	Agrez *et al.*, 1994
Enhanced gene expression	Of integrins, and ECM proteins in response to substrate composition	Delcommenne & Streuli 1995
	Of β-casein	Roskelley *et al.*, 1994
	Of collagenase	Tremble *et al.*, 1995
Apoptosis	Prevented by ligation to a number of ECM ligands (section 1.4.4)	Ruoslahti and Reed, 1994
Protein kinase C and arachidonic acid		Woods and Couchman, 1992
Accumulation of signal transduction adapters and enzymes	Association of growth factor receptor-bound protein 2 (Grb2) to FAK and activators of the Ras pathway (mSos1)	Schlaepfer *et al.*, 1994
ERK activation		Chen *et al.*, 1994a
JNK activation		Miyamoto *et al.*, 1995b

FAK, unlike other tyrosine kinases lacks both Src homology domains (SH2 and SH3 domains-responsible for intermolecular interactions that couple signalling proteins), but phosphorylation of tyrosine-397 of FAK appears to act as a gateway for activation of a large number of other protein kinases and recruitment of cytoskeletal proteins in a controlled hierarchy of interactions, dependent on clustering and activation state of integrins (Clark and Brugge, 1995; Miyamoto *et al.,* 1995b) as shown in table 1.5, overleaf. Studies using swaps or truncations of integrin subunits indicate that the initiation of many specific signal transduction pathways is integrin-specific, resulting in changes in cell adhesion, migration and focal adhesion formation (Pasqualini and Hemler, 1994). Additionally, specific integrin subunits are responsible for initiation of a growing number of individual pathways (Vuori and Ruoslahti, 1994; Agrez *et al.,* 1994).

α integrin cytoplasmic domains have also been found to associate with cytoplasmic proteins, particularly a 60kDa calreticulin homologue at the conserved GFFKR motif (Rojiani *et al.,* 1991). Calreticulin is a nuclear inhibitor of receptor mediated transcription and will only associate to α integrin domains in a high affinity conformation. It has been suggested that this association with integrins not only stabilises a high affinity state but sequesters calreticulin away from the nucleus enhancing gene transcription (Dedhar *et al.,* 1994).

Very recent studies have shown that the membrane proximal sequences significant for long range inside out "activation" of integrins (or the integrin "hinge", as discussed above) are additionally significant for outside in signal transduction (Hughes *et al.,* 1996). Disruption of a potential salt bridge between conserved membrane proximal sequences KvGFFKR (α subunit) and KLLitihD (β subunit, lower case symbols represent less conserved residues) by point mutation constitutively activates signalling pathways mediated by integrins, such as FAK phosphorylation.

This recent discovery will have tremendous implications upon the elucidation of further integrin mediated signalling pathways, through the examination of cells transfected with integrins mediating this constitutive activation.

Table 1.5. Range and hierarchy of cytoplasmic molecules interacting with β integrin cytoplasmic domains, and their relationship to integrin clustering and ligation.

	State of receptor			
Cytoplasmic molecules	integrin aggregation	integrin aggregation + ligand occupancy	integrin aggregation + tyrosine phosphorylation	aggregation tyrosine phosphorylation ligand occupancy
Cytoskeletal proteins	Tensin	Tensin α-actinin Vinculin		Tensin Talin α-actinin Vinculin Paxillin F-actin Filamin
Src substrates	FAK Tensin	FAK Tensin	FAK Tensin Cortactin pp120	FAK Tensin Cortactin pp120
Src kinase family			c-Src c-Yes c-Fyn c-Csk	c-Src c-Yes c-Fyn c-Csk
Signalling molecules			GAP PLC-γ PI3-kinase PTP-1D RhoA Rac1 Grb2 Sos Ras Raf1 MEKK MEK1 ERK1 ERK2 JNK1	GAP PLC-γ PI3-kinase PTP-1D RhoA Rac1 Grb2 Sos Ras Raf1 MEKK MEK1 ERK1 ERK2 JNK1

Table reproduced from Miyamoto *et al.* (1995b)

1.4. Role of integrin receptors in malignant melanoma

Integrins have a critical role to play in mediating the malignant phenotype of melanoma. This process requires complex changes in the degree of normal cell-cell and cell-substratum interactions which can manifest as increases or decreases in integrin expression or changes in receptor activation and affinity (Juliano, 1987). An active malignant melanoma will be able to undergo substrate independent growth and survival and be able to complete the metastatic cascade of detachment from the primary tumour, invasion of basement membranes of the surrounding stroma, passage within the lymphatic system or vasculature and migration to remote sites of the body before secondary substrate attachment, invasion of endothelia and metastatic growth (Clark *et al.,* 1984; Clark *et al.,* 1986). Control of this cascade of events cannot be assigned to a single integrin heterodimer or to the influence of a single oncogenic signalling pathway. Here we shall examine the changes in integrin and ECM expression that occur in transformed melanocytes and examine the role of key integrins in the migratory phenotype of malignant melanoma.

1.4.1 Changes in integrin expression in transformed cells

Oncogenic transformation of any cell type results in altered expression of integrin receptors in comparison to untransformed cells (Plantefaber and Hynes, 1989). Changes in integrin expression profiles appear to be both tumour specific and integrin specific, and this is very much the case in transformed melanocytes. Table 1.6, overleaf, gives an indication of the range of changes that have been reported in the expression profile of transformed melanocytes.

Distinct differences are hard to elucidate as integrins expressed upon melanocytes are difficult to detect *in situ* due to their isolated nature and close

association with keratinocytes. Comparisons with cultured cell lines is additionally difficult since expression of many surface proteins are changed in a tissue culture system (Herlyn *et al.,* 1987). A more significant indicator of the importance of integrins on tumour progression can be found from comparisons of integrin expression at different stages of tumour progression *in vivo* (Albelda *et al.*, 1990; see section 1.4.2). It must be noted that it is not clear whether changes in integrin expression patterns in melanoma are a contributor to the malignant state or a consequence of it.

Oncogenic transformation of cells will have a significant impact upon integrin mediated signalling pathways. Constitutive activation of intracellular signalling proteins such as oncogenes Src and p21Ras will uncouple the requirement of integrin ligation and clustering for substrate dependent intracellular signalling and survival (as described above). Constitutive activation of integrin associated signalling pathways will also have an impact upon the subsequent expression of specific genes, including integrins and ECM proteins.

Transformed cells express altered levels of ECM components (such as fibronectin) and changes in ECM composition can play an active part in changes in adhesiveness, motility and morphology of transformed cells (Yamada, 1983).

1.4.2. Role of integrins in migration, invasion and metastasis of malignant melanoma

Functional studies have shown that integrins play an active role in the motility of melanoma. Synthetic peptides containing the ligand mimetic RGD motif inhibit the invasion of human melanoma cells through amniotic basement membrane models *in vitro* (Gehlsen *et al.,* 1988). RGD peptides also reduce the number of metastatic lung nodules *in vivo* when co-injected into C57 mice with B16F10 melanoma cells (Humphries *et al.,* 1986; Saiki *et al.,* 1989; Humphries *et al.,* 1988).

Table 1.6. Changes in integrin expression between untransformed melanocytes and melanoma cells *in vivo*

α1β1	α2β1	α3β1	α4β1	α5β1	α6β1	α6β4	α7β1	αIIbβ3	αvβ3	αvβ5	References
	↑	↑	↑↑	↑					↑↑		Albelda *et al.*, 1990
									↑↑		McGregor *et al.*, 1989
↓	↓↓		↑↑	↑↑							Schadendorf *et al.*, 1993
	↑↑										Van Duinen *et al.*, 1994
									↑↑		Si and Hersey, 1994
							↑↑				Kramer *et al.*, 1991
		↑↑									Natali *et al.*, 1993
					↓↓						Natali *et al.*, 1991
		↑	↑↑	↑↑	↓	↓			↑↑		Danen *et al.*, 1994
										↓↓	Danen *et al.*, 1995
								↑↑			Chang *et al.*, 1992[1]

1. It must be noted that identification of αIIbβ3 has only been identified in vitro in murine cultures of B16a cells. A double arrow represents a large change (or de novo expression, in the instance of αvβ3 expression by Albelda et al,1990) in the marked integrin heterodimer. A single arrow represents a small, but reproducibe change in expression. No arrow denotes either no change or that the integrin subunit was not studied.

As described in section 1.4.1, in situ monoclonal antibody detection of integrins on sections of human melanoma from benign naevi, non-invasive radial growth phase (RGP) primary melanotic lesions, vertical growth phase (VGP) lesions and metastatic melanoma have revealed significant alterations in integrin profiles (McGregor *et al.*, 1989; Albelda *et al.*, 1990). Most striking amongst these differences is that VGP and metastatic melanoma express β3 integrins whereas non-invasive melanoma lesions (and native melanocytes) do not. There are two identified β3 integrins, αIIbβ3, the major platelet integrin (Phillips *et al.*, 1988) and αvβ3, the classical vitronectin receptor (Cheresh and Spiro, 1987). Integrin αvβ3 has become closely implicated with an invasive tumour phenotype.

Further evidence for αvβ3 integrin involvement in melanoma metastasis has been obtained through a number of studies: Antibody treatment of human melanoma cell lines with an anti αvβ3 antibody inhibits subcutaneous growth of human melanoma xenografts (Boukerche *et al.*, 1989). Ligand binding to αvβ3 integrin with soluble vitronectin or antibodies is associated with an increased *in vitro* invasive potential of A375M human melanoma cells (Seftor *et al.*, 1992). It has been postulated that this ligand binding results in induction of signal transduction pathways, increasing expression of type IV collagenase enzymes (Seftor *et al.*, 1992). Further studies have shown that αvβ3 can also recognise a cryptic ligand binding site exposed upon denaturation of collagen I matrix (Davis, 1992), exposed by collagenase digestion of the basement membrane by invading tumour cells (Montgomery *et al.*, 1994) and allowing invasion of collagen matrices. Further important evidence of a co-ordination between proteolytic enzymes and αvβ3 has recently been published by

Brooks *et al.* (1996) who provide evidence for a co-localisation and interaction between αvβ3 and activated receptor bound matrix metaloproteinase (MMP-2).

A similar pattern of β3 integrin expression has also been elucidated in a murine melanoma cell model B16a, except the functionally active integrin is the classic platelet integrin αIIbβ3 (Chen *et al.,* 1992b). Similar to expression of αvβ3 in human melanoma, αIIbβ3 expression in B16a cells has been implicated with increased metastatic capacity (Chang *et al.,* 1992), which is reduced (but interestingly, not totally prevented) by treatment with specific anti αIIbβ3 monoclonal antibodies.

The ability of tumour cells to migrate to distant sites of the body has been closely linked to their association with platelets in several studies (reviewed by Honn *et al.,* 1992). During this process, many tumour cells can induce platelet aggregation and subsequently form co-aggregated thrombi in the bloodstream. This is followed by arrest at distant sites in the vasculature, and tumour cell invasion. The mechanisms behind this process have long been thought to be due to the passive entrapment of tumour/platelet thrombi in narrow capillary vessels. However, the site specific nature of many tumour types and increased shear conditions at sites of capillary occlusion have lead to the discovery of the importance of β3 integrins in this process.

Induction of platelet aggregation by tumour cells can be mediated by a number of factors including ADP release (Grignani and Jamieson, 1988; Longenecker *et al.,* 1989), generation of tissue factors (Bastida *et al.,* 1984) or thrombin release by tumour cells (Tohgo *et al.,* 1985). These interactions can "activate" the platelet integrin, αIIbβ3 into a high affinity state, resulting in the aggregation of platelets using soluble plasma proteins (such as fibrinogen, von Willebrand factor, fibronectin or

thrombospondin) as bridging ligands (Peerschke *et al.*, 1980). Recent studies (Felding-Habermann *et al.*, 1996) have shown that tumour cell arrest under flow is influenced by adhesion events mediated by this platelet activation. Tumour cells expressing either β3 integrin (αIIbβ3 or αvβ3) can use activated platelet arrest to vessel walls as an primary anchor for their arrest via the soluble bridging ligands described.

Vitronectin expression in the ECM is vital for melanoma progression mediated by αvβ3 (Sanders *et al.*, 1992). Vitronectin is produced in the liver and accumulates in the serum from where it deposits into the ECM at the lungs, striated skeletal muscle, lymph nodes, skin and kidneys. Vitronectin deposits in the skin have been shown to increase with age and exposure to sunlight (Dahlback *et al.*, 1989) - both are in part factors in the development of melanoma. Co-injection of vitronectin with M21 human melanoma cells into nude mice results in an increase in tumour proliferation (Sanders *et al.*, 1992). Adhesion to lymph nodes, a primary target for melanoma metastasis is mediated through αvβ3 mediated attachment to ECM vitronectin, and is blocked by specific antibodies to αvβ3 or vitronectin (Nip *et al.*, 1992).

Integrin signaling events following ligand binding are vital to αvβ3 mediated invasion and metastasis, as deletions or changes in integrin cytoplasmic domains prevents cell spreading, focal adhesion formation and migration (La Flamme *et al.*, 1994; Ylänne *et al.*, 1993). Deletion of a highly conserved NPXY sequence in the cytoplasmic domain of the β3 subunit (residues 744-747) results in the loss of the metastatic phenotype of melanoma cells (Filardo *et al.*, 1995). The NPXY sequence is closely linked with recruitment of secondary signalling molecules and cytoskeletal

contacts, although deleted β3 subunits can still attach to soluble ligand (Filardo *et al.*, 1995).

Post-ligand binding signalling pathways have been implicated in the urokinase-type plasminogen activator system of basement membrane proteolysis which is closely linked to cell invasion (Seftor *et al.*, 1992). Lowering the expression of αv integrin subunits (using antisense αv phosphorothioate oligonucleotides) lowers expression of urokinase plasminogen activator receptor (uPAR), mAb ligation of αvβ3 also causes a transcriptional increase in uPAR (Nip *et al.*, 1995).

Although αvβ3 integrin has been closely linked to invasive and metastatic capacity of human melanoma cells, several important contradictions and complications have been elucidated which complicate understanding of the specific role of β3 integrin mediated melanoma progression (discussed below). Due to the complex nature of the metastatic cascade, a spectrum of other integrins (with different ligand affinities) are also closely linked with melanoma migration, invasion and metastasis as suggested by the range of integrins highlighted by table 1.6. Many isolated metastatic melanomas (up to 25%) do not express the αvβ3 heterodimer (Albelda *et al.*, 1990; McGregor *et al.*, 1989; Boukerche *et al.*, 1994) and it is most likely that metastatic activity is compensated by altered expression of other integrins. Additionally, Seftor *et al.* (1993) have reported that reduction of αvβ3 surface expression using fluorescence activated cell sorting (FACS) of A375M human melanoma cells causes an increase in ability of cells to invade *in vitro*. This appears to contradict αvβ3 mediated increases in invasion *in vitro* seen by Seftor *et al.* (1992).

1.4.3. Role of integrin αvβ3 in tumour cell Angiogenesis and apoptosis

Recent evidence has closely implicated integrin αvβ3 with angiogenesis (the growth of new blood vessels) during many processes such as wound repair, inflammation, development and pathological conditions such as diabetic retinopathy, rheumatoid arthritis and tumour cell development (Brooks *et al* 1994a; Brooks *et al.*, 1995).

Angiogenesis is vital for both blood supply to primary tumours and to aid passage of invading metastatic cells into the vasculature. In many tumour types (for instance prostatic and breast cancer) the degree of blood vessel infiltration of primary tumours provides a prognostic indication of disease status (Weidner *et al.*, 1992, 1993) as this has direct impact upon metastasis. Angiogenesis requires invasion, migration and proliferation of smooth muscle and endothelial cells of the vasculature (Clark et al., 1982). Examination of this phenomenon in *in vivo* models of chick chorioallantoic membranes (CAM) challenged with cytokine impregnated discs or fragments of solid human melanoma (not expressing αvβ3) has revealed that infiltration of blood vessels involves αvβ3 integrin (Brooks *et al.*, 1994a). Treatment of these models with cyclic RGD peptides or mAb's against αvβ3 dramatically decreases blood vessel infiltration and directly affects primary tumour cell growth (Brooks *et al.*, 1994b). Similar αvβ3 dependent tumour cell angiogenesis has also been seen in human mammary tumours (also not expressing αvβ3) grown upon human foreskin tissue grafted onto immunocompromised mice (Brooks *et al.*, 1995).

One interesting observation of anti-αvβ3 monoclonal antibody treatment of angiogenesis is that antibodies have no effect upon preformed tumour vascularisation.

However, treatment of forming angiogenic vessels at the peak of αvβ3 expression (12-24 hours) results in programmed cell death, or apoptosis of forming blood vessels detected with antibodies to DNA fragmentation (Brooks *et al.,* 1994b). Therefore, αvβ3 ECM interactions appears vital for survival and maturation of newly forming blood vessels.

Other integrin influenced apoptotic events have also been noted in the aberrant survival of human melanoma cells in a three dimensional dermal collagen I matrix. Human M21-L melanoma cells, selected (from wild type M21 cells) for lack of αvβ3 expression will initially spread through dermal collagen (type I, mediated by α2β1) but will rapidly lose their spread dendritic morphology after 24 hours. They subsequently undergo apoptosis after a two day period unless supplemented with growth factors or insulin to supplement inactive signaling pathways (Montgomery *et al.,* 1994). Wild type M21 cells (αvβ3 positive) in this system do not undergo apoptosis due to ligation of αvβ3 integrins with cryptic RGD binding sites revealed by melanoma cell proteolysis of collagen I (through integrin mediated collagenase synthesis, section 1.4.2.). This has been proposed as a major factor in tumour progression (Marx, 1993). It has therefore been suggested that αvβ3 ligation is vital to melanoma survival and growth before angiogenesis or in poorly vascularised areas of the tumour.

1.5. Integrins as targets for drug and gene therapy

It has been shown that integrin molecules are vital mediators in the regulation of many pathogenic and non pathogenic cell functions (Juliano and Varner, 1993;

Clark and Brugge, 1995). Their nature as a contact between the extracellular environment, and intracellular signalling pathways makes them a very interesting target for drug or gene therapy of any condition involving aberrant cell aggregation, migration, growth or differentiation. Potential target conditions could be as diverse as control of haemostasis, treatment of primary tumour spread or metastasis, or inflammatory conditions such as arthritis. This may be tackled using downregulation or inactivation of integrins involved in a pathogenic process, or stimulation of integrin expression or integrin conformation mediating a non-pathogenic phenotype.

They potentially pose an additionally interesting role as sites for drug (or gene) targeting to specific cell types, or even specific cell types in a certain stage of development. These topics are discussed in the following few chapters, with special consideration for studies that have already taken place.

1.5.1. Inhibition of gene expression using antisense DNA or catalytic RNA

Inhibition of protein translation through the use of single stranded DNA or RNA that hybridises in a sequence specific manner to target mRNA sequences in the cell have been extensively studied since its discovery and suggestion that it may have a clinical potential (Zamecnik and Stephenson, 1978). Several gene inhibition techniques, based on this approach have been suggested over the last 15 years including triplex DNA formation, catalytic RNA (ribozymes) and antisense RNA/DNA. All techniques utilise base pair hybridisation to DNA or mRNA to disrupt transcription and translation of proteins and are briefly reviewed here.

(a) Triplex DNA:

This technique of gene therapy is different to others in that it involves colinear association of specific DNA oligonucleotides (short lengths of linear single stranded

DNA) to double stranded genomic DNA in the nucleus. Complimentary oligonucleotides will form a triplex with purine rich double stranded DNA by forming non-Watson-Crick hydrogen bonds to the major groove of the double helix and causing a shift in the helix structure in a cation dependent manner. Consequences of this triplex formation are believed to be both a steric and conformational hindrance of mRNA transcription (Maher *et al.*, 1989). Conjugation of triplex forming DNA oligonucleotides with a number of modifying groups such as EDTA-Fe (Moser and Dervan, 1987) has also shown that triplex DNA conjugates can cause sequence specific double strand breaks. Triplex formation has also been shown to occur when using all-purine methylphosphonate oligonucleotides (see antisense oligonucleotides, below) complementary to all-pyrimidine mRNA targets (Reynolds *et al.*, 1994). Triplex DNA therapy has applications in both gene mapping and gene therapy although specific examples of effective use *in vivo* and *in vitro* are limited. Specific limitations of triplex therapy include the requirement of purine rich target DNA sites and reluctance of DNA to form triplexes due to charge repulsions between DNA phosphate backbones (Maher *et al.*, 1989).

(b) Ribozymes

Ribozyme therapy utilises the discovery that RNA can have catalytic cleavage activity upon endogenous mRNA (Cech and Bass, 1986) without the association of proteins, in a divalent cation and pH dependent manner. Several ribozymes have been discovered which selectively cleave mRNA, primarily the "hairpin" and "hammerhead" ribozymes, named due to their two-dimensional structural appearance. From their discovery, sequence specific ribozymes have been engineered, using two target mRNA specific antisense flanking sites (12-13 base pairs), connected together

with a short unpaired catalytic core. Modification of the structure to DNA/RNA chimeras has additionally reduced ribozyme susceptibility to ribonuclease attack (Bratty *et al.,* 1993).

One problem with ribozyme therapy is their inability to cross the Plasma membrane into cells due to their size and anionic charge. As a consequence, ribozyme therapy is either mediated through transfection methods such as liposomes or by endogenous cellular production after transfection of mammalian expression vectors coding for specific ribozymes with expression driven by viral or bacterial promoters.

Few studies have examined the potential role of ribozymes against malignant melanoma, with the majority of ribozyme studies focusing on their use against oncogenes, such as H-*ras* (Ohta *et al.,* 1994). Studies using ribozymes against integrins, or even other adhesion molecules are limited.

(c) Antisense RNA/DNA oligonucleotides

Antisense technology uses single stranded RNA or DNA to hybridise to and cause the intermediary metabolism of mRNA, interrupting the translation pathway between gene and protein. This alteration relies on sequence specific hybridisation of the single stranded RNA or DNA to a target mRNA and therefore in theory can affect target genes without altering expression of any other genes, although this is dependent upon non-specific sequence homology.

Antisense DNA or RNA is known to inhibit mRNA processing by a number of mechanisms. Primary amongst these is the physical inhibition provided by oligonucleotide binding to mRNA. This can occur in many forms, from nuclear inhibition of mRNA splicing, polyadenylation and transport from the nucleus, to cytoplasmic effects such as ribosomal translation and elongation (Hélène and Toulme,

1990). Some workers have suggested that targeting the 5' translation initiation site (AUG) of mRNA will afford additional inhibition of translation initiation factors (Leonetti *et al.,* 1993). An unexpected inhibition can also occur from the action of ribonucleases such as RNase H on mRNA/DNA duplexes (Walder and Walder, 1988) and RNase L on mRNA/RNA duplexes (Maitra *et al.,* 1995). These ribonucleases will hydolyse the mRNA strand and lead to degradation of the target strand. It is thought that unmodified phosphodiester oligonucleotides function primarily through the cleavage of RNase H (Walder and Walder, 1988)

Many problems occur with antisense treatment of cells. Synthetic single stranded phosphodiester oligomers are very sensitive to 3' exonucleases in extracellular fluids and have a half life of 5-60 minutes (usually around 20 minutes) (Akhtar *et al.,* 1991). Synthetic modification of DNA oligonucleotides by substitution of the non-bridging oxygen atom in the phosphate backbone can lead to nuclease resistant oligomers. For example, phosphorothioate oligonucleotides have the oxygen substituted for a sulphur atom (Matsukura *et al.,* 1987), increasing half life to over 1 hour, or methylphosphonate oligonucleotides with substituted methyl residues (Smith *et al.,* 1986). Modification of oligonucleotides can lead to inherent problems associated with degraded modified oligonucleotides entering the nucleotide pool and potential mutagenic effects (Stein and Cheng, 1993).

A second common problem associated with oligonucleotide delivery is their inefficient uptake into cells, particularly the nucleus. Untreated phosphodiester or phosphorothioate oligonucleotides are taken up into the cell by both receptor mediated endocytosis and passive absorbtive pinocytosis and tend to accumulate in endosomes and lysosomes with little transport to the nucleus (Wagner, 1994). Cell

permeabilisation techniques such as liposomes or microinjection greatly increase delivery to the nucleus and in some studies are found to be absolutely necessary for antisense activity (Bennett *et al.*, 1992).

Another technique to combat this delivery problem is by transfection of cells with mammalian expression vectors containing DNA encoding target specific antisense sequences with expression driven by a viral promoter (such as the Cytomegalovirus, CMV, or Rous Saracoma virus, RSV promoter). By the use of specific vectors and promoters, expression can be engineered to allow either episomal expression of constructs (using vectors based on the Epstein-Barr Virus) or an integration of DNA into the nucleus. Antibiotic markers such as geneticin or purimicin, encoded within the expression vector, allow for the *in vitro* selection of stable transfected cells. This technique ensures constant transcription of antisense mRNA and no subsequent need for cell permeabilisation to achieve adequate oligonucleotide targeting. Drawbacks of this method are that these RNA oligonucleotides are exonuclease sensitive, tend to be of longer length and therefore less specific and can give a gradual loss of antisense affect over time in some systems, possibly due to pathway redundancy.

As suggested above, other potential problems associated with antisense treatment are non-specific effects, particularly with longer oligonucleotides. This can include steric hindrance of non-target mRNA but is most likely a result of non-specific ribonuclease activity, for instance Woolf *et al.* (1992) have shown that RNase H activity can be seen if 6-10 base pairs of a 20-24mer oligonucleotide hybridise to non-target mRNA. Non-specific inhibition can also potentially arise from polyanionic

phosphodiester or phosphorothioate oligonucleotide binding to various proteins in the cell (Stein and Cheng, 1993).

1.5.2. Gene therapy of integrin expression.

Most studies with the techniques described above have been in the field of cancer therapy, with the most intensive body of work concentrating on the use of modified oligonucleotide delivery to cells in culture and *in vivo* studies. In the field of integrin targeting, most work has been in the field of non-therapeutic characterisation of integrin depletion through the use of antisense DNA or RNA oligonucleotides. Phosphorothioate DNA oligonucleotides have been used to great apparent effect in quail neural crest cells, using 18-21 mers coding for antisense α1 or β1 subunits (Lallier and Bonner-Fraser, 1993). Treatment of cells in culture with 0.02-50μM oligonucleotides gave a dose dependent reduction in both adhesion to laminin and fibronectin (up to 70%) and of protein levels (detected using immunoprecipitation of biotinylated surface integrins), up to 90% after a 4-6 hour incubation of cells with phosphorothioate oligonucleotides. Cells regained the ability to bind to substrata 8 to 16 hours after treatment.

Many other studies have been carried out using antisense RNA, particularly against the α2 subunit (Keely *et al.*, 1995; Riikonen *et al.*, 1995a; Riikonen *et al.*, 1995b). These studies all used partial or total (1.1kb to the entire 4.5kb) antisense cDNA constructs coding for the 5' end of the cDNA ligated into either integrating or episomal mammalian expression vectors in an antisense orientation. Keely *et al.* (1995) demonstrated a decrease (30-70%) in surface expression (and apparently protein levels using Western blots although data is not shown) of the α2 subunit via flow cytometry in isolated antisense treated human melanoma clones, although α2

mRNA levels in these clones appeared similar to wild type expression. Riikonen *et al.* (1995a, 1995b) used a total antisense RNA against human osteosarcoma cell lines and produced reductions in both α2 protein (data yet again not shown) and mRNA levels, where a decrease in expression of up to 50% was observed in selected clones. This study however fails to produce a clear link between antisense RNA expression and α2 downregulation. Other studies have also shown conflicting data on antisense effects upon mRNA levels, which can possibly be explained by the varied nature of any potential antisense effect and that it may exert an antisense effect which does not lead to the degradation of its target mRNA.

Antisense RNA studies of β1 integrin subunit downregulation (Koivisto *et al.*, 1994) have used a 1.1kb cDNA fragment of the 3' end of human β1 (1227-2357bp) ligated into the integrating expression vector pcDNA1neo. This study failed to produce any apparent decrease in surface expression of the β1 subunit in human osteosarcoma cells, however it specifically decreased total β1 protein and expression in intracellular β1 precursor pools resulting in an increased maturation rate of the β1 integrin subunit. Steady-state surface levels in this study were therefore not affected due to cellular reserves of receptor, although total levels of β1 subunits were reduced.

None of these antisense RNA studies have examined the possibility of non specific effects occurring from the use of long antisense oligonucleotides. Additionally, most studies have described the effects of antisense cDNA vectors by selection of individual clones after antibiotic selection. Great care must be taken in this course of events that any downregulation of integrin expression is due to a specific antisense effect rather than simply natural variation in expression.

1.5.3. Antiadhesive therapy of integrins

As explained in section 1.2.2, proteins of the extracellular matrix act as ligands for integrins by the presentation of specific amino acid sequences, such as arginine-glycine-aspartic acid (RGD) (Summarised in table 1.3). Synthetic peptides of RGD or peptide fragments from ECM proteins can compete with natural ECM ligands and will inhibit adhesion and spreading of many cell types to substrates coated with adhesion proteins containing an RGD motif (Pierschbacher and Ruoslahti 1984). Additionally, soluble RGD containing peptides have been found to inhibit human melanoma cell invasion through amniotic basement membrane *in vitro* (Gehlsen *et al.,* 1988) and in murine models of experimental metastasis *in vivo* (Humphries *et al.,* 1986). YIGSR peptides against laminin have also shown this ability in similar models (Iwamoto *et al.,* 1987). The inhibitory effect of these peptides can be additionally increased by the use of polymeric peptides containing repeating units of the active sequence (Saiki *et al.,* 1989).

Although monomeric and polymeric soluble peptides will inhibit integrin functions, their stability, potency and affinity for integrins is low (Pierschbacher and Ruoslahti 1984). The discovery of the importance of focal adhesive contacts and flexible nature of ligand binding sites helps to explain that conformational elements play a significant part in ligand/receptor affinity. A family of small proteins isolated from the venom of *Crotalidiae* and *Viperidae* snake species and termed "disintegrins" (Gould *et al.,* 1990) have been shown to contain RGD or KGD sequences and have high affinity (1000-2000 times linear RGD; Williams, 1992) for integrins. These proteins have shown to be potent inhibitors of platelet aggregation (Huang *et al.,* 1987), thrombotic disease (Gould *et al.,* 1990) and experimental metastasis models of

melanoma cells (Trikha *et al.,* 1994). Their lack of specificity for integrins and potential for antigenicity however have limited the potential use of disintegrins to experimental aids.

Recent studies have used natural forms of ECM proteins with very high integrin affinity and low toxicity which could potentially be used in anti-melanoma therapy (Morla *et al.,* 1994). Multimers of fibronectin, created by induction of spontaneous disulphide crosslinking using a fragment type-III repeat of the ECM protein produces a high molecular weight "superfibronectin" resembling *in vivo* matrix fibrils and having greatly enhanced adhesive properties although solubility is poor.

1.5.4. Integrins as targets for drug therapy

Studies of pathways for adenovirus endocytosis into host cells have shown that attachment and internalistaion of the virus is mediated by interactions with integrins. Adenovirus have been found to express five RGD motifs upon a penton base of the virus fibre protein (Wickham *et al.,* 1993). Antibodies against αvβ3 and αvβ5 block internalisation of this virus but not attachment. Further studies have shown that interactions between this RGD motif and αvβ5 (and to a lesser extent αvβ3) are necessary for virus internalisation in a receptor mediated manner (Wickham *et al.,* 1994). This novel biological role for integrins has interesting implications for delivery of not only engineered adenovirus-mediated gene transfer but also for the targeting of drugs. RGD motifs of the adenovirus penton base have been replaced by the peptide motif EILDVPST which mediates binding to α4β1 (Wickham *et al.,* 1995). Further studies should indicate the potential of this active motif replacement upon adenovirus targeting to specific integrins (and therefore delivery to specific cells).

An integrin-specific targeting technique has been used by Smith *et al.* (1995), who have grafted the complementary determining region of a β3 specific antibody into the epidermal growth factor module of human tissue type plasminogen activator (t-PA). The resulting molecule binds to platelet integrin αIIbβ3 with nanomolar affinity and retains full enzymatic activity and may be highly useful as its thrombolytic activity is more actively targeted to platelet rich arterial thrombi that lead to acute myocardial infarction.

1.6. Aims and Objectives

It is clear that integrin αvβ3 plays a unique role in the progression of human malignant melanoma. Although many other integrins undoubtedly play a vital role in melanoma dynamics, αvβ3 is a particularly attractive target for integrin therapy due to its de-novo expression upon vertically migrating primary melanomas (Albelda *et al.*, 1990) and host of recently discovered actions upon invading melanoma such as angiogenesis and control of apoptosis.

As a parallel model to the involvement of β3 integrins in human melanoma, the role of integrin αIIbβ3 has been carefully examined in the B16a murine melanoma system (Chen *et al.*, 1992b). There is no evidence for the existence of integrin αIIbβ3 expression on the surface of human melanoma cells, however, expression seems to parallel the relationship between αvβ3 levels and metastatic potential (Chang *et al.*, 1992). A murine model for melanoma metastasis is an attractive prospect due to this laboratory groups' experience with the B16 murine cell line and its use *in vivo* with C57 mice.

Neither murine integrin subunit has been fully cloned and characterised at cDNA level. Chen *et al.* (1992b) have generated αIIb and β3 integrin sequence fragments (423bp and 711bp respectively) through reverse transcription polymerase chain reaction (RT PCR) with degenerate PCR primers to potentially homologous human sequences. Further characterisation has been carried out by Cieutat *et al.* (1993) who have cloned further portions of the murine β3 integrin subunit from murine kidney cells using RT PCR.

The initial aim of this project is to fully characterise these integrin subunits by cloning cDNA sequences for both αIIb and β3 subunits from B16a cells. This will be accomplished by screening a λZAPII (Stratagene) phage-based cDNA library of B16a cells with integrin-specific probes generated from RT PCR of B16a mRNA. Clones obtained using this method will be useful in the characterisation of integrin homology between species and identification of active homologous residues within integrin subunits.

They will be additionally useful in two separate studies to examine the possibility of using the integrin β3 subunit as a target for melanoma gene therapy. Firstly, antisensed (reversed) portions of the β3 integrin cDNA will be cloned into the mammalian expression vector pcDNA3 - a potent mammalian expression system driven by the cytomegalovirus (CMV) promoter. This non-viral vector based expression system is simple to purify and transfect and allows analysis of cell transfection in both transient and stable systems (see below).

A number of different sized antisense fragments will be cloned to ascertain the effect of antisense fragment size upon integrin expression. These vectors will be

transfected into B16a cells using electroporation and effects upon β3 surface expression will be examined using fluorescence activated cell sorting (FACS) analysis with a specific β3 monoclonal antibody.

Studies will be carried out, both in transient expression systems (24 to 96 hours after transfection) and in selected cell populations transfected with antisense vectors and selected for stable antisense expression using the geneticin (G418) antibiotic marker expressed by pcDNA3. Effects of antisense therapy will also be examined using a range of *in vitro* assays designed to give an indication of metastatic potential such as static adhesion, spreading, and invasion on a variety of ECM proteins.

A second approach will be the competitive inhibition of active αvβ3 heterodimers present on the surface of human melanoma cell-lines such as A375 cells using murine β3 subunits carrying inactivating point mutations. Mutation of functional cloned murine β3 cDNA, such as at position D119 or equivalent in the murine sequence (discussed in section 1.2.3) will enable the integrin subunit to form heterodimer complexes with specific α subunits but render the complex incapable of binding ligand and activating secondary signalling pathways. Mutated murine β3 integrin cDNA will then be ligated into mammalian expression vector pcDNA3 and transfected into A375 human melanoma cells using electroporation. The degree of competitive integrin inhibition will be examined using a range of *in vitro* tumorigenicity assays.

Human melanoma cells will be useful in these assays as expression of mutated murine β3 subunit will be distinct from that of endogenous β3 using specific murine monoclonal antibodies which do not cross react with human β3 using FACS analysis.

Chapter Two: Materials and Methods

2.1. Bacterial strains

General cloning procedures using pBluescript, and λZap II plaque screening were performed using the host strain *E. coli* XL1-Blue MRF' (Stratagene). Excision of pBluescript from λZap II plaques was carried out with the *E. coli* strain SOLR (Stratagene). Cloning procedures using the mammalian expression vector pcDNA3 (Invitrogen) were performed using the host strain *E. coli* TOP10F' (Invitrogen). Cloning procedures using the expression vector CDM8 (Invitrogen, obtained from Dr J. C. Loftus section 2.3) were carried out with the *E. coli* host strain MC1061/P3 (Invitrogen). The host strain used for pRSV*lac*Z was *E. coli* XL1-Blue MRF'. Bacterial growth media and other solutions are defined in appendix C. Growth media plates were produced by adding 15% Bacto Agar (Difco) to the media of choice before autoclaving, allowing the solution to cool to 55°C before addition of antibiotics (see section 2.5) and pouring into 90mm polystyrene petri dishes.

2.2. Plasmid vectors

General cloning procedures were carried out using the plasmid vector pBluescript pSK(-) (Strategene). Mammalian expression experiments were all carried out using the mammalian expression vector pcDNA3 (Invitrogen), derived from the human cytomegalovirus (CMV) major intermediate early promoter/enhancer region (illustrated by figure 2.1, below). Selection of stable transformants was carried out using the neomycin resistance marker as described in section 2.28.3. Control

expression studies were carried out using the mammalian expression vector pRSV*lac*Z obtained with thanks from Dr D. Ogllvie (Zeneca Pharmaceuticals, Alderley Edge, Cheshire, U.K.). This is a 7.8kb reporter plasmid based on the Rous Sarcoma Virus long terminal repeat (RSV LTR) promoter and driving expression of a 3.1kb cDNA insert for the β-galactosidase enzyme, used in assays to examine the efficiency of cell transfection (section 2.28.2).

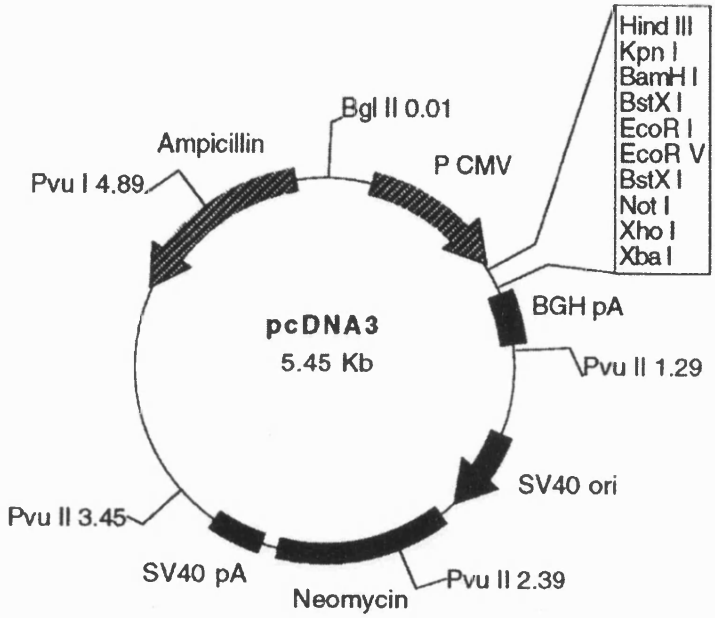

Fig 2.1 Plasmid map of mammalian expression vector pcDNA3. Abbreviations, P CMV CMV promoter, BGH pA bovine growth hormone polyadenylation signal, SV40 ori SV40 promoter and origin for transient episomal replication in cells expressing SV40 large T antigen. The boxed region represents endonuclease restriction sites within the multicloning site (in order).

2.3. cDNA constructs

The cDNA for a wild-type human integrin subunit β3, CD3A, and a mutant β3 clone CD3A D119A were obtained with thanks from Dr Joseph C. Loftus, Dept of Vascular Biology, Scripps Research Institute, La Jolla, CA, USA. Both inserts were cloned into the mammalian expression vector CDM8 (Invitrogen) at a *BstX* I

endonuclease restriction site. The entire 3.9kb insert using either clone could be removed as an *Xba* I restriction fragment (Fig 2.2 below). The cDNA clone for wild-type human integrin subunit αv, VnRα, was obtained from Dr. J. C. Loftus as a ~4kb insert cloned into the *EcoR* I site of pBluescript pSK-.

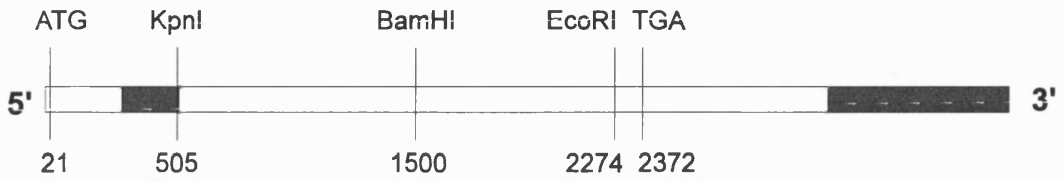

Fig 2.2 Diagram showing the human β3 integrin subunit cDNA clone obtained from Dr. J. C. Loftus. Endonuclease restriction sites of interest are marked with corresponding nucleotide positions. The shaded area at the 5' end of the cDNA (position 327-513) shows the position of the ligand binding site. The ATG site at position 21 indicates the start codon while the TGA site at position 2372 indicates the stop codon. The shaded area at the 3' end of the cDNA (3170-3900) indicates an untranslated region of unknown nucleotide sequence. The map of this cDNA was obtained using the MAP software as detailed in section 2.16 and is based on that described by Fitzgerald *et al.* (1986).

2.4. Preparation of electrocompetent *E. coli* host strains.

An overnight starter culture of *E. coli* XL-1 Blue, *E. coli* TOP10F' or *E. coli* MC1061/P3 cells was diluted 1:100 and grown to an OD_{600} of 0.5-1.0 in 500ml LB medium. The cells were chilled briefly on ice and centrifuged at 4000*g* for 15 minutes at 4°C using a Beckman J2-MC centrifuge. The ionic strength of the suspension was reduced by washing the cells in 500 ml ice cold sterile water, followed by 250 ml of sterile water, then 10 ml of sterile ice cold 10% glycerol, and finally resuspending in 0.5-1 ml of 10% glycerol. The ice-cold cell suspension was dispensed into 40µl aliquots in sterile microfuge tubes and snap-frozen in cardice/methanol. The electrocompetent cells were stored at -70°C until required.

2.5. Transformation of *E. coli* cells using electroporation.

Electroporation of all bacterial cells was carried out using a modified protocol to that described by Dower et. al (1988). Concentrated electrocompetent cells were thawed slowly on ice. Chilled recombinant plasmid DNA (up to 1µg in water) was added, and the cell mix was pipetted into a sterile pre-chilled 0.2cm electroporation cuvette (Bio-Rad Laboratories, Richmond, CA). The cuvette was placed in the pre-chilled cuvette carrier of a Gene Pulser and Pulse Controller (Bio-Rad) and subjected to a single 2.5kV pulse, capacitance and resistance of the power supply having been set to 25µFarads and 200Ω, respectively, to produce a nominal time constant for the capacitor discharge of ~5ms. Following electroporation, cells were allowed to recover in 1 ml SOC medium at 37°C with shaking for 1 hour (to allow expression of plasmid-coded antibiotic resistance). Transformed cells were selected by spreading onto L-agar plates containing ampicillin (50µg/ml or 30µg/ml for MC1061/P3 cells) and tetracycline (12.5 µg/ml or 7.5µg/ml for MC1061/P3 cells).

Transformations using *E. coli* XL1 Blue with pBluescript were plated onto L-agar plates surface coated with 40 µl X-gal (Melford Laboratories, 20 mg/ml in DMF) and 4 µl 0.84M IPTG. After growing for 18 hours at 37°C, cells containing recircularised pBluescript plasmids appeared as blue colonies, recombinants grew as white colonies. From each transformation, several white colonies (or several random colonies for pcDNA3 and MC1061/P3 transformations) were picked with a sterile wire and grown overnight in LB broth containing ampicillin (50µg/ml) and tetracycline (12.5µg/ml). Plasmid DNA was recovered by miniprep (see section 2.6.) and analysed by restriction endonuclease digestion.

2.6. Small scale preparation of bacterial plasmids (minipreps).

Small scale preparation of plasmids was carried out using an alkali lysis method based upon the methods of Birnboim and Doly (1979) and Ish-Horowicz and Burke (1981) as described in Molecular Cloning (Sambrook, J., Frisch, E.F. and Maniatis, T. Cold Spring Harbor Laboratory Press, 1989). Briefly, 1.5ml of an overnight culture of bacterial host was centrifuged at 10,000*g* for 1 minute. Pellets of cells were resuspended into 100µl solution I (for this and other solutions see appendix C). Cells were lysed by addition of 200µl solution II, mixed gently by inversion and incubated on ice for 10 minutes. 150µl solution III was added and mixed by vortexing before incubation on ice for 5 minutes. The reaction was centrifuged at 12,000*g* for 5 minutes at 4°C and the supernatant transferred to a clean tube.

Extraction of DNA from the supernatant was carried out using an equal volume of phenol:chloroform (Amresco Ltd) to precipitate polluting proteins. The upper aqueous layer was transferred to a clean tube and contaminating phenol removed using an equal volume of chloroform/isoamyl alcohol (24/1, Amresco Ltd). DNA was then precipitated using ethanol as described in section 2.10 and resuspended in 50µl TE buffer supplemented with 20µg/ml RNase.

2.7. Large scale preparation of bacterial plasmids (maxipreps).

Large scale plasmid preparation was carried out with a Qiagen Maxiprep Kit (Qiagen, Hilden, Germany) in accordance with manufacturers' protocols. This modified alkaline lysis method plus an anion exchange resin column purification step routinely produced approximately 500µg of ultrapure pcDNA3 plasmid from 300ml L Broth cultures of *E. coli.* TOP10F'.

2.8. Spectrophotomeric determination of nucleic acid concentration.

For quantification of aqueous solutions of DNA or RNA, spectrophotomeric readings were taken at 260nm and 280nm using 1ml matched quartz cuvettes in a Specronic 601 spectrophotometer (Milton Roy). An OD of 1 at 260nm corresponds to a solution at 50μg/ml for double stranded DNA and 39μg/ml for single stranded DNA and RNA. Contaminating phenol and protein absorbs at 280nm. Nucleic acid solutions with a 260nm:280nm absorbency ratio of less than 1.8 were considered too impure for routine use.

2.9. Digestion of DNA with restriction endonucleases.

DNA restrictions were performed using New England Biolab (NEB) restriction enzymes and buffers, in accordance with manufacturer's instructions. For complete plasmid digestion, reaction mixtures were allowed to incubate at 37°C for 1 hour. For digestion with *Pvu I*, mixtures were allowed to incubate at 37°C overnight in the presence of 50mM KCl. Standard endonuclease restrictions, used in size analysis and cloning, were carried out using 1μg DNA in a 10μl total reaction mix volume. Large-scale endonuclease restriction of plasmids for mammalian cell transfection was carried out using 20μg plasmid DNA and subsequently purified by phenol/chloroform extraction (section 2.6) before use.

2.10. Concentration of DNA by ethanol precipitation

DNA was precipitated from aqueous solutions by the addition of 3M sodium acetate pH 5.2 to a final concentration of 0.3M, followed by two volumes of ethanol at -20°C. The solution was vortexed well and allowed to precipitate at -70°C for 15

minutes. A pellet of DNA was recovered by centrifugation at 12,000*g* using a Jouan A14 centrifuge at 4°C for 30 minutes. Ethanol was aspirated off and the pellet washed with 70% ethanol at 4°C before drying the pellet at 37°C for 20 minutes. DNA was finally resuspended in TE buffer.

2.11. Horizontal agarose gel electrophoresis

Agarose gels were cast and run in Bio-Rad DNA sub-cells. Ultrapure agarose (Bethesda Research Laboratories) was dissolved in 0.5x TBE buffer at 100°C. The solution was allowed to cool to approximately 60°C, and 1mg/ml ethidium bromide (Sigma) was added to a final concentration of 0.5µg/ml. The gel was poured and allowed to set at room temperature for 45 minutes. Once set, gels were submersed in 0.5x TBE. DNA samples were mixed with 0.2 vol 5x DNA loading buffer (appendix C) and electrophoresis was carried out at 70-200V until the tracking dye reached the end of the gel. DNA bands were visualised on a UV light box (Mighty Bright, Hoefer). Photographs were taken using Polaroid 655 film in a Polaroid MP4 camera.

2.12. Denaturing agarose electrophoresis

In order to maintain denaturing conditions during electrophoresis of RNA samples, denaturing formaldehyde/agarose gels were used. All procedures involving formaldehyde and formamide were carried out in a chemical hood, in RNase free conditions (see below). To 30 ml of a molten 1.28% agarose solution (DEPC treated), 9.4 ml of 5x formaldehyde gel-running buffer was added (appendix C) with 8.6 ml of 12.3M formaldehyde. Gels were quickly cast, and allowed to set for at least 30 minutes at room temperature.

RNA samples for electrophoresis were prepared as follows. Five to ten micrograms of RNA in 4.5µl water were added to 2µl 5x formaldehyde running buffer, 3.5µl formaldehyde and 10µl formamide and heated to 65°C for 15 minutes then chilled on ice. Two microlitres of formaldehyde gel-loading buffer (50% glycerol, 1mM EDTA, 0.25% bromophenol blue), and 1µl of ethidium bromide 1mg/ml was added, and the samples electrophoresed at 100V. Gels were viewed on a UV light box and photographed if required.

2.12.1 Maintenance of RNase free conditions

In order to protect RNA samples from degradation by contaminating RNase enzymes, all RNA manipulation techniques were carried out in RNase-free conditions. All water, glassware and salt solutions were treated with diethyl pyrocarbonate (DEPC) to inactivate RNase's. Briefly, solutions (except Tris solutions which DEPC reacts with) were treated with 0.1% DEPC overnight at 37°C before autoclaving (appendix C). Tris solutions were made with sterile DEPC treated water Glassware was soaked in DEPC treated water overnight before autoclaving. Laboratory plasticware (such as electrophoresis kit) was rinsed in chloroform before use.

2.13. Purification of DNA using Geneclean

DNA was purified from agarose gels by adsorption of DNA to silica matrix using the Geneclean II DNA purification system (Bio-101, La Jolla, CA, USA). Following agarose gel electrophoresis, the section(s) of the gel containing restriction fragment(s) of interest were excised and purified into TE buffer or water as detailed in the manufacturers' protocol.

2.14. Ligation of DNA fragments into plasmid vectors

Plasmid vectors (pBluescript pSK-, pcDNA3 or pcDM8) were linearised by restriction at one or two sites within the vector polylinker as described in section 2.5. Vectors linearised with a single enzyme were subsequently dephosphorylated with calf intestinal alkaline phosphatase (CIAP, New England Biolabs) in accordance with manufacturers' protocol to prevent re-ligation of linearised vector. Enzymes used were subsequently denatured (as specified in the protocols) and 1μg vector run on a horizontal TBE agarose gel and recovered using Geneclean. Fragments to be subcloned were similarly recovered to ensure purity. The DNA samples were mixed together, with a five fold molar excess of insert DNA over vector and ligated with T4 DNA ligase (NEB) in accordance with the manufacturers' protocol. Mixtures were incubated at 16°C for four hours in the case of sticky end ligations, or at 16°C overnight for blunt end ligations. Reaction mixtures were purified using Geneclean before transformation of host cells by electroporation.

2.15. Nucleotide sequencing

Nucleotide sequencing was performed by the dideoxy mediated chain termination method of Sanger *et al.,* (1977). Sequencing reactions were performed using the Sequenase II system (United States Biochemical), using double-stranded template DNA. Subsequent electrophoresis was performed using the Bio-Rad Sequi-Gen system (21cm x 40cm x 0.04cm), and Severn Biotech acrylamide/bis acrylamide sequencing solution (6% w/v acrylamide ratio 19:1, 7M urea, 1x TBE) in accordance with manufacturers' protocols.

2.15.1. Preparation of double-stranded template DNA

Double-stranded plasmid DNA (1µg) was denatured in 0.2M NaOH, 0.2mM EDTA at 37°C for 30 minutes, then precipitated with ethanol as described in section 2.10 before resuspending in 7µl sterile water.

2.15.2. Sequencing reactions

Using double-stranded templates, approximately 5µg of DNA was used per sequencing reaction with 0.5pmol of sequence specific primer. Template DNA was sequenced using the Sequenase (version 2.0) kit according to the manufacturers' instructions, incorporating [^{35}S dATP] 1000-1500Ci/mmol, 12.5mCi/ml (NEN). Sequencing gels were subsequently soaked in 10% acetic acid/15% methanol for 15 minutes follow by drying for 2 hours at 80°C using a Bio Rad 583 gel dryer in accordance with manufacturers instructions.

2.16. Analysis of Nucleotide sequence.

DNA sequence analysis was performed using the GCG (University of Wisconsin Genetics Computer Group) package at the SERC Seqnet computing facility at Daresbury, UK. Genbank database searching was performed using the SEQED, FASTA and TFASTA software. Restriction mapping of sequences was carried out using MAP software.

2.17. Mammalian Cells lines

The B16a murine melanoma cell line were a kind gift of Dr K. V. Honn, Dept of Radiation Oncology, Wayne State University, Detroit, and were obtained as solid

lung tumours from C57 black mice (obtained from Dr David Hayes, Wellcome PLC, Beckenham, Kent). Parental human melanoma cell-lines A375P (passage 182) and a more metastatic sub-population, A375MM (passage 21) were obtained with thanks from Dr A. Fabra, Cancer Research Institute, Hospital Duran I Reynals, Barcelona, Spain. The SV40 transformed monkey kidney cell line, COS7 was obtained from the European Collection of Animal Cell Cultures (ECACC, Porton Down, Salisbury, UK)

2.18. Tissue culture media and conditions

All cell lines were cultured in Eagles' Minimal Essential Medium (MEM) with Earles' salts, supplemented with 10% foetal calf serum, 200μM L-glutamine, 5IU/ml penicillin and 5IU/ml streptomycin and 1x non essential amino acids. All reagents were purchased from Gibco Life Sciences. Cells were maintained in an LEEC anhydric incubator at 37°C in an atmosphere of 95% air/ 5% CO_2 and a humidified atmosphere. Cells were grown in Falcon polystyrene flasks (Beckton and Dickinson) or 6-, 24- and 96-well plates (Nunc). Adhesion assays were carried out using 96-well flexible assay plates (Falcon Microtest III, N° 3912, Beckton Dickinson)

2.18.1. Cell line maintenance and subculture

All cell lines were routinely subcultured from adherent semi-confluent monolayers of cells every 2-3 days, except COS7 cells which were subcultured every 4 days. Subculture was carried out by washing twice with calcium and magnesium free phosphate buffered saline (PBS, Oxoid), and adding a sufficient volume of trypsin/EDTA (Gibco) to cover the cells. Flasks were incubated at 37°C for 5 minutes or until total detachment had taken place MEM (~20ml) was added to detached cells which were transferred to a 50ml centrifuge tube (Falcon) and pelleted at 200*g* for 10

minutes using a Jouan B3.11 centrifuge. The pellet was resuspended into 5ml media and 0.5ml was re-seeded into a fresh flask.

Where necessary, viable cell numbers were evaluated using a grid haemocytometer, visualising cells on an M40 inverted biological microscope (Wiold Heerbrugg Ltd) after staining with 0.1% w/v trypan blue (Sigma) in PBS as described in the Sigma biochemicals catalogue (1996, p1702-3).

2.18.2. Dispersion of B16a cells from solid lung tumours

Tumours of approximately 2g size were minced with a sterile razor blade and pieces transferred to a sterile 50ml centrifuge tube (Corning). 25 ml of tumour dispersion solution (appendix C) was added to this tube and incubated with shaking at 37°C for 15 minutes after which it was strained through two sterile pieces of cheesecloth and discarded. A further 25ml of dispersion solution was added to the tube and incubated shaking at 37°C for 45 minutes. This fraction was collected after straining through cheesecloth, and pooled with a second fraction collected after a third, 60 minute incubation with a further 25ml dispersion solution. The pooled fraction was centrifuged at 200*g* for 7 minutes, and washed twice with 20ml MEM before resuspending the final cell pellet in 2ml MEM. This was then used to seed a 75cm^2 Falcon flask.

2.18.3. Cell storage and recovery

Cells were stored in 2ml cryogenic ampoules (Falcon) in the vapour phase of a Union Carbide LR-40 liquid nitrogen refrigerator at approximately -148°C. Cells were prepared for storage by trypsinising semi-confluent flasks of cells (as described in section 2.10.1.), washing once with MEM and resuspending cells in 1ml MEM with 10% DMSO (Aldrich, spectophotometric grade) as a cryoprotectant. Cells were

slowly frozen in a BF6 biological freezer unit plug (Union Carbide) inserted into a Union Carbide LR-33 liquid nitrogen refrigerator.

Recovery of cells was carried out by rapidly defrosting cryotubes at 37°C, followed by washing cells twice in 20ml MEM and seeding a 175cm^2 tissue culture flask.

2.19. Preparation of a cDNA library

2.19.1. mRNA purification from B16a cells

Polyadenylated RNA (or messenger RNA, mRNA) was obtained from B16a cells using a "Quickprep" mRNA Purification Kit (Pharmacia) in accordance with manufacturers' protocol. All preparations were carried out in RNase-free conditions as described in section 2.12.1. Each isolation was carried out with 1x10^7 cells, trypsinised from a semi-confluent 175cm^2 tissue culture flask and centrifuged at 200*g* for 10 minutes before extraction. To ensure greater purity of mRNA, eluate from the first purification step was applied to a second oligo (dT)-cellulose column as described in the manufacturers' protocol. Purity (from polluting ribosomal RNA bands), and size distribution of mRNA was ascertained by visualisation of sample using denaturing agarose electrophoresis as described in section 2.12.

2.19.2. cDNA synthesis by reverse transcription

2μg of polyadenylated RNA was reverse transcribed using a cDNA synthesis kit (Pharmacia) in accordance with manufacturers' protocols. Briefly, 20μl of denatured mRNA was added to a first-strand reaction mix containing 5μg oligo(dT)$_{12\text{-}18}$ primer and 60 units of Moloney Murine Leukaemia Virus (MMLV) reverse transcriptase. The mix was incubated at 37°C for 1 hour. This was then added to a second-strand

reaction mix containing 1 unit RNase H and 25 units DNA polymerase I and incubated at 12°C for 1 hour then 22°C for 1 hour. Finally, 5 units of Klenow fragment were added to blunt end any double stranded cDNA from the reaction.

2.19.3. *Ligation of EcoRI linkers*

Linker ligation to newly synthesised cDNA was carried out using *EcoR* I linkers supplied with the cDNA synthesis kit (Pharmacia).

AATTCGCGGCCGC

GCGCCGGCGp

The "p" designates a dephosphorlyated blunt end, while the other end of the linker is a non-dephosphorylated *Eco* RI overhang. The linker also contains an internal *Not* I restriction site. Briefly, cDNA from the procedure described above was column purified and the eluate (100µl) was added to 2ng *EcoR* I linkers, 1µl 100mM ATP and 3µl DNA ligase (3 units/µl). The mixture was incubated at 12°C overnight.

2.20. Preparation of λZAP II library

For cloning purposes the Stratagene system, Lambda Zap II was used. This system has a standard lambda phage library construction plus the pBluescript phagemid cloning vector, to allow rapid *in vivo* excision of plasmid with cloned insert.

2.20.1. Ligation of cDNA into λZAP II arms

To approximately 100ng cDNA (calculated from initial mRNA in reaction), 1µl (1µg) λZAP II *EcoR* I/CIAP arms, 1µl 10x ligase buffer, 1µl 100mM ATP, 1µl T4 DNA ligase (5 units/µl) and sterile water to 10µl was added. The mixture was incubated at 12°C overnight. Parallel reactions with 0.5x and 2x cDNA in the reaction mix were also carried out to maximise efficiency of ligation.

2.20.2. Packaging into λZAP II

Packaging was carried out according to manufacturer's instructions, using Gigapack II packaging extracts (Stratagene). Following ligation, 4µl of DNA was added to one melting 'freeze-thaw' extract. Sonic extract (15µl) was added and the tube contents and mixed by pipetting. Packaging was allowed to continue for 2 hours at 22°C then stopped with 500µl of SM and 20µl chloroform. The library was stored at 4°C.

2.21. Screening λZapII cDNA library

Lambda Zap II libraries were screened from plaque lifts of 90mm petri dishes using 82mm Hybond N+ Nylon membrane discs (Amersham) as described below.

2.21.1. Titration of the cDNA the library

This was carried out as detailed in the Lambda Zap II Cloning Kit protocol (Stratagene). Briefly, the *E. coli* strain XL1-Blue MRF' was grown overnight (30°C shaking) in LB/10mM $MgSO_4$/0.2% maltose. Cells were spun down at 2,000*g* for 10 minutes, resuspended in 10mM $MgSO_4$ to an OD_{600} of 0.5 and divided into aliquots of 200µl. To each aliquot, 1µl packaged phage suspension (of a 1:1, 1:10, 1:100 or 1:1000 dilution in SM buffer) was added, and incubated for 15 min at 37°C to allow phage to attach to cells. Each mixture was then added to 3ml of molten top NZY agar (with 0.7% agarose) at 48°C and poured onto the surface of a pre-warmed and dried NZY plate. Plates were incubated overnight at 37°C. Number of plaque forming units (pfu) was subsequently counted on each plate (if possible) and titre of the original solution calculated.

2.21.2. Plaque screening

DNA screening was carried out using a slightly modified protocol from that described in the Lambda Zap II Cloning Kit. Briefly, 99mm plates were plated with approximately 15,000 pfu as described in section 2.22.1 and incubated at 37°C for 8 hours. Plates were chilled at 4°C for two hours before transferring DNA. An 82mm Hybond N+ nylon membrane (Amersham) was placed over the surface of the plate, orientated by pricking through the filter using a syringe needle and allowed to transfer for 2 minutes. Membranes were then removed and placed colony side up onto three layers of 3MM paper soaked in denaturing solution for 7 minutes. This was then transferred to a pad of 3MM paper soaked in neutralising solution for 5 minutes. Finally, the filter was rinsed for 30 seconds in 2 x SSC buffer. A duplicate plate was produced by placing onto the plate for 5 minutes, marking for orientation using a syringe needle. Membranes were fixed by rinsing in 0.4M NaOH solution for 20 minutes. All membranes were stored at 4°C wrapped in clingfilm.

2.22. Preparation of oligonucleotides

Oligonucleotides used for PCR amplification of cDNA were synthesised by Dr. A. Wolstenholme (School of Biochemistry, University of Bath, U.K.). They were eluted from their synthesis columns using 1ml concentrated ammonia solution, drawn through the column using a 5ml syringe in 0.2ml aliquots every 20min. The resulting solution was transferred to a 1.5ml screw-capped microcentrifuge tube and placed into a glass universal bottle containing 0.5ml concentrated ammonia solution. This was incubated overnight in a water bath at 55°C, to remove the amino-protecting groups. The concentrated ammonia solution was removed by vacuum drying in a DNA

Speedvac (Savant) and the oligonucleotide pellet resuspended in 100µl sterile ddH_2O. Oligonucleotides were precipitated using ethanol as detailed in section 2.8 and the dried pellet resuspended in 1ml ddH_2O. Yield of oligonucleotide was calculated as described in section 2.2 and diluted accordingly. Typical yield was between 1-2mg.

2.23. Polymerase Chain Reaction (PCR) of cDNA probes for murine integrin αIIb and β3 subunits

cDNA, generated as explained in section 2.19 was used as a template for PCR using the GeneAmp PCR Core Reagent Kit (Perkin Elmer Cetus, Norwalk, CT) with settings and reagent concentrations as detailed in the manufacturers protocol. Briefly, 10x Buffer, 10mM dNTP's, 1µM oligonucleotide primers (described in section 2.22) and 2.5 units Amplitaq were combined into a "master mix" to which 1-4mM magnesium chloride and approximately 1-100ng template cDNA was added. The reaction was exposed to standard temperature cycling parameters of 94°C for 1 minute, 55°C for 1 minute and 72°C for 1 minute, repeated for 30 cycles using a Crocodile II temperature cycler (Appligene). This *Taq* DNA polymerase based protocol is based upon a method described by Saiki *et al.* (1985) and Mullis and Falonna (1987). Any bands obtained from this process were gel purified using Geneclean before ligation into cloning vectors.

2.24. Preparation of ^{32}P-labelled cDNA probes

PCR fragments of αIIb and β3 obtained as described in section 2.23 were recovered from a horizontal agarose gel using Geneclean. This DNA was used as a template for generation of an [α-^{32}P]dATP labelled probe using DNA polymerase

primed by random hexanucleotides. Approximately 25ng of purified DNA in 9µl water was added to 2µl random hexanucleotide mixture (Boehringer Mannheim), 3µl of a mixture of dTTP, dCTP and dGTP, all at 20 mM (Pharmacia), 5µl [α-^{32}P]dATP (3000 Ci/mmol, 10µCi/µl) (NEN) and 1µl (10 units) Klenow fragment of DNA polymerase (NEB). The reaction mixture was incubated at 37°C for 30 minutes and stopped by heating to 65°C for 5 minutes. Unincorporated nucleotides were removed by passing the final mixture through a Nuc-Trap column (Stratagene) in accordance with manufacturers' protocols. This method generates probes of very high specific activity 10^8-10^9 cpm/µg. Such high activity probes were used within a week of synthesis, as high energy α-^{32}P emissions can cause destruction of the molecular structure of the nucleotide sequence.

2.25. Hybridisation of labelled DNA probes to fixed nylon membranes

Hybond N+ Membranes (Amersham) for screening were hybridised and washed in accordance with manufacturers protocols. Briefly, fixed membranes were prehybridised in 25ml of 5x Denhardts' solution, supplemented with 0.5% SDS, 5x SSC and 0.5mg denatured sonicated salmon sperm DNA (Strategene) at 65°C for at least 1 hour. Labelled probe was prepared as described in section 2.24 and denatured at 100°C for 5 minutes. An aliquot of the labelling mix (5-20µl, dependant on age of the isotope) was then added to the membranes and allowed to hybridise at 65°C for 12 hours. After hybridisation, membranes were washed once with 50ml 2x SSC at 65°C for 15 minutes, once with 50ml 2x SSC, 0.1% SDS at 65°C for 30 minutes and once with 50ml 0.1x SSC, 0.1% SDS at 65°C for 10 minutes. Membranes were wrapped in clingfilm and developed as described in section 2.26.

2.26. Autoradiography

Hybridised nylon membranes from library screens were exposed to Kodak X-omat film for 12-24 hours in a light proof cassette with intensifying screens (Amersham) at -70°C. Dried sequencing gels were exposed to Kodak X-omat AR film for 24-48 hours at room temperature in a light-proof cassette. Hybridised nitrocellulose membranes from western blots were exposed to Kodak X-omat film for 1-30 minutes at room temperature. After exposure, film was developed using a Fuji RG II X-ray film processor in accordance with the manufacturers' protocol.

2.27. *In vivo* excision of pBluescript from λZAP II

Plaques of interest were isolated from plates using a fine pasteur pipette to core an agar plug. Phage from this plug was resuspended by adding 500µl SM buffer (see appendix C) and 20µl chloroform and incubated for 2 hours at 4°C. *In vivo* excision of pBluescript SK(-), containing clones of interest from phage suspensions was carried out using the ExAssist/SOLR excision system as described in the Lambda Zap II Cloning Kit protocol.

2.28. MTT assay for determination of cell number

Cell number determination, for use in growth, and survival assays was carried out using a modified MTT assay as described by Mosmann, (1983) and Arnould *et al.* (1990). Briefly, cells were seeded into 96-well plates at a desired density. After treatment or at regular time points for growth assays, media was removed by inversion and the cells washed twice with serum free MEM. 200µl of 1mg/ml solution of 1-

[4,5-dimethylthiazol-2-yl]-3,5-diphenylformazan (MTT formazan, Sigma) in complete MEM was added to each well and the plate was incubated at 37°C for 3 hours. MTT solution was carefully removed from the plates by gentle inversion and resultant crystals of formazan blue were solubilised with 200µl DMSO and agitation on an orbital mixer for 5 minutes. Cell number was calculated by reading optical density of wells (on a Titretek plate reader) at 540nm with a reference wavelength of 690nm.

2.28.1. Calibration of MTT assay

Calibration of this assay was carried out by seeding 96-well plates with a known number of cells, ranging from $1x10^3$ to $5x10^5$. Cells were allowed to adhere for 1 hour, followed by a standard MTT assay.

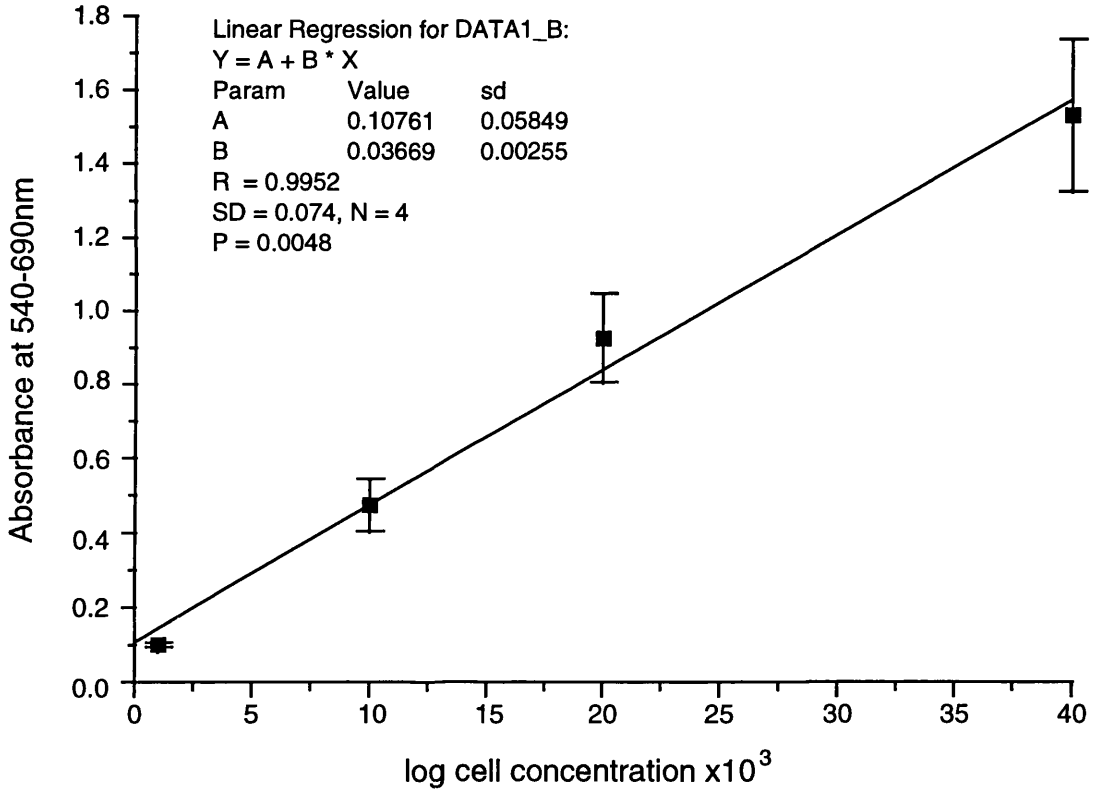

Fig 2.3 MTT assay showing the effect of B16a cell number upon mean absorbance of treated cells at lower absorbance values. Each point represents a mean absorbance value ± standard deviation of samples (n=8). This experiment is representative of two experiments.

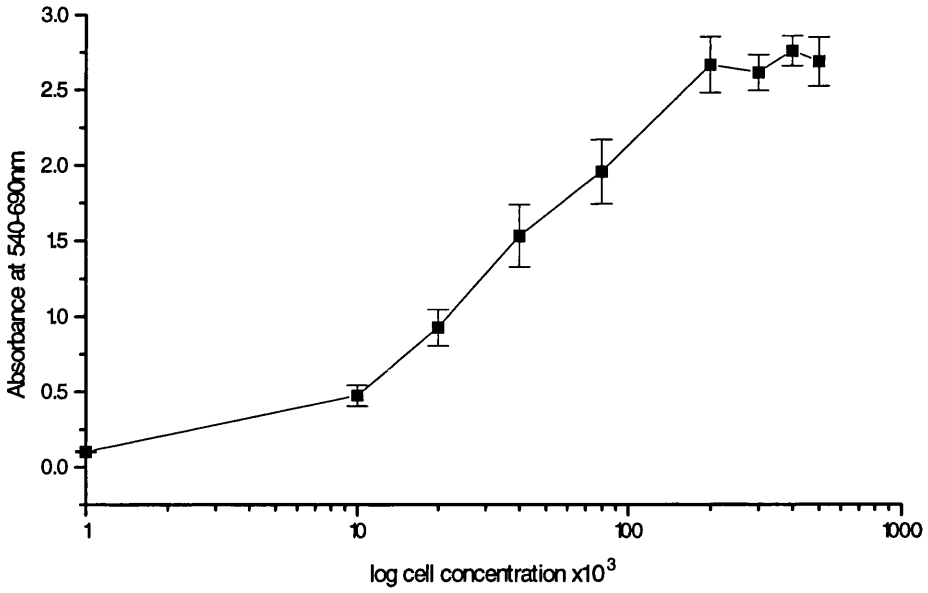

Fig 2.4 Effect of B16a cell number upon mean absorbance of treated cells over the whole range of cell concentrations tested (represented as a logarithmic scale). Each point represents a mean absorbance value ± standard deviation of samples (n=8). This experiment is representative of two experiments

Figure 2.3 indicates that a linear relationship between the number of cells and absorbance is obtainable up to ~$4x10^4$ B16a cells per well (or up to an absorbance of ~1.5). Figure 2.4 illustrates the limitations of the MTT assay at higher, saturating cell concentrations. Subsequent growth and viability assays were carried out upon tissue culture grade plastic with no added ECM substrate.

2.28.2. Optimisation of G418 treatment of cells using an MTT viablity assay

B16a cells were seeded at a density of $5x10^3$ cells per 96-well plate and allowed to adhere in full media for 4 hours before addition of 0-2 mg/ml of the antibiotic Geneticin (G418, Gibco). Cells were cultured under standard conditions for 3 days before a standard MTT assay was carried out to ascertain surviving cell numbers.

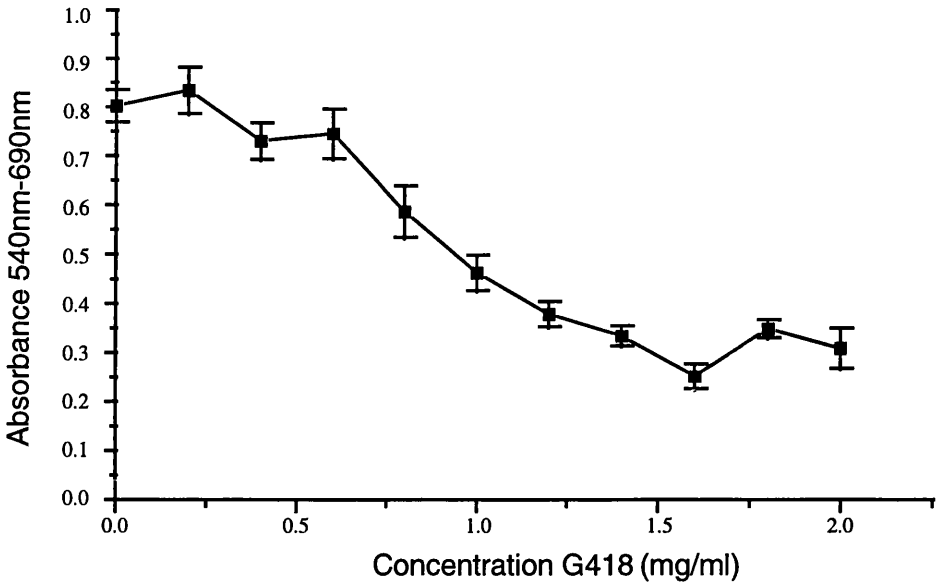

Fig 2.5 MTT assay showing the effect of G418 concentration upon growth of $5x10^3$ B16a cells after 3 days of treatment. Each point represents a mean absorbance value ± standard deviation of samples (n=8).

Figure 2.5 illustrates that the optimal G418 concentration for treatment of B16a cells is approximately 1.5 mg/ml or higher as this results in the greatest suppression of cell growth, as represented by the lowest MTT absorbance after three days incubation with G418.

2.29. Transfection of mammalian cells with DNA using electroporation

Transfection of B16a, A375 and COS7 cells with plasmid DNA was carried out using electroporation and protocols based on procedures described by Neumann *et al.* (1982) and Wong and Neumann (1982). Electroporation was additionally modified using lower voltage and higher capacitance settings as described by Chu *et al.* (1987). Cells were electroporated in a Bio Rad Gene Pulser connected to a Bio Rad Capacitance Extender using 4mm electroporation cuvettes (Bio Rad). Briefly, semi-confluent cells from $175cm^2$ tissue culture flasks were trypsinised and washed three

times with 20ml ice cold PBS. The contents of one 175cm^2 flask (approximately 5-10x10^6 cells/ml) was resuspended into 500µl ice cold PBS. Twenty micrograms of plasmid for transfection, generated by Qiagen maxi-preps (section 2.7) was added to this suspension as an aqueous solution (1µg/µl) and incubated on ice for 5 minutes. The mixture was transferred to a 4mm electroporation cuvette (Bio-Rad, pre-chilled) and electroporated at optimal transfection settings for the cell line used. After transfection, cuvettes were incubated at 4°C on ice for 20 minutes before transferral to tissue culture flasks. Plasmids used for stable transfection of cells were linearised and purified before electroporation as described in section 2.9.

2.29.1. Determination of efficiency of electroporation using FITC labelled dextran

Optimisation of electroporation settings was carried out by measuring cellular uptake of FITC labelled dextran (Sigma, average MW 71,200) in a protocol based on that described by Andreason and Evans (1989) and Graziadel (1991). Briefly, 50µl (of a 10mg/ml stock) FITC dextran was added to 1x10^6 cells in 500µl ice cold PBS and transfected using a standard electroporation protocol. Cells were seeded into 99cm^2 tissue culture dishes and incubated at 37°C for 4 hours. After this period, all cells (including non-adherent and dead cells) were removed by trypsination, washed, and resuspended into 50µl PBS and analysed for FITC fluorescence by FACS. Cell death was measured by labelling cells with 100ng/ml propidium iodide and measuring fluorescence of the same population of cells in the FL-2 region of fluorescence emission in a protocol based on that described by Sasaki *et al.* (1987). Refer to section 2.30 for details of FACS.

2.29.2. Determination of efficiency of electroporation using β galactosidase activity

A secondary method utilised to ascertain the efficiency of electroporation settings was transfection of a reporter vector, pRSV*lac*Z expressing the β-galactosidase enzyme (section 2.2). Efficiency of transfection was visualised by light microscopy following incubation with chromogenic substrate 5-bromo-4-chloro-3-indolyl-β-galactosidase (X-Gal) in a protocol based on that detailed by MacGregor *et al.* (1991). Briefly, 20μg of pRSV*lac*Z was transfected into $1x10^7$ cells by electroporation using optimised electroporation settings. Aliquots of transfected cells were seeded into $99cm^2$ tissue culture dishes and incubated at 37°C for 24-96 hours before being washed twice with PBS and fixed with 1% glutaraldehyde in PBS at 4°C for 5 minutes. Fixed cells were washed twice with PBS and overlaid with 10ml X-Gal solution (see appendix C) and incubated at 37°C overnight. After this period X-Gal solution was removed and cells washed twice with PBS before visualisation under an M40 inverted light microscope.

2.29.3. Selection of stable transfectants using geneticin (G418)

Selection of stable transfected cells was carried out with the antibiotic selection marker geneticin (G418, Gibco), in accordance with manufacturers' protocols. Briefly, cells were transfected with recombinant pcDNA3 vectors (section 2.2). Two days post-transfection, media was removed from cells and replaced with 1.5 mg/ml G418 in complete MEM (optimised in section 2.28.2). G418 media was replaced every 48 hours (or as necessary on initial treatment) and colonies were trypsinised once they had attained a sufficient size.

2.30. Adhesion assays of cells to ECM proteins

2.30.1. Coating surfaces with ECM proteins

Extracellular matrix proteins, fibronectin (1mg/ml solution, Sigma) and fibrinogen (Sigma) were used to coat tissue culture plasticware. Proteins for coating were diluted in PBS to 2-50μg/ml and 50μl of solutions added to 96-well plates, and incubated at 4°C overnight. Fibrinogen is insoluble at low temperatures, so solutions were made up with pre-warmed PBS and surfaces coated at 37°C for 90 minutes. Plates were subsequently washed twice by immersion in PBS and then treated with 200μl 0.1%w/v Bovine serum albumin (BSA, Sigma) solution in PBS and incubated at 37°C for 1 hour to prevent non-specific binding. Coated wells were washed twice with PBS before use.

2.30.2. Static cell adhesion assay to coated 96-well plates

Adhesion assays were carried using ECM protein coated Falcon MicroTest III flexible assay plates. Cells for testing were trypsinised from flasks and washed once with 20ml complete MEM before resuspended into 300μl complete MEM. Sodium chromate [^{51}Cr] (Amersham, CJS1) was used to label cells in a modified protocol to that described by Holden *et al.* (1973).

To 1ml stock ^{51}Cr, 110μl 10x Hanks buffered salt solution (HBSS, Gibco) was added to make isotonic. 100μl of this solution was added to cells and incubated at 37°C for 45 minutes, agitating every 10 minutes. Cells were washed 3 times in 1ml serum free MEM and a 100μl aliquot removed to determine cell number and viability. Cells were resuspended in serum free MEM at $2x10^5$ cells/ml and 50μl aliquots added to protein treated wells (8 repeats per point). Cells were incubated at 37°C for 30-120 minutes and non-adherent cells removed by slowly immersing titre plates in PBS

supplemented with cations (1mM Ca^{2+}/0.5mM Mg^{2+}) and gently tapping the underside of the plate. This was repeated and counts in each well taken by cutting up plates, placing wells into scintillation tubes and taking counts in a Gammamaster 1277 (Wallac). γ-Counts from coated wells were then compared to counts obtained by a parallel adhesion assay carried out in BSA treated wells, and a percent adhesion generated by comparison of adherent cell counts to counts obtained from 50µl initial labelled cell suspension.

2.30.3. Cell spreading assay upon coated surfaces

Six well-plates (Falcon) were coated with 200µl of 2µg/ml fibronectin as described. Cells were trypsinised from 175cm^2 tissue culture flasks and resuspended at 1x10^4 cells/ml in MEM. 1ml aliquots were transferred to wells and at regular time intervals from 0-120 minutes, medium was carefully removed, cells were washed once with PBS at 37°C and fixed with 1% formaldehyde (Sigma) in PBS. Morphology of cells was recorded by taking pictures of cells using an M40 inverted biological microscope.

2.31. Fluorescence activated cell sorting (FACS) of cells

2.31.1. Antibodies

Purified hamster anti-mouse IgG monoclonal antibody (mAb), Hmβ3, against the murine β3 integrin subunit was obtained from Pharmingen (Sorrento Valley Road, San Diego U.S.A.). Monoclonal mouse anti-human IgG1 antibody, Y2/51, against the human β3 integrin subunit was obtained from Dako (Glostrup, Denmark). Monoclonal mouse anti-human IgG1 antibody, P2W7, against the human αv integrin subunit was obtained as a kind gift of Dr. Ian Hart (ICRF, London). Fluorescein

isothiocyanate (FITC) conjugated mouse anti-hamster IgG monoclonal antibody cocktail (clones G70-204 and G94-56), specific for Hmβ3 was obtained from Pharmingen. R-phycoerythrin (RPE) conjugated $f(ab')_2$ fragment of goat anti-mouse immunoglobulins, specific for Y2/51 and P2W7 was obtained from Dako. Mouse IgG1 negative control was obtained from Dako.

2.31.2. Labelling cells for FACS analysis

Cells for analysis were detached by trypsinisation and allowed to recover in 20ml fresh MEM for 30 minutes at 37°C. Cells were counted as described and approximately $5x10^5$ cells used for each analysis. Cells were washed in cold PBS at 4°C and resuspended into 50µl PBS with a sufficient excess of primary antibody (generally between 1:50 and 1:500). Tubes were incubated at 4°C for 30 minutes, washed once with 1ml PBS and resuspended into 50µl of PBS plus 0.1% BSA and incubated for 10 minutes at 4°C. Cells were subsequently washed with 1ml PBS and resuspended into 50µl with a sufficient excess of fluorescently labelled secondary antibody (in accordance with manufacturers' protocols) and incubated at 4°C for 30 minutes. Excess antibody was removed by washing three times with 1ml PBS before analysis on a FACS Vantage analyser (Beckton Dickinson). For FACS samples measured in the FL-1 emission spectrum (530 ± 15nm), viability was estimated by the addition of 100ng/ml propidium iodide as described in section 2.29.1. If necessary, cells were fixed with 1% formaldehyde in PBS before analysis. Prior to FACS analysis, formaldehyde was washed off with 1ml PBS.

Where cell sorting was desired, the procedure above was carried out in a sterile environment, and approximately $5x10^6$ cells were sorted into sterile 6ml sample tubes (Falcon) containing 500µl MEM.

2.31.3. FACS analysis of intracellular proteins

Comparisons of the amount of surface protein to intracellular protein were carried out using a cell permeabilisation assay based on a protocol suggested by Pollice *et al.* (1992). Briefly, three samples of cells were treated by either: (1) FACS labelling cells with mAb as described. (2) Fixing the cells with 0.25% paraformaldehyde at room temperature for 15 minutes before washing once with PBS and carrying out a standard FACS analysis. (3) Fixing cells as described, washing once with PBS and treating cells with 1ml cold (4°C) 70% methanol for 60 minutes to make both the cell and nuclear membranes permeable before FACS analysis. Control scans (1) and (2) give an indication of the degree of background fluorescence.

2.32. Western blotting of total cell proteins

2.32.1. Preparation of cell extracts

Cell protein extracts were obtained from semi-confluent 75cm^2 tissue culture flasks which were washed twice with PBS before aspiration of washings and addition of 1ml solubilisation buffer (appendix C). Cells were solubilised through scraping with a sterile cell scraper (Costar) and transferred to a sterile microfuge tube. Samples were centrifuged at 12000*g* for 2 minutes in a Jouan A14 centrifuge at 4°C. The supernatant was transferred to a clean tube and stored at -20°C before use.

2.32.2. Sodium dodecyl sulphate-polyacrylamide gel electrophoresis (SDS-PAGE)

Separation of *B16a* proteins was carried out by electrophoresis in the Bio-Rad Protean and Mini Protean system, using an 8% denaturing polyacrylamide gel (formula shown below) in a protocol based on that described by Lugtenberg *et al.*, (1975), under reducing conditions.

Constituent	Running Gel (8%)	Stacking Gel
H_2O	4.6ml	1.4ml
30% acrylamide mix*	2.7ml	0.33ml
1.5M Tris pH 8.8	2.5ml	-
0.5M Tris pH 6.8	-	0.25ml
SDS 10% W/v	0.1ml	0.02ml
AMPS 10% W/v	0.1ml	0.02µl
TEMED	0.006ml	0.002ml

*29.2% W/v acrylamide and 0.8% W/v N,N'-methylene-bis-acrylamide (Bis) (Bio-Rad)

Table 2.1. Composition of running gel and stacking gel for SDS-PAGE.

Briefly, 10µl protein samples were boiled with 2µl 5x SDS sample loading buffer (appendix C) for 5 minutes. These were spun briefly and loaded onto the gel. Electrophoresis was carried out at 200V in 1x SDS-PAGE running buffer (appendix C) until the tracking dye reached the bottom of the gel. After electrophoresis, the gel was removed from the glass plates, and proteins either stained directly (to ascertain loading) or transferred to nitrocellulose for subsequent probing with antibodies (see Immunoblotting).

Directly stained gels were soaked with gentle agitation in 0.1%W/v Coomassie Brilliant Blue R-250 in 50% methanol/10% acetic acid for 30-60 mins. Gels were then destained in 10% methanol/20% acetic acid until background stain was removed. Gels could then be dried onto filter paper.

2.32.3 Immunoblotting

Following separation by SDS-PAGE, cell components were transferred onto nitrocellulose membranes (0.45 µm pore size, Bio-Rad) according to the western blotting method modified from Towbin *et al.,* (1979). Semi-dry transfer of proteins was carried out using a Multiphor II transfer block (Pharmacia) in accordance with

manufacturers' protocols. Briefly, the gel was transferred onto a cut piece of nitrocellulose placed onto a stack of 4 sheets of 3MM paper, soaked in transfer buffer. This stack was covered in another 4 sheets of soaked 3MM paper and proteins transferred for 60 minutes at 0.8mA/cm^2. Transferred nitrocellulose was then rinsed in ddH2O and stained with diluted Ponceau S (Sigma) to ascertain transfer efficiency, protein loading and positions of markers (which were marked by pencil).

Transferred proteins were immunodetected using monoclonal antibody Hmβ3 specific for murine β3 integrin subunit. Blots were first blocked overnight with gentle agitation in 10ml TBS containing 1% ovalbumin and 0.05% sodium azide. This blocked unbound sites on the nitrocellulose. Membranes were then rinsed with 1x TBS followed by hybridisation with primary antibody diluted in 5ml blocking buffer (dilution sufficient to give minimal background hybridisation) for 4 hours. Blots were then washed once with 10ml TBS then three times with 10ml TBSN and finally, once with 10ml TBS (~10min per wash) and incubated for 2 hours with a 1/10,000 dilution of horseradish peroxidase (HRP) conjugated mouse immunoglobulins (Dako) in 10ml TBSN. A second round of TBS/TBSN washes was then followed by developing blots using ECL (Amersham) for 1 minute in accordance with manufacturers' protocol. Membranes were blotted briefly on 3MM paper then developed as described in section 2.26.

Chapter 3: Cloning and sequencing of murine αIIbβ3 from B16a melanoma cells

Expression studies involving the transfection of complete, functional genes into mammalian cells require an entire cDNA, free from sequence errors. For this purpose, screening of complete cDNA libraries packaged into λ phage with homologous probes remains one of the most reliable methods for retrieving full length target genes. The information detailed below describes work carried out on this cloning procedure in an attempt to obtain complete murine αIIb and β3 cDNA sequences. This includes generation of library probes specific to the integrins of interest using RT-PCR, generation of a B16a cDNA library and its packaging into λZapII and subsequent screening of recombinant lambda phage.

3.1. Construction of a B16a cDNA library in λZAP II

Messenger RNA was extracted from B16a cells in culture as described in section 2.19.1 and approximately 2μg (quantified by spectrophotomeric determination) was used as a template for the generation of double stranded DNA (section 2.19.2). A parallel control reverse transcription, labeled with 20μCi [α-^{32}P]dCTP revealed a good size distribution of synthesised cDNA of between approximately 0.5 and 10 kbases after analysis in a 1% denaturing alkaline agarose gel. Analysis of the subsequently packaged phage library on IPTG/X-Gal plates showed that it contained 6.89x10^6 phage of which 99% were recombinants (did not stain blue).

3.1.1. Calculation of average insert size using random excision of plaques

An additional step to ascertain packaging efficiency was carried out using random excision of six plaques as described in section 2.27. Six host *E. coli* XL1-Blue MRF' recombinants were generated, all of which grew in LB under ampicillin and tetracycline selection. pBluescript plasmid was recovered by miniprep and the average cDNA insert size observed by endonuclease restriction with *Not* I to cut plasmids at *Not* I sites within the cDNA insert linkers, releasing any packaged murine cDNA.

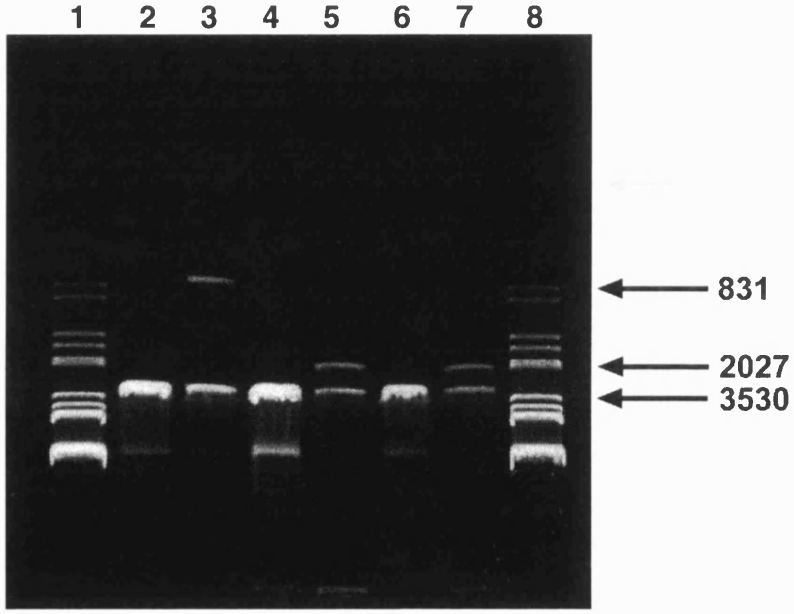

Fig 3.1 1% horizontal agarose gel stained with 0.5µg/ml ethidium bromide showing restriction digest of six randomly excised pBluescript SK(-) plasmids from a λZAPII B16a cDNA library. Counting lanes left to right, Lanes 1 & 8 show λ *Hind* III/*Eco* RI DNA markers. Lanes 2-7 show *Not* I restriction of 1µg of randomly excised recombinant pBluescript SK(-) (See text for explanation).

Fig 3.1 shows restriction of the six pBluescript plasmids, revealing a single band at ~3kb of linearised pBluescript and second, lighter bands of cDNA inserts. Half of the isolated plasmids showed no visible insert, probably indicating insertion of insignificant inserts too small to visualise. Other plasmids contained 50 (lane 2, insert

not visible above), 400 (lane 3), and two ~2000 base pair fragments (lanes 5 & 7). Therefore although 99% of phages were apparently recombinant under IPTG/X-Gal visualisation, approximately 50% contain insignificant inserts. The clones of interest are approximately 3300bp (β3) and 2370bp (αIIb). Although no inserts of this size were observed, the sample size was very low and the presence of 2000 base pair inserts indicated packaging of inserts in the kilobase range.

3.2. Generation of αIIb and β3 specific probes by reverse transcription PCR of B16a cDNA

Two pairs of PCR oligonucleotide primers were generated as described in section 2.22 using primers specific for portions of human αIIb and β3 with known homology between different species. Specific primers described below were used with a standard PCR protocol (section 2.23) and cDNA template generated using the cDNA synthesis kit as described.

3.2.1. Generation of an αIIb fragment from RT PCR of B16a cDNA

αIIb oligonucleotide primers were synthesised using sequences based on primers described by Chen *et al.* (1992b) and homologous for a 709bp fragment in the region of 2370-3079 of both human and rat platelet integrin αIIb. Primer αs was designed to incorporate three nonsense bases plus an endonuclease restriction site for *Eco* RI (underlined). Primer αas was similarly synthesised, but with a *Hind* III endonuclease site to allow directional cloning into pBluescript (underlined).

αs 5' - CCCGAATTC TGGTGGTGGCAGCAGAA - 3'

αas 5' - CCCAAGCTT GTTCCGCTTGAAGAAGCC - 3'

PCR of approximately 1ng cDNA using reaction conditions as detailed and 2mM magnesium chloride gave rise to a single ~700bp DNA fragment (Fig 3.2B). Approximately 1μg of this PCR fragment was removed from a 1.5% horizontal TBE gel using Geneclean and dual-restricted with both *Hind* III and *Eco* RI and ligated into *Hind* III/*Eco* RI dual-restricted pBluescript SK for sequence analysis.

3.2.2. Generation of a β3 fragment from RT PCR

Integrin β3 oligonucleotide primers were synthesised using sequences based on primers described by Cieutat *et al.* (1993) and are homologous to a 657bp fragment in the region of 1684-2358bp of human integrin β3 cDNA.

Ds 5' - TCCGCTACAAAGGGGAGAT - 3'

A1h 5' - TACGTGATATTGGTGAAGGT - 3'

PCR using these primers with ~1ng cDNA template and 2mM magnesium chloride generated a single band of around 650bp (fig 3.2A). No incorporation of restriction site was carried out with the PCR primers described above. Therefore, 1μg PCR fragment was removed from a 1.5% horizontal TBE agarose gel using Geneclean and cloned into pBluescript by dual-restriction with both *Eco* RV and *Pvu* II to release a 322bp fragment which was removed from a TBE gel using Geneclean. Prior to

ligation, 1µg pBluescript was restricted with *Eco* RV and dephosphorlyated with alkaline phosphatase before a standard blunt-end ligation.

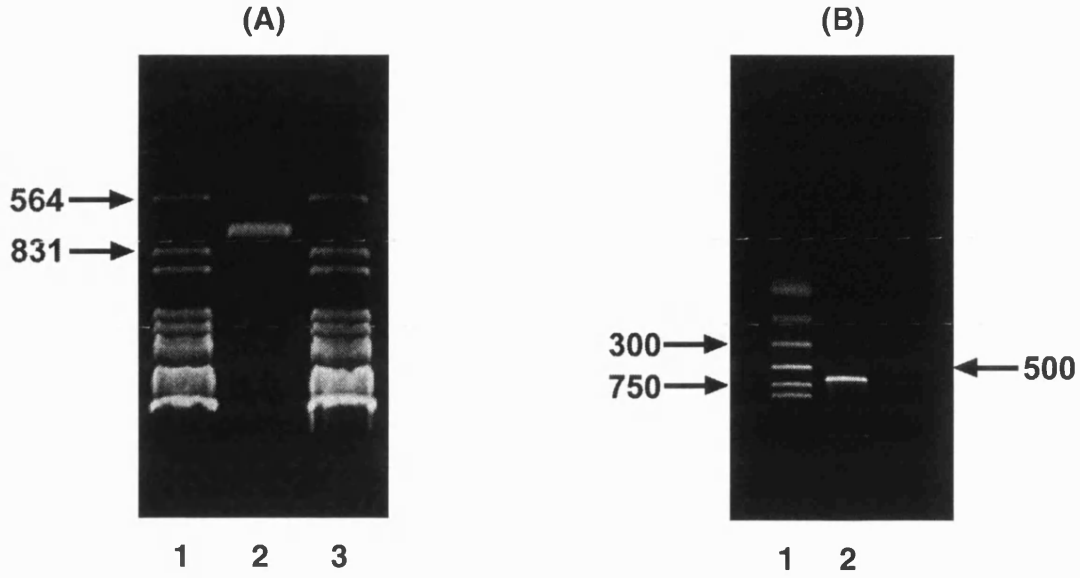

Fig 3.2 1.5% TBE agarose gel stained with 0.5µg/ml ethidium bromide showing RT PCR fragments generated using B16a cDNA template and integrin specific oligonucleotide primers. (A) From left, lanes 1&3: λ *Hind* III/*Eco* RI markers, lane 2: RT-PCR fragment generated using integrin β3 specific primers Ds and A1h,. (B) From left, lane 1: Promega low MW markers, lane 2: RT-PCR fragment generated using integrin αIIb specific primers αs and αas.

3.2.3. Verification of PCR fragments by nucleotide sequencing

Sequencing of both pBluescript PCR fragment clones was carried out using denatured double stranded vector and the Sequenase II protocol as described in section 2.15. PCR clones were sequenced using a Sequenase II -40 kit primer, specific to a pBluescript sequence upstream (5') of the multicloning site. After sequencing, nucleotide sequences were entered into the Daresbury database using the GCG SEQED software, as described in section 2.16. Comparison of sequenced portions of PCR products was carried out against human αIIb and β3 cDNA using GCG FASTA software. This sequence comparison identified each PCR fragment as having significant homology to a corresponding region of published human αIIbβ3 sequences.

Degree of homology using FASTA was 82.7% for αIIb PCR fragment and 85.7% for the β3 PCR fragment (fig 3.3 and fig 3.4).

```
                                          90        100       110
m αIIb                                   GTGGTGGCAGCAGAAGAAGGTGACAGGGAG
                                         ||||||||||||||||||||||||| ||||||
h αIIb CTGCGAGGGAACTCCTTTCCAGCCTCCCTGGTGGTGGCAGCAGAAGAAGGTGAGAGGGAG
            2350      2360      2370      2380      2390      2400

         120       130       140       150       160       170
m αIIb CAGGAAGACTTGGACAGATGGGTCTCCAGGCTGGAGCACAACCTATGAGCTCCACAACAT
       ||| |   ||||||||| ||||   |||   |||||||| ||||||||||||||||||
h αIIb CAGAACAGCTTGGACAGCTGGGGACCCAAAGTGGAGCAC-ACCTATGAGCTCCACAACAA
            2410      2420      2430      2440       2450      2460

         180       190       200       210       220       230
m αIIb TGGCCCTGGCACTGTGAATGGCCTCAGACTTCTCATCCACATTCCTGGCCAGTCCCAGCC
       ||||||||| |||||||||||  ||    ||   ||||||| |||| || ||||||||||
h αIIb TGGCCCTGGGACTGTGAATGGTCTTCACCTCAGCATCCACCTTCCGGGACAGTCCCAGCC
            2470      2480      2490      2500      2510      2520

         240       250       260       270
m αIIb CTCGGATCTGCTCTACAT-CTGGATGTGCAGCCGCAGGAGGTT
       ||| || |||||||||||  |||||| | |||||  |||| ||
h αIIb CTCCGACCTGCTCTACATCCTGGATATACAGCCCCAGGGGGGCCTTCAGTGCTTCCCACA
            2530      2540      2550      2560      2570      2580
```

Fig 3.3 Sequence alignment of murine αIIb PCR fragment with human αIIb cDNA (accession J02764) using the Wisconsin gcg package and FASTA software

```
                                             100       110       120
murine β3                                   GATCTGTGTGTGCGTCCAGCCAGGCTCCTAT
                                            | ||||||  ||  ||||||| |||||||||
hum β3 TGCAGCGGCCGCGGCAAGTGTGAATGTGGCAGCTGTGTCTGTATCCAGCCGGGCTCCTAT
            1830      1840      1850      1860      1870      1880

           130       140       150       160       170       180
mur β3 GGAGACACCTGTGAGAAGTG-CCCACCTGCCCAGATGCCTGCTCCTTTAAGAAGGAGTGT
       ||  |||||||||||||||| |||||||||||||||||||| |||||||||  ||  |||
hum β3 GGGGACACCTGTGAGAAGTGCCCCACCTGCCCAGATGCCTGCACCTTTAAGAAAGAATGT
            1890      1900      1910      1920      1930      1940

190       200       210         220      229
mur β3 GTGGAGTGTAAGAAGTTCAACCGGGAACGCTCCATGA--AGAAACACCTG
       ||||||||||||||||  ||||||| | ||  |||||    |||  |||||
hum β3 GTGGAGTGTAAGAAGTTTGACCGGGAGCCCTACATGACCGAAAATACCTGCAACCGTTAC
            1950      1960      1970      1980      1990      2000
```

Fig 3.4 Sequence alignment of β3 PCR fragment with human β3 cDNA (accession J02703 using the Wisconsin gcg package and FASTA software

3.3. Screening of λZAP II plaques with cDNA probes

Phage were plated at 15,000 pfu per 82mm plate, lifted onto Hybond N+ circles and screened with 1-5μl of denatured [α-^{32}P]dATP labeled PCR probe (see section 2.21-2.25). Screening of 25 plates for each integrin subunit revealed 12 αIIb reactive plaques and 16 β3 reactive plaques. These plaques were removed from each plate and eluted into 500μl SM buffer plus 15μl chloroform. Secondary screening with a titre of approximately 150 pfu per plate revealed only one αIIb and one β3 reactive clone under high stringency washes. Excision of single reactive plaques into *E. coli* SOLR (section 2.27) and extraction of plasmids from host cells by miniprep gave two clones which were examined by restriction with both *EcoR* I and *Not* I, both of which restrict at the cDNA linker of cloned plasmids, releasing a cDNA insert (section 2.19.3).

3.4. Examination of reactive λZAP II plaques

Size analysis of both reactive clones was carried out by restriction with either *Eco* RI or *Not* I endonuclease enzymes. Fig 3.5A indicates restrictional analysis of the αIIb clone. Both *Eco RI* and *Not* I restriction released a single insert band of ~750bp and linearised pBluescript (~3kb). Fig 3.5B indicates restrictional analysis of the β3 clone. Restriction with *Not* I released a single ~1.5kb cDNA insert while *Eco* RI restricted the insert twice internally to give two ~550bp bands and a single ~250bp band (not visible below).

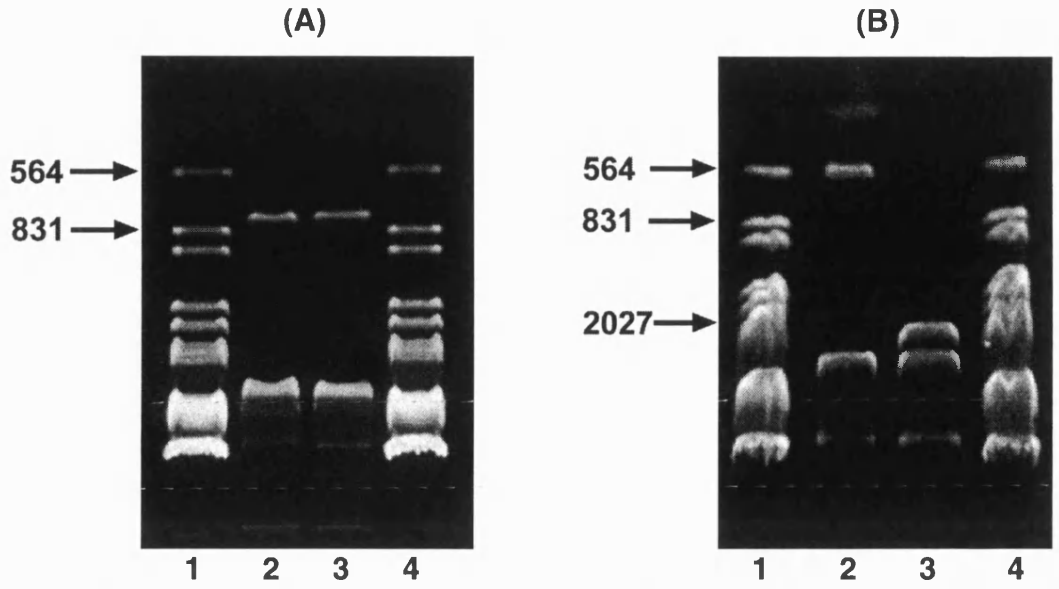

Fig 3.5 1% horizontal TBE agarose gel stained with 0.5μg/ml ethidium bromide showing endonuclease restriction of αIIb and β3 cloned pBluescript plasmids. (A) Restriction of αIIb clone: from left, lanes 1&4: λ *Hind* III/*Eco* RI markers, lane 2: *Eco* RI, lane 3: *Not* I. (B) Restriction of β3 clone: from left, lanes 1&4 λ *Hind* III/*Eco* RI markers, lane 2 *Eco* RI, lane 3 *Not* I restriction.

3.4.1. Sequence analysis of reactive cDNA clones

Sequence analysis of these two isolated clones was carried out using denatured double stranded plasmid templates with the Sequenase II protocol as described. Template was primed using kit -40 primers. Resulting sequences gave two ~200 base pair nucleotide sequences which were compared using FASTA software against their human counterpart integrin cDNA sequences and to the entire Genbank database.

The murine αIIb clone nucleotide sequence has a reasonable homology to the 3' untranslated end of the human αIIb sequence (68.7%, fig 3.6), however large portions of the sequence carry no homology, and further FASTA searches revealed poor homology to other α integrin subunits within the Genbank database. Wider scale searches using the entire Genbank database showed little homology to any gene (murine or otherwise). Therefore, homology of this αIIb clone to sections of the PCR

fragment used may have been sufficient to give hybridisation even at high stringency washes.

Searches using the sequenced section of the β3 clone showed virtually no homology to either human, rat, or known sections of mouse β3 (fig 3.7). FASTA searches against the entire Genbank database showed no significant homology to any relevant gene. It is possible that the sequenced portion of the clone detailed here represents a distant 3' post-translational site of β3 and that the 5' end of this sequence is specific to murine β3. Clones of human β3 as isolated by Fitzgerald *et al.* (1987) do contain ~700 bases of 3' information, so if the region sequenced is specific to murine β3, the majority of this fragment will be untranslated 3' sequence. Otherwise, it is possible that regions of this clone (not sequenced here) are sufficiently homologous to the β3 PCR probe to result in a hybridisation.

```
119        109         99         89          79         69
alphac  GTTTCAGCCAGTTGCCTTGCTCAGAACTCCATGGGGTC-TTCCCTTTCCAGCAGACCGG
                                          | ||| ||| || || | ||| |||| | |
j02764 CTTTGGGTTGGAGCTGTTCCATTGGGTCCTCTTGGTGTCGTTTCCCTCCCAACAGAGCTG
             3210       3220       3230       3240       3250       3260

          59         49         39         29         19          9
alphac GTGCATCCCTTTTCCTAATACCTAATAAAGAGCTTGACAGTGAAAAAAAAAGCGGCCGGC
       |    | |||    ||||   | ||||||||||||  |||
j02764 GGCTACCCCCCCTCCTGCTGCCTAATAAAGAGACTGAGCCCTG
             3270       3280       3290       3300
```

Fig 3.6 Sequence alignment of αIIb library clone fragment to the human αIIb cDNA (accession J02764) sequence

```
49         39         29         19          9
betacl GGTTTTCAGGTGAGCTCTGGGGTTACACTACAGTCCGCTGCCTAGCTGAGCGGCCGCG
                                          || |  |||||   ||  ||||||||||
j02703 TACCACGCGTACTGACACCTGCATGTCCAGCAATGGGCTGCTGTGC--AGCGGCCGCGGC
      1780       1790       1800       1810       1820         1830

j02703 AAGTGTGAATGTGGCAGCTGTGTCTGTATCCAGCCGGGCTCCTATGGGGACACCTGTGAG
        1840       1850       1860       1870       1880       1890
```

Fig 3.7 Sequence alignment of β3 library clone fragment to the with human αIIb cDNA (accession J02703)

3.5. Discussion

It is clear from the sequences described above that the PCR probes generated from RT-PCR of B16a were highly homologous to the same fragment contained in human αIIb and β3. The sequences described above are completely homologous to the published partial PCR sequence information obtained by Chen *et al.* (1992) and Cieutat *et al.* (1993) thus confirming the expression of integrin αIIbβ3 by murine B16a melanoma cells. Screening of a B16a cDNA library with these probes recovered only two small fragments with low homology to any human integrin, or integrin-related sequences (confirmed using the FASTA software contained in the Wisconsin GCG package). Hybridisation of these sequences to PCR probes was probably due to partially homologous sequences further downstream from those sequenced. The limited size of these fragments also precluded isolation of full length cDNA sequences for either integrin subunit.

Time became an important consideration and limited the screening of further library plaques. Due to inexperience with the process of library screening within the lab, significant time was required to set up the necessary equipment and optimal conditions for efficient hybridisation. High levels of background counts were encountered in early experiments, so that a number of probe labeling protocols, hybridisation conditions and blocking solutions were used before the eventual protocol described was chosen. Further library screening could have been carried out, but the length of time that this screening takes, and the low number of recombinant phages recovered from a high number of plaque screens indicated that the library generated from reverse transcription of B16a mRNA was unlikely to yield full length clones of αIIb or β3.

In retrospect, it would have been constructive to attempt to determine the abundance of αIIb and β3 mRNA amongst total cellular mRNA (using methods such as immunoprecipitation of integrin markers and comparison to other cellular proteins such as actin). This would have given an indication of the number of clones necessary to screen. The modal size within a mammalian mRNA population is usually around 1.8kb. Both integrin subunits of interest are larger than this (αIIb is 3300bp while β3 is 2370bp) and it may have also been wise to have enriched the proportion of larger mRNA by size fractionation, either of mRNA (before reverse transcription) or of cDNA (before ligation into λZapII). Rather than carry on with time-consuming cloning work, it was decided that the original objectives to down-regulate expression in the murine system would be continued, but using full length human integrin β3 cDNA obtained from other groups.

Human integrin β3 subunit (clone CD3A) cDNA, was obtained from Joseph Loftus (Scripps Institute, La Holla, CA., USA). Additionally, human αv cDNA (clone VnRα) and a mutant β3 clone CD3A D119A containing a point mutation in the ligand binding site and resulting in a single residue substitution at position 119 of the amino acid sequence, inactivating the integrin (detailed in Loftus *et al.,* 1990) were also received (all are detailed in section 2.3, verification of this mutation is detailed in section 6.2).

The use of human cDNAs introduced interesting problems in that any antisense work carried out with human β3 vectors upon murine cell lines used cDNA which was not 100% homologous to murine β3 cDNA. Data presented here and by Cieutat *et al.* (1993) suggest a DNA homology of around 86% between human and murine β3

integrins, and there are precedents for use of species variants in antisense experiments. Saelman *et al.* (1995) have successfully used a human α2 antisense construct, ligated into an integrating expression vector, to specifically reduce expression of canine α2 integrin subunits. The homology between the latter two genes is not detailed, however Woolf *et al.* (1992) suggest that RNase H activity can be seen with oligonucleotides with as little as 6-10 concurrent base pairs of homology (section 1.5). Therefore, the likelihood of producing activity using antisense fragments of human β3 integrin against endogenous murine β3 is reasonable, however, the degree to which this inhibition would be specific is unknown. As a result of this incomplete homology, it was decided that antisense experiments would be carried out in parallel in the human melanoma cell line A375, and its more metastatic sub-population A375M.

Use of the mutant β3 clone (CD3A D119A) presents an immediate problem in that transfection of inactive human β3 clones into cells already expressing functional β3 subunits would make selective identification of the mutant subunit difficult without attaching a marker. Therefore it was decided to continue this work in the murine B16a cell line, by electroporation with the human mutant β3 clone. This strategy potentially allows identification of expressed human β3 using antibodies which do not bind to murine β3.

It should be possible to inhibit expression of native murine αIIbβ3 by transfection of murine cells with mutated human β3 subunits, as long as CD3A D119A is capable of forming a heterodimer with murine αIIb. Examination of the sequences of different β integrin subunits indicates a high homology, both between

integrin subunits and between species (Hynes, 1992), suggesting that CD3A D119A is likely to form a heterodimer with murine αIIb.

An additional interesting experiment would be to transfect human αv clones into murine B16a cells already expressing αIIbβ3, which may give an insight into changes in tumorigenicity and on competition between different α subunits for β3 integrins.

Chapter 4: Characterisation of β3 integrin expression in murine and human melanoma cell lines.

Effective gene therapy techniques upon melanoma cells cannot be characterised unless a fairly detailed knowledge of β3 expression in cells studied has been undertaken. The role of β3 integrins (as αIIbβ3) in the B16a murine melanoma cell line was examined through comparison of cell populations selected on the basis of β3 expression using fluorescence activated cell sorting (FACS). Further, more limited examination of αvβ3 expression in the human A375 melanoma cell line was also carried out, using FACS to ascertain expression of β3 integrins in cell lines isolated on the basis of metastatic potential.

4.1. Characterisation of β3 integrin subunit expression of B16a cells using FACS

Surface expression of β3 integrin subunits (expressed as the heterodimer αIIbβ3) upon the surface of wild-type B16a cells was quantified using FACS as described in section 2.31. Characterisation of the interaction of murine β3 with hamster anti-mouse IgG, Hmβ3 was necessary before this antibody could be used in assays. These studies included the effect of cell-detachment conditions upon detection of integrins by Hmβ3, and the effect of integrin ligands upon antibody binding.

FACS was then subsequently used to generate control models for integrin αIIbβ3 modulation by isolating two populations of B16a cells from a wild-type population on the basis of β3 expression. These sub-populations were further

characterized for stability of β3 expression and a number of other in vitro techniques were used to investigate the effect of differential expression of β3 upon cellular phenotype.

4.1.1 FACS analysis of B16a cells using mAb Hmβ3.

Initial FACS experiments using B16a cells were designed to ascertain the level of β3 expression on the surfaces of wild-type cells and to characterise the nature of binding of antibodies specific for murine β3. FACS experiments were carried out using the labeling protocol described in section 2.31.2. All assays for the detection of murine β3 used the hamster anti-mouse IgG, Hmβ3 in dilutions of 1:50 as described. Secondary labeling of Hmβ3 with fluorescent IgG was carried out using FITC conjugated mouse anti-hamster IgG cocktail in dilutions of 1:50 as described.

The nature of this antibody binding is displayed by figures 4.1 and 4.2. The FL1-height axis refers to the level of fluorescence emission measured from cells at wavelength 530 ± 15nm, while the events axis describes the relative number of cells at each flourescence intensity. Shaded regions indicate fluorescence of Hmβ3 labeled cells while the unshaded region indicates non-specific IgG binding of the FITC conjugated anti-hamster IgG cocktail alone. Many of the FACS scans shown below have associated numerical values for the scan mean and peak channel. This represents the average surface fluorescence of the cell sample in the FL-1 wavelength and the associated fluorescence channel in which cells are maximally fluorescent.

Figure 4.1 overleaf, illustrates that detection of β3 expression with mAb Hmβ3 did not appear to be affected by proteolytic cell detachment arising from trypsin/EDTA treatment

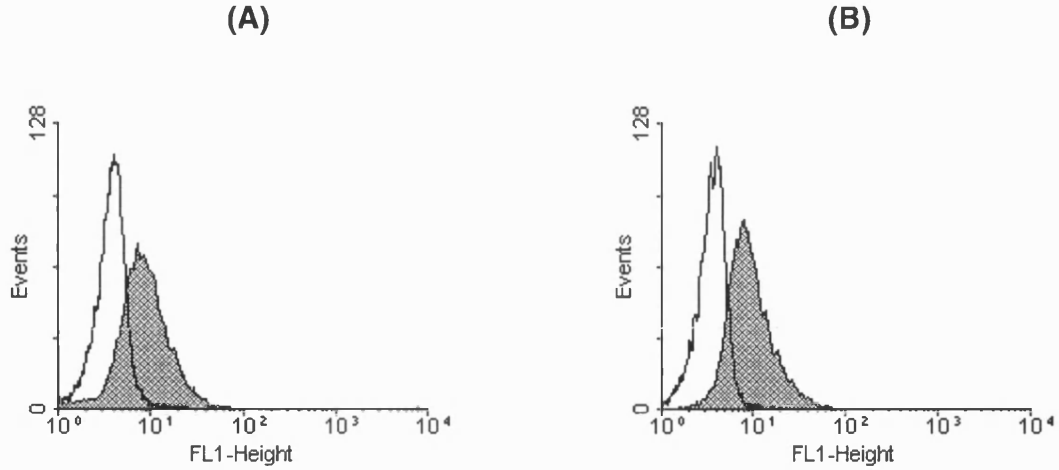

Fig 4.1 Effect of cell detachment method upon detection of murine β3 integrin surface expression by FACS using antibody Hmβ3 against wild type B16a cells (I_2). (A) Expression of β3 integrin subunit from B16a cells stripped from a 175cm^2 flask by scraping. (B) Expression of β3 integrin subunit from B16a cells stripped from a 175cm^2 flask with 1.5ml trypsin/EDTA. The non-shaded area represents non-specific binding of FITC conjugated anti-hamster IgG alone. These scans are representative of two experiments.

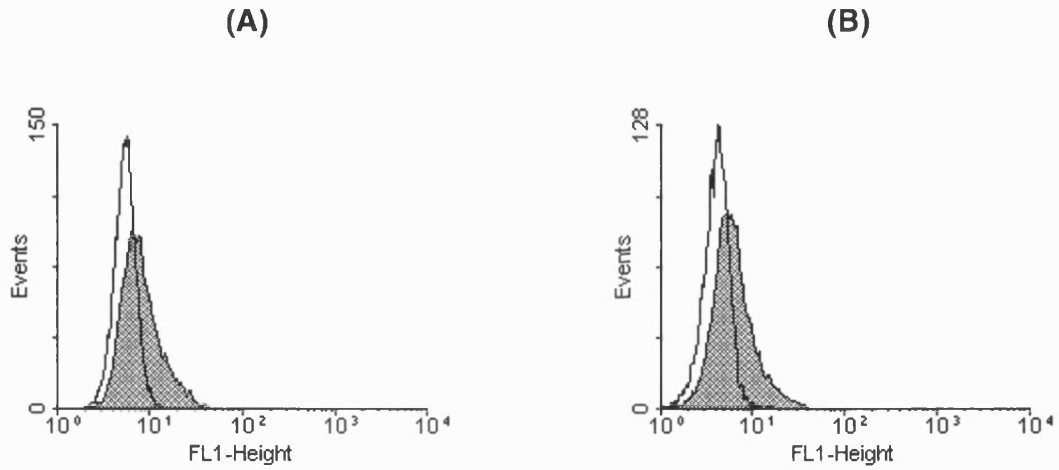

Fig 4.2 FACS analysis of wild type B16a cells (I_2) showing the extent of mAb Hmβ3 binding in the presence of an excess of soluble ligand for αIIbβ3. (A) Fluorescence of control wild type B16a cells treated with Hmβ3 antibody and secondary FITC labeled anti-hamster IgG. (B) Fluorescence of B16a cells labeled with Hmβ3 antibody in the presence of 10μg/ml fibronectin. The non-shaded area represents non-specific binding of FITC conjugated anti-hamster IgG alone. These scans are representative of two experiments.

Subsequent FACS experiments were therefore carried out using cells detached with trypsin/EDTA treatment. Figure 4.2 shows the that presence of saturating concentrations of soluble fibronectin during the labeling procedure does not interfere with labeling efficiency (concentrations of fibronectin used were determined using information derived from static adhesion assays, detailed in section 4.2). This also indicates that antibody Hmβ3 does not bind to the ligand binding site of αIIbβ3 and will probably therefore not interfere with cell adhesion to ligand substrates.

Both figures indicate that wild type B16a cells are weakly positive for murine β3 integrin subunits, giving a small shift in FL1 fluorescence from control IgG-FITC treated cells. The intensity of this fluorescence was similar between cell samples (as illustrated by both figures), although unpredictable levels of fluorescence were often obtained from FACS of cells of higher passage number or from confluent density cultures. As a result, all FACS samples were generated from low passage ($< P_{10}$) cells recovered from semi-confluent flasks.

4.1.2. FACS of B16a cells using β3 expression as a selectable marker

FACS sorts were carried out as explained in section 2.31.2 under sterile conditions. Two populations of B16a cells were isolated on the basis of β3 expression using a starting population of 5×10^6 wild type B16a cells (P_1). After treatment with Hmβ3 and FITC anti-hamster IgG, the fluorescent cell population was sorted into two tubes, isolating the top and bottom 5% of fluorescent cells. Samples from each tube were re-run through the FACS Vantage machine to check sorting efficiency (displayed by fig 4.3). Cells were subsequently seeded into $25cm^2$ tissue culture flasks and subcultured as usual for further analysis. Passaged cells from this sorting procedure were termed high β3 expressing (HBE) or low β3 expressing (LBE) B16a cells.

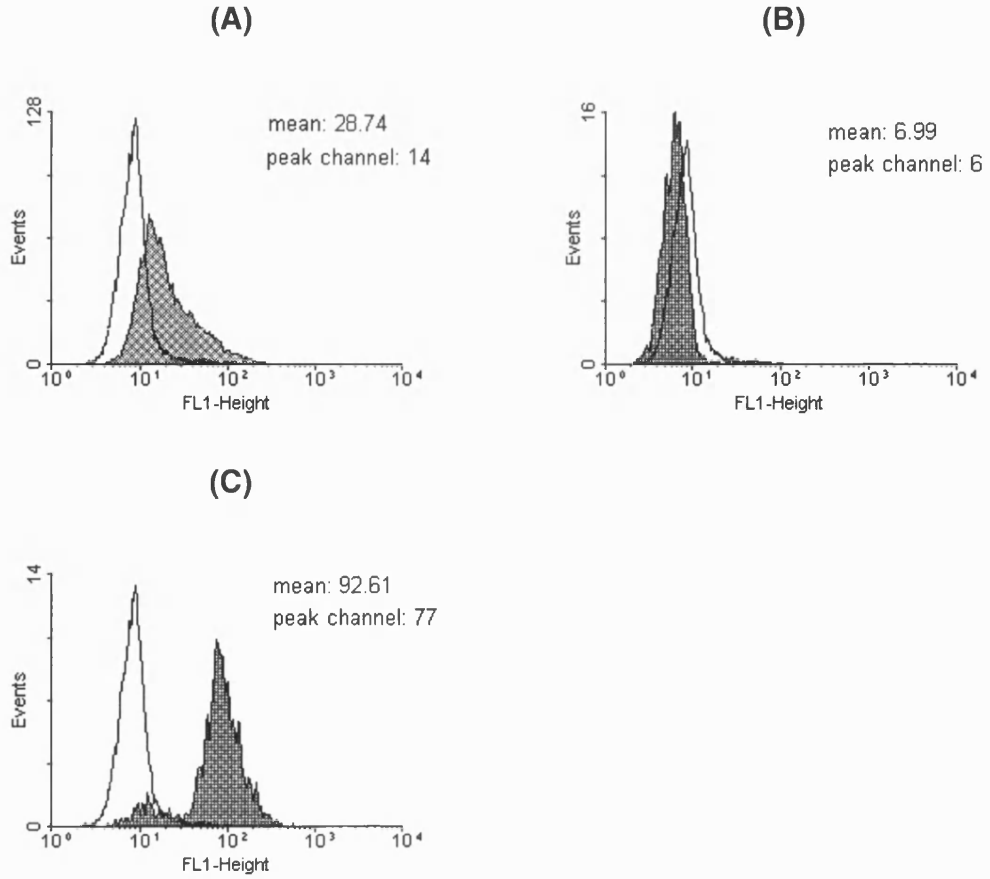

Fig 4.3 FACS analysis of wild type B16a cells before and after fluorescence activated cell sorting of cells labeled with Hmβ3 and anti-hamster FITC conjugated IgG. (A) Wild type B16a cell population used for cell sort. (B) Sample of cells isolated from the bottom 5% of fluorescent cells. (C) Sample of cells isolated from the top 5% of fluorescent cells. The shaded areas represents fluorescence of cells labeled with mAb Hmβ3 while the non-shaded areas represents non-specific binding of FITC conjugated anti-hamster IgG alone.

4.1.3. Stability of β3 expression from FACS isolated cells

The ability of these sorted cell lines to retain a heterologous integrin expression profile was examined by FACS analysis of B16a cells using Hmβ3 antibody over a number of successive passages (figure 4.4). Each passage number represents a 3 day period where cells were trypsinised, counted, and two aliquots of

$5x10^5$ cells were removed for FACS analysis. Remaining cells were split 1/10 into a fresh $175cm^2$ flask, for harvesting three days later.

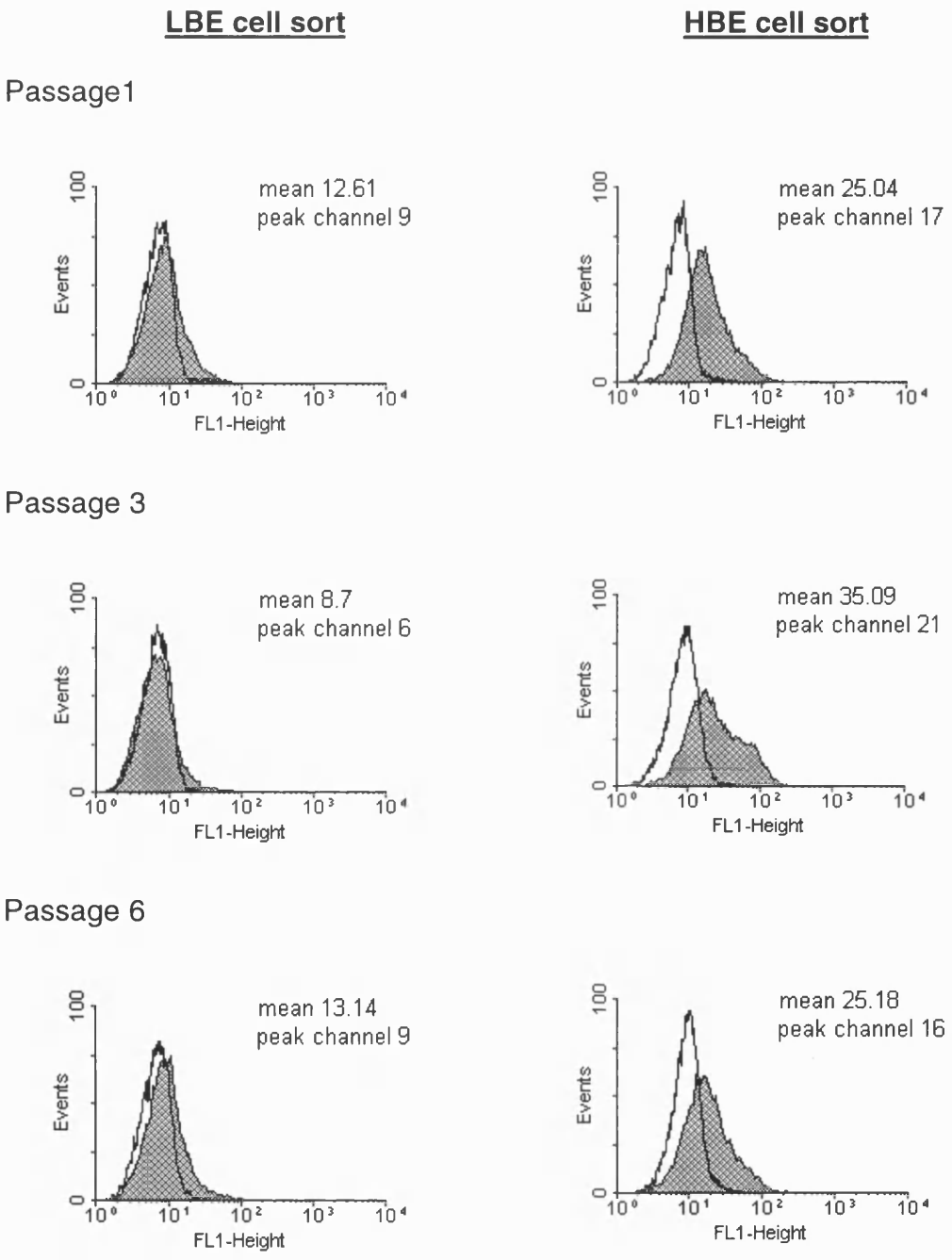

Fig 4.4 FACS analysis of B16a cells using mAb Hmβ3 for murine β3 expression, showing the effect of time in culture upon expression of β3 integrin subunits in the isolated B16a populations described. The shaded areas represent the fluorescence of cells labeled with hamster anti mouse Hmβ3 and FITC conjugated anti-hamster IgG while the non-shaded areas represents non-specific binding of FITC conjugated anti-hamster IgG alone.

Figure 4.4 illustrates that expression of murine β3 (detected using Hmβ3) is fairly constant over the time period shown after isolation of HBE and LBE cell populations. Level of mean fluorescence does appear to settle down in the HBE cell line after sorting when compared to that of HBE cells immediately after cell sorting, although the degree of cell fluorescence still appears significantly higher than that of the LBE cell population.

4.1.4 Morphology of FACS isolated cells

Morphology of HBE and LBE cell populations was examined by photography of typical cell populations using a M40 inverted microscope under normal culture conditions, grown on tissue culture grade plastic. Fig 4.5 represents a typical semi-confluent population of HBE and LBE cells two passages after sorting of cells by FACS.

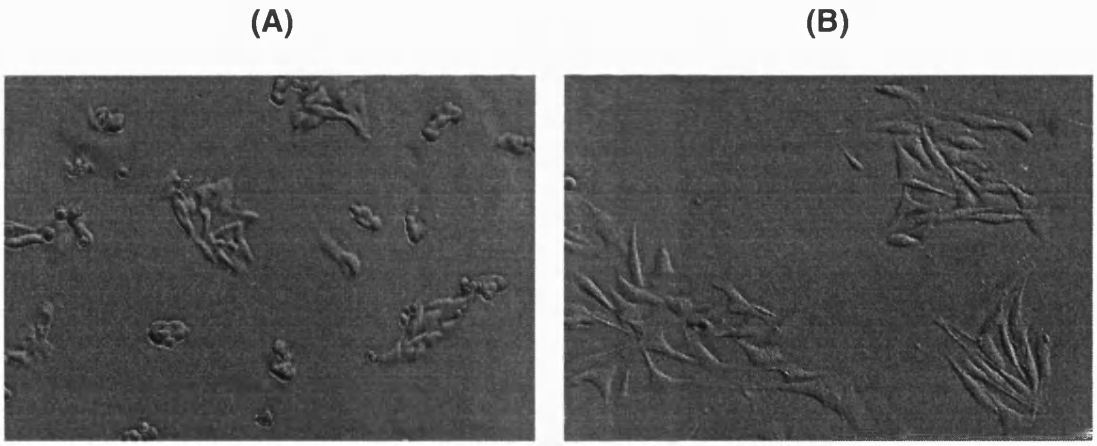

Fig 4.5 Typical morphology of isolated B16a populations, grown on tissue culture plastic. Cells shown are magnified x300. (A) Low β3 expressing (LBE) population. (B) High β3 expressing (HBE) population. Unsorted cells have a characteristic mixed morphology of spread and rounded cells (not shown).

Figure 4.5 illustrates the differences observed between LBE and HBE cells clearly. LBE cells commonly have a much more rounded morphology and grow in much more concentrated colonies. No focal contact points are obvious with the

culture surface and cells are poorly spread upon it. HBE cells typically appear to have a much more dendritic appearance and cells spread from colonies in a much more disperse manner. Contacts with the substratum appear to be concentrated at focal points.

4.2. Static adhesion assays using B16a cell populations

A primary function of integrin heterodimers is the mediation of adhesive contact formation with proteins of the ECM. Static adhesion assays were used to determine the binding of B16a cells to matrices of ECM proteins. Assays were carried out using the [Cr^{51}] labeling technique described in section 2.30, which was used to label live cells (Cr^{3+} is absorbed into cells through active uptake, Holden *et al.* 1973) using 96-well plates coated with known ligands for αIIbβ3 (see table 1.3). The effect of surface expression of murine β3 integrins from B16a cells upon adhesion to these ECM proteins is shown below.

4.2.1. Calibration of chromium-based cell detection protocol

The relationship between the number of cells, labeled using the standard [Cr^{51}] treatment protocol and γ emission was examined by aliquotting known numbers of labeled cells into scintillation tubes, and measuring the mean γ emission of eight separate samples. Figure 4.6 illustrates the linear relationship between radiolabeled cell number and γ radiation emission of these cells. Due to the relatively short half-life of [Cr^{51}] (27.7 days) and variation in the efficiency of uptake, the actual radioactive emission of cells was found to vary between labeling experiments. However, figure 4.6 shows that γ emission is directly proportional to the number of labeled cells counted. All subsequent static adhesion assays carried out were therefore

expressed as a percentage of the mean counts per minute (CPM) of eight control sample aliquots of cells.

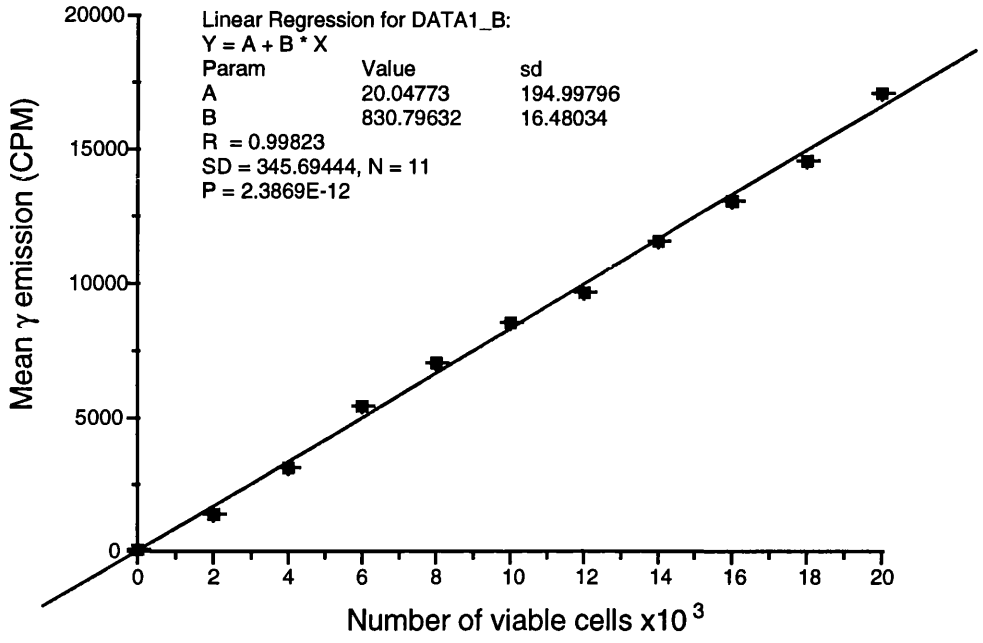

Fig 4.6 Relationship between the number of viable Cr^{51} labeled B16a cells and γ emission measured as mean counts per minute (CPM). Each point represents the mean γ emission of samples ± standard deviation of samples (n=10). These data are representative of two replicated experiments.

4.2.2. Adhesion to surfaces coated with fibronectin

Fibronectin is a widely distributed glycoprotein, synthesised by most cells and present in high concentrations in most extracellular matrices and plasma (~300μg/ml). It is a known ligand for αIIbβ3, which recognises fibronectin via an RGD ligand-binding motif (Pierschbacher and Ruoslahti, 1984). Experiments were carried out to study both the optimal coating concentration of fibronectin (fig 4.7) and the rate of adhesion to optimal concentrations of fibronectin, using both HBE and LBE cell lines (fig 4.8).

Figure 4.7 indicates that the efficiency of adhesion of B16a HBE cells for fibronectin is high and cells saturate the surface of 96-well plates at fairly low concentrations of ligand. The surface area of a single well in a 96 well-plate is $0.32cm^2$. Therefore, the HBE B16a cells shown in figure 4.7 are maximally bound to 96-well plates coated with 1μg/ml fibronectin. Experiments were carried out using a coating concentration of 1.5μg/ml, equating to a coating concentration of $0.234\mu g/cm^2$ fibronectin.

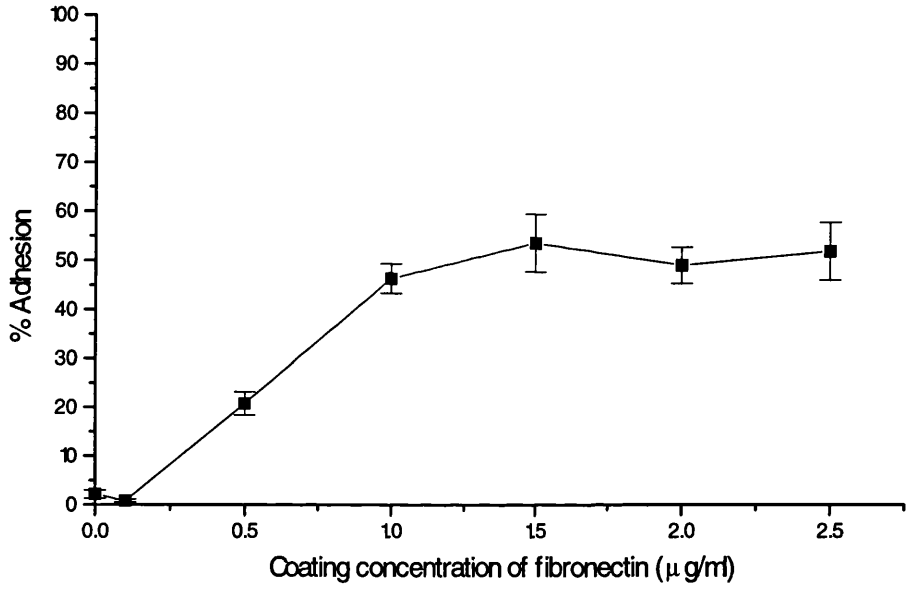

Fig 4.7 Relative adhesion of HBE B16a (I_{10}) cells to 96-well plates coated with various amounts of fibronectin. Emission of cells is standardised by comparison with emission of cells added to wells coated with 1% BSA alone. Adhesion is represented as the percentage of emission of total cells added to wells, adjusted by emission of cells adhered to BSA coated wells. Each point represents the mean γ emmission of cells adhered to coated wells minus the mean γ emission of cells adhered to BSA coated wells (n=4) divided by the mean γ emission of total cells (n=8) ± standard deviation between samples of adhered and non-adhered cells. These data are representative of two replicated experiments.

Figure 4.8 illustrates the rapid rate of B16a cell adherence to substrates coated with fibronectin. Cells saturate fibronectin coated 96-well plates within 30 minutes and the majority of cells attaching within 15 minutes. Two repeats of this assay failed to show a reliable difference in the binding rate of isolated cell populations to fibronectin.

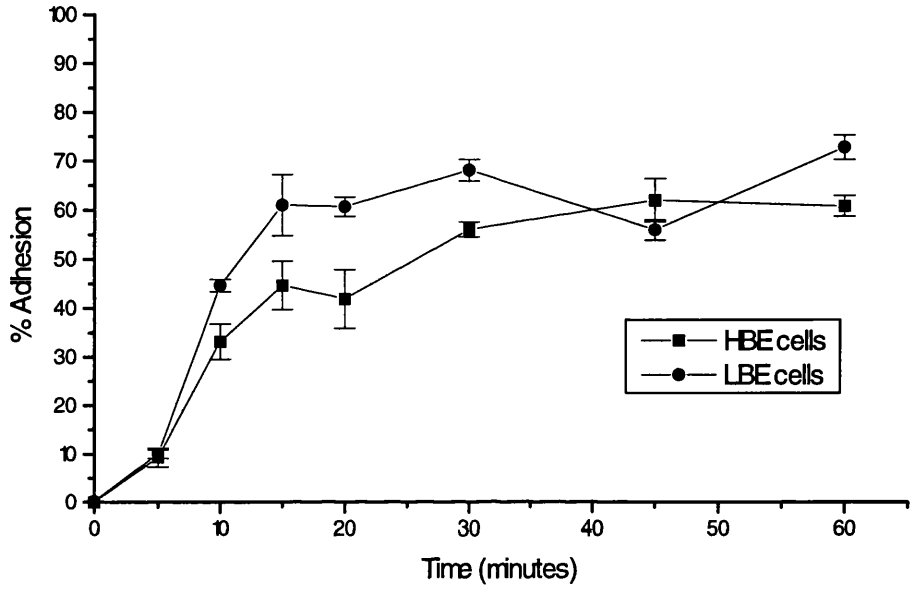

Fig 4.8 Relative adhesion of sorted B16a populations to fibronectin coated wells (0.24μg/cm^2) over time. Emission of cells is standardised by comparison with emission of cells added to wells coated with 1% BSA alone. Adhesion is represented as the percentage of emission of total cells added to wells, adjusted by emission of cells adhered to BSA coated wells. Each point represents the mean γ emission of cells adhered to coated wells minus the mean γ emission of cells adhered to BSA coated wells (n=4) divided by the mean γ emission of total cells (n=8) ± standard deviation between samples of adhered and non-adhered cells. These data are representative of two replicated experiments.

4.2.3. Adhesion to surfaces coated with fibrinogen

Fibrinogen is a soluble plasma protein, derived from hepatocytes and cleaved in the haemostatic pathway by thrombin from where it forms insoluble fibrin clots

with platelets (Ginsberg *et al.*, 1993). Integrin αIIbβ3 represents the primary receptor for fibrinogen, recognised through a KQADGV ligand-binding motif and is responsible for the recognition of fibrinogen by platelets in the blood (D'Souza *et al.* 1991). Coating concentration and adhesion kinetics experiment were carried out in a similar fashion to 4.2.2.

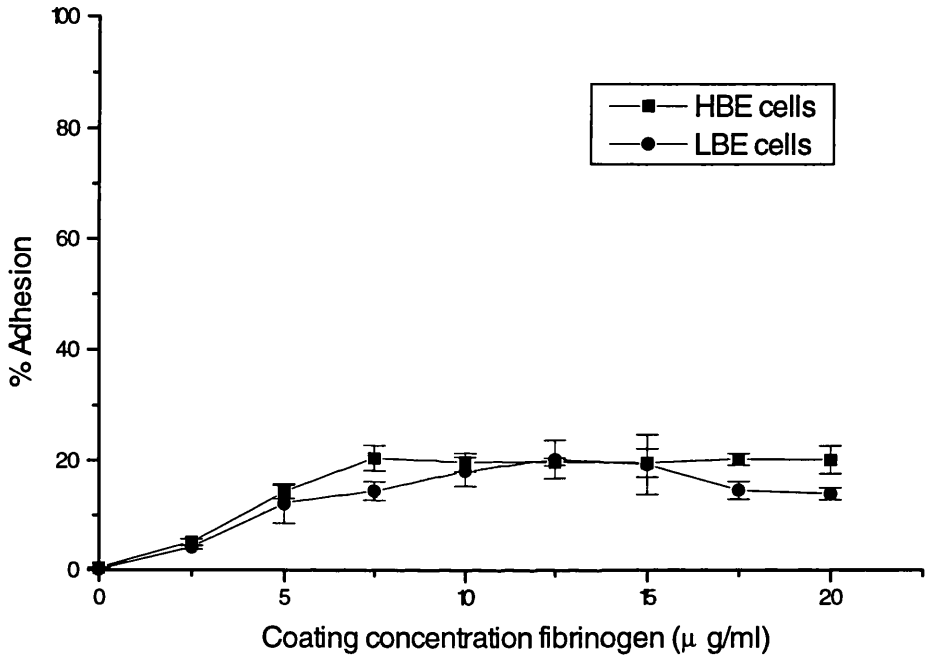

Fig 4.9 Relative adhesion of HBE and LBE B16a cells to 96-well plates coated with various amounts of fibrinogen. Emission of cells is standardised by comparison with emission of cells added to wells coated with 1% BSA alone. Adhesion is represented as the percentage of emission of total cells added to wells, adjusted by emission of cells adhered to BSA coated wells. Each point represents the mean γ emission of cells adhered to coated wells minus the mean γ emission of cells adhered to BSA coated wells (n=4) divided by the mean γ emission of total cells (n=8) ± standard deviation between samples of adhered and non-adhered cells.. These data are representative of two replicated experiments.

Both LBE and HBE B16a cell populations have a similar adhesion efficiency to fibrinogen coated 96-well plates (Figure 4.9). A repeat of this experiment also failed to show any difference in cell binding between cell strains. The degree of this binding is much lower than that of cell adhesion to fibronectin and cells bind maximally at higher coating concentrations, of approximately 7.5μg/ml. Subsequent timed adhesion assays were carried out using surface concentration 10μg/ml equating to a coating concentration of 1.56μg/cm^2 (assuming fibrinogen coats wells with 100% efficiency).

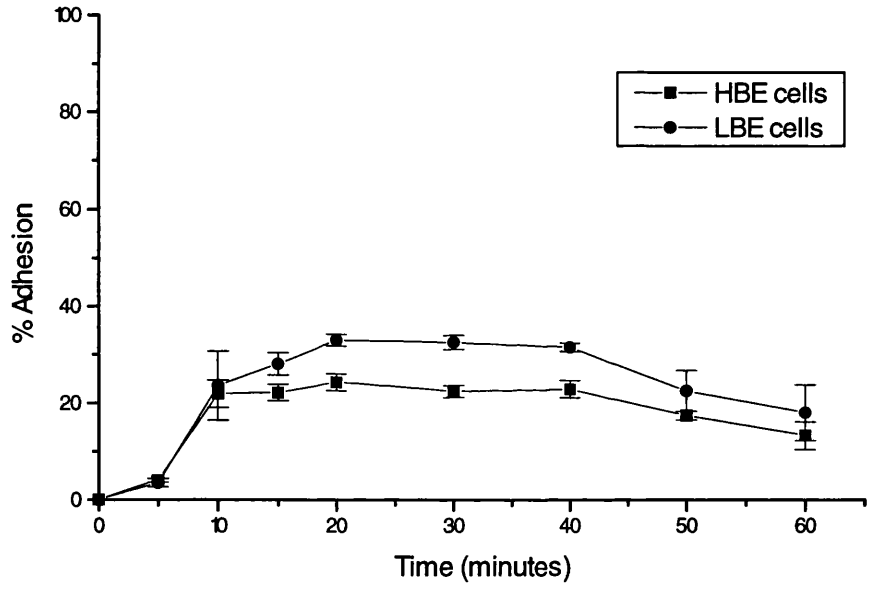

Fig 4.10 relative adhesion of sorted B16a populations to fibrinogen coated wells (1.56μg/cm^2) over time. Emission of cells is standardised by comparison with emission of cells added to wells coated with 1% BSA alone. Adhesion is represented as the percentage of emission of total cells added to wells, adjusted by emission of cells adhered to BSA coated wells. Each point represents the mean γ emission of cells adhered to coated wells minus the mean γ emission of cells adhered to BSA coated wells (n=4) divided by the mean γ emission of total cells (n=8) ± standard deviation between samples of adhered and non-adhered cells. These data are representative of two replicated experiments.

The rate of cell attachment to fibrinogen coated surfaces are as rapid as that of attachment to fibronectin (Figure 4.10). Cells are maximally bound to 96-well plates after 20 minutes, with the majority of cells attaching within 10 minutes. However, adhesion of cells to fibrinogen is at a lower level than adhesion to fibronectin. Repeats of this experiment failed to produce any reproducible differences between HBE and LBE cell attachment.

4.2.4. Spreading of B16a cells upon surfaces coated with fibronectin

Assays were carried using protocols described in section 2.30.3. Six well-plates were coated with 0.24μg/cm^2 fibronectin and cell morphology studied over a 120 minute time course. For clarity, only the first 30 minutes of the assay have been shown below, as cell morphology did not significantly change from 30-120 minutes in either cell population.

Figure 4.11 illustrates the differences in morphology between LBE and HBE cells when adhering to substrates coated with fibronectin over time. HBE cells show a considerably more spread morphology over time, with approximately 50% of cells flattening out and losing a well defined shape after 20 minutes. After 30 minutes, all HBE cells were seen to have attained a spread morphology upon the substrate. The majority of LBE cells did not spread considerably upon fibronectin over the time period studied. As indicated by the static assays described above, LBE cells adhere to fibronectin rapidly, however, the appearance of these cells once attached to substrate does not seem to significantly alter. The morphology of LBE cells was similar when coated to plastic (Fig 4.5) and is potentially linked to cellular ECM secretion (see discussion, section 4.5).

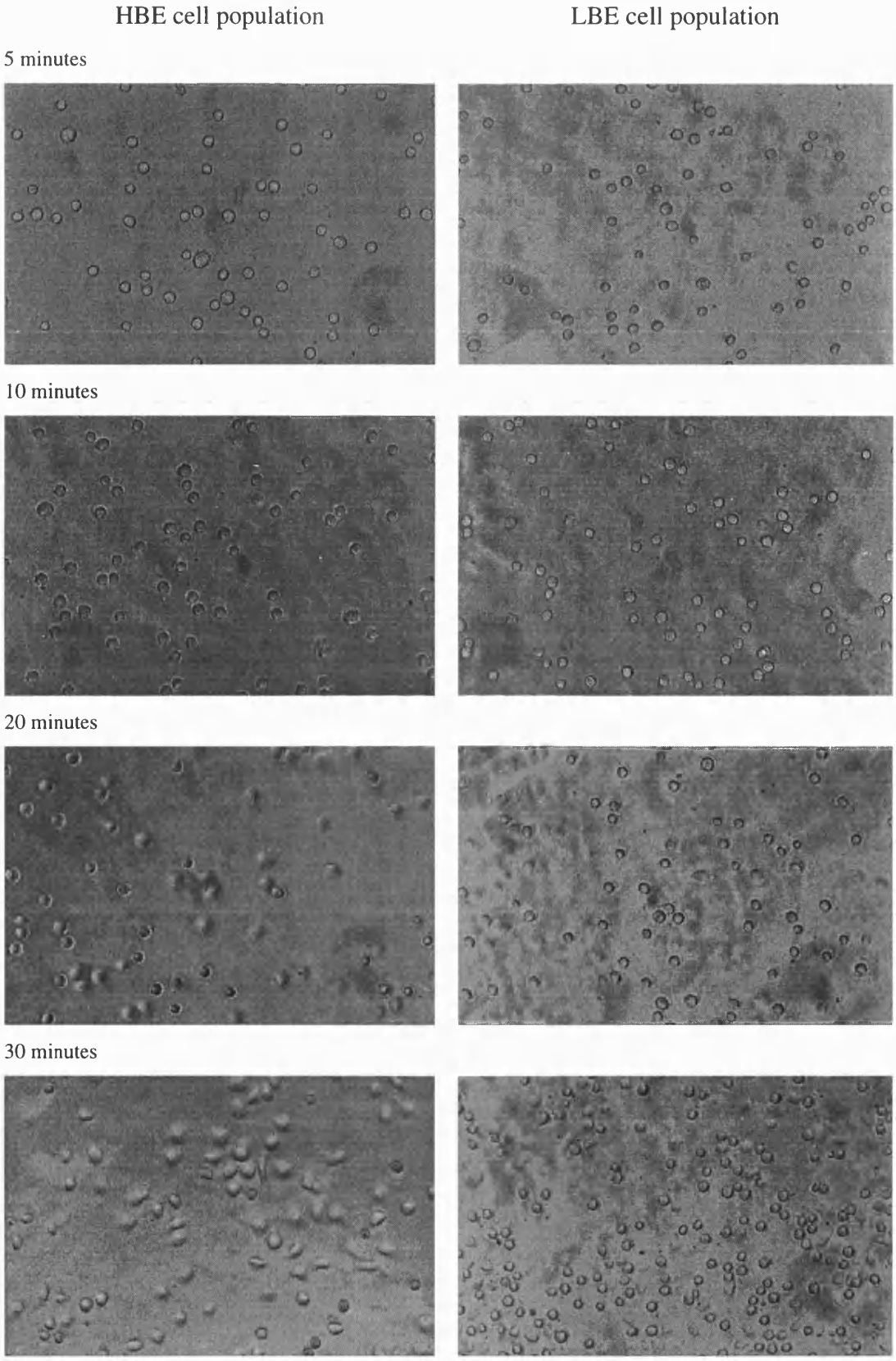

Fig 4.11 Spreading of sorted B16a populations on tissue culture plastic coated with 0.24μg/cm^2 fibronectin over a 30 minute time course. Cells are shown at x200 magnification. These photographs are representative of three replicate wells per time point.

4.3. Proliferation of FACS isolated B16a cell populations

Examination of the proliferation rates of both HBE and LBE B16a cell-lines was carried out using standard tissue culture conditions and uncoated tissue culture plastic substrates. A standard MTT assay (as described in section 2.28) was used to ascertain this growth within 96-well plates, determining the total number of viable cells at controlled time points. The effect of cell density upon this proliferation was additionally observed by carrying out a number of parallel assays, seeding wells with different starting concentrations of cells ranging from $1x10^3$ up to $5x10^4$ cells per 96 well-plate. Cells used for this study were both 2 passages from the original isolation of cells by FACS and harvested from semi-confluent flasks.

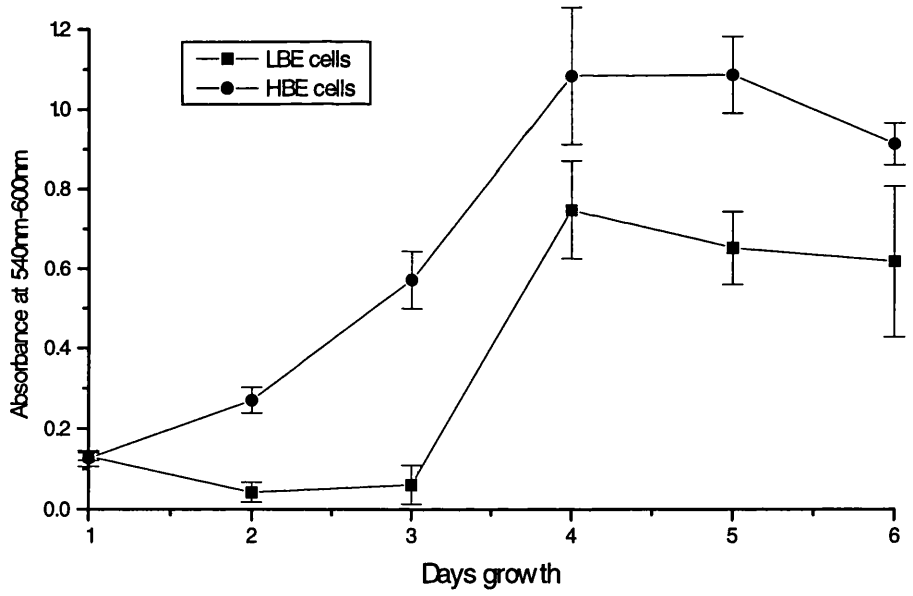

Fig 4.13 MTT assay of B16a sub-populations showing B16a cell proliferation from an initial seeding concentration of $1x10^3$ cells per well. Data points represent mean absorbance ± standard deviation of the mean (n=8). Difference in cell number is statistically significant to a level of $p<0.001$ (with 14 degrees of freedom) at all points after day 1. These data are representative of six assays carried out at seeding densities of $1x10^3$ cells per well to $5x10^4$ cells per well.

Figure 4.13 shows the rate of growth of LBE and HBE cells from a low initial number of cells. An apparent difference between cell lines was observed at all seeding concentrations, although saturation of the well plate occurred much more rapidly at higher concentrations. Using a low initial number of cells, LBE cells appear to exhibit a significant "lag period" before any increases in cell number. The overall saturating cell density at longer time periods also appeared to be lower with LBE cells.

4.4 Characterisation of β3 expression on the surface of human A375 melanoma cells using FACS.

Examination of B16a cells under the influence of antisense β3 vectors lead to further experiments with these vectors in a human melanoma cell line, A375 (detailed in chapter 6). Due to time limitations, characterisation of β3 expression was limited to only brief FACS analysis of these cells using antibodies specific for human β3 and αv. FACS analysis was carried out using a standard labeling protocol as described in section 2.31.

Previous reports have suggested that A375 cells express integrin αvβ3 and that this integrin is closely linked to a metastatic phenotype (Seftor *et al.*, 1992). A375 cells were obtained as a parental ("wild type") cell line A375P cells and a highly metastatic sub-line of parental cells, A375MM cells. These were isolated by harvesting cells from secondary tumours, grown from injection of A375P cells into immunocompromised mice (carried out by Dr A Fabra, Cancer Research Institute, Hospital Duran I Reynals, Barcelona, Spain).

Detection of surface αv was carried out using a mouse anti-human αv IgG1, P2W7 at dilutions of 1:100-1:500. Detection of surface β3 was carried out using a mouse anti-human β3 IgG1, Y2/51 at dilutions of 1:50. An R-phycoerythrin (RPE) conjugated $F(ab')_2$ fragment of goat anti-mouse IgG was used as a secondary labeling antibody for both P2W7 and Y2/51 in dilutions of 1:20. FACS profiles for these cells are displayed in a similar format to those shown in section 4.1, although PE labeled cells have a longer fluorescence emission waveband than FITC labeled cells. Fluorescence is therefore measured in the FL-2 emission range of 575 ± 13nm. The unshaded region of each profile indicates the degree of fluorescence of cells labeled with mouse IgG1 negative control at the same dilution as primary antibodies, followed by labeling with a 1:20 dilution of RPE conjugated anti mouse $F(ab')_2$ fragment of IgG1.

Figure 4.14 overleaf, shows that A375MM cells appear to express more αv and β3 subunits than their parental cell line, A375P. Both cell lines appear to exhibit higher levels of cell fluorescence after FACS analysis than the level of fluorescence from B16a cells for the murine β3 subunit. Whether this is due to higher intensity of fluorescene from RPE labeled antigen, or due to a larger number of surface receptors is unclear.

Examination of the morphology of A375 cells reveals significant differences to that of B16a cells. The metastatic A375MM cells can be seen to express higher levels of integrin αvβ3 than A375P cells, however, parental A375P cells are a highly adherent cell line while their metastatic counterpart are only weakly adherent in normal tissue culture conditions. This appears to be in direct contrast to the adhesive

profiles of B16a cells in normal tissue culture conditions and upon ECM protein substrates.

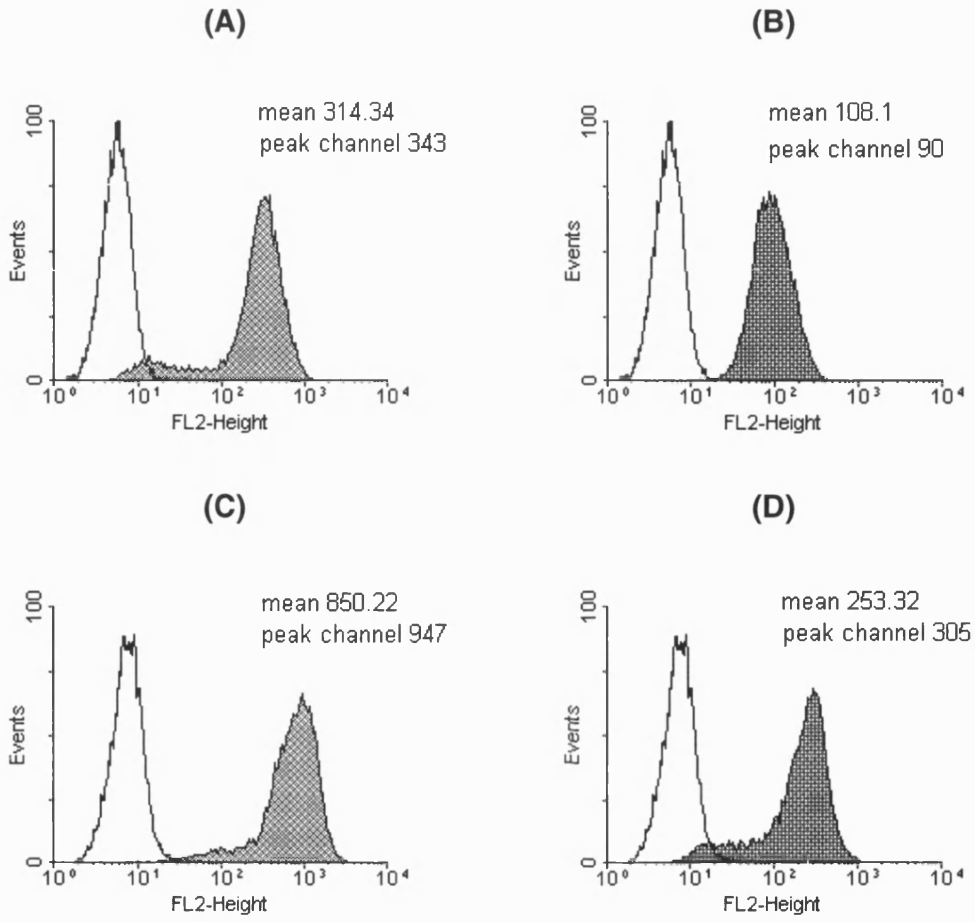

Fig 4.14 FACS analysis of integrin αvβ3 surface expression upon human melanoma A375P and A375MM cell lines (n=2). The shaded area represents the fluorescence of cells treated with either mAb P2W7 for αv (dark shading) or Y2/51 for β3 (light shading). The unshaded area represents non-specific fluorescence of cells treated with mouse IgG1 negative control. (A) Scan of A375P cells for the αv integrin subunit. (B) Scan of A375P cells for the β3 integrin subunit.. (C) Scan of A375MM cells for the αv integrin subunit. (D) Scan of A375MM cells for the β3 integrin subunit. These data are representative of two replicated experiments.

4.5 Discussion

FACS analysis appears to be an excellent system for the detection of β3 integrin expression upon the surface of B16a cells and selection of cells on this basis. Monoclonal antibody Hmβ3 binding was not affected by the use of trypsin, or by the presence of soluble ligand, indicating that it is not an inhibitor of ligand binding, nor is it binding to a ligand induced binding site.

Sorting of wild type B16a cells on the basis of β3 expression generated stable (at least up to 6 passages) cell populations with distinctly different behavioural patterns. The specificity of selection of murine cell populations on the basis of β3 expression, however, was difficult to establish without further FACS analysis of other murine α and β integrin subunits and this must be taken into consideration when judging these results. Integrins known to be present on the surface of B16a cells include β1, α3 and α5 (Chen *et al.,* 1992b; Qian *et al.,* 1994) - all of which may have contributed to the adhesive and signaling profile of these cells.

Changes in β3 surface expression in B16a cells appeared to have dramatic effects upon cellular morphology and ability to spread upon fibronectin. The spread, dendritic appearance of HBE cells indicated the formation of focal contacts by the clustering of integrin receptors to ligand. LBE cells were much less willing to spread upon fibronectin and had a considerably more spherical appearance, suggesting adhesion of a less focal nature. These morphological differences were found to be independent of the nature of cell substratum used, be it a ligand for αIIbβ3 or tissue culture plastic. However, adhesion of cells to tissue culture plastic in itself may

increase cellular synthesis of ECM proteins and even expression of integrins (Streuli and Bissell, 1990; Delcommenne and Streuli, 1995). Therefore it is likely that observed interactions were occurring between ECM ligands and integrins even when they were examined "on plastic".

In direct contrast to observed differences in cell spreading, the static adhesion of HBE and LBE cells to fibronectin or fibrinogen was not significantly changed. Although significant differences between HBE and LBE cells were observed at some individual points of timed assays (figures 4.8 and 4.10), repeats of these experiments failed to reproduce any significant differences. Assuming that HBE and LBE populations were specifically isolated on the basis of β3 expression, the high level of binding of cells to fibronectin was most likely due to the expression of other adhesion molecules. Both integrin α5β1 and α3β1 have an affinity for fibronectin (via the RGD motif). It is therefore possible that these (or other) integrins present in significant numbers on the surface of B16a cells mediate adhesion to fibronectin. The spreading and morphological effects suggest that integrin αIIbβ3 may have a significant role in the formation of focal adhesive contacts leading to ligand-induced cell spreading through signal transduction.

Both HBE and LBE cell lines bound with poor efficiency to fibrinogen. Since αIIbβ3 is reported to be the major receptor integrin for this ligand (Ginsberg *et al.*, 1983) it is not clear why no differences were observed between HBE and LBE cells. One possible explanation is that αIIbβ3 integrins expressed by HBE cells were not presented in a high affinity state. However, a counter-argument is that αIIbβ3 has a high affinity for insoluble matrices (but not soluble ligand) of fibrinogen which is independent of activation state (Sims *et al.*, 1991). Another consideration is that

fibrinogen has a QAGDV motif which is specific for αIIbβ3, however, it also contains two RGD sequences in its α chain and these can mediate adhesion through other integrins (Cheresh *et al.,* 1989). Another possible explanation for the lack of difference in binding between HBE and LBE cells for either ligand could be that integrin αIIbβ3 is not expressed in significant enough numbers on the surface of B16a cells (even in the sorted HBE line) to influence primary binding to ligand.

Differences in static ECM adherence have been commonly reported using B16a cells (and other melanoma cell lines, such as A375, Seftor *et al.,* 1992) with highly metastatic and poorly metastatic potential (Chang *et al.,* 1992; Honn *et al.,* 1992). Often, these changes in B16a cells have been correlated with altered αIIbβ3 integrin expression. However these alterations in static adhesion are possibly the result of large-scale differences in the expression of a number of different adhesion molecules. The process of FACS selection for β3 expressing cell populations used here results in cell lines isolated on the basis of a single cell marker, not on the basis of *in vivo* tumorigenicity, and is possibly a more powerful tool for the specific characterisation of individual integrin function in tumour cells. This differences observed between cells isolated by different methods shall be discussed further in chapter 7.

Although αIIbβ3 modulation does not appear to alter static adhesion profiles it does have a clear affect upon ligand-integrin associated signaling events such as focal adhesion formation and proliferation. LBE cells showed a reproducible reduction in the ability to proliferate on tissue-culture plastic, at all seeding densities, but particularly at low density. This may be an effect of integrin-related ECM matrix synthesis (Streuli and Bissel, 1990), or due to increased activation of specific signal

transduction pathways in cells selected for high β3 expression. Rates of growth on ECM protein matrices were not determined, but could possibly have an effect upon these differences in proliferation rate.

Numerous reports in the literature have indicated that activity of αIIbβ3 in B16a cells is a close parallel to that of αvβ3 integrin in a number of human melanoma cell lines (Chang *et al.* 1992, Honn *et al.* 1992). Characterisation in this study of A375 cells with different lung-colonising ability agreed with this pattern of expression in that A375MM cells expressed significantly more αvβ3 than their less metastatic counterpart. However, the A375MM cell had a much less adherent phenotype despite reports that they are significantly more invasive (Seftor *et al.,* 1992). The data suggest that αIIbβ3 and αvβ3 may have similar roles in the progression of these two melanoma though they may function in a significantly different manner. Though integrins may have different mechanisms for their separate roles in malignancy, it is clear that β3 integrins have an important role in tumour progression. The data presented here additionally identifies a number of quantitative markers for the down-regulation of β3 expression in B16a cells.

Chapter 5: Treatment of melanoma cells with antisense mRNA against β3 integrins

The aim of this chapter is to ascertain the efficiency and efficacy of using antisense β3 constructs for the down-regulation of integrin β3 expression. Work carried out below details the generation of a number of antisense β3 fragments and ligation into mammalian expression vector pcDNA3. Transfection studies were subsequently carried out using B16a and A375 melanoma cells, and the transient effect of this treatment upon integrin expression was investigated using FACS analysis. Further studies have been carried out, using the antibiotic selection facility of pcDNA3 based vectors to select for stable polyclonal B16a transfectants using the neomycin analogue geneticin (G418). Further studies have been carried out using these polyclonal populations to study the effect of antisense β3 constructs upon total β3 expression and tumour cell proliferation.

5.1. Cloning of antisense β3 cDNA constructs into pcDNA3

The human integrin β3 cDNA clone, CD3A, obtained from Dr. Joseph Loftus is described in section 2.2. Samples of CD3A were obtained as lyophilized vector which was resuspended with 20μl of sterile water. A 1μl aliquot of this solution was transformed into host strain *E. coli* MC1061/P3 as described in section 2.5 and vector isolated by miniprep before restrictional analysis with *Bst* XI and *Xba* I to verify presence of the β3 insert cDNA.

5.1.1. Cloning of an entire antisense β3 insert

The entire 3.9kb cDNA insert was cloned into pcDNA3 by endonuclease restriction of CD3A with *Xba* I and isolation of the insert from a 1% horizontal gel band using Geneclean. This was ligated into pcDNA3, restricted with *Xba* I and dephosphorylated using calf intestinal alkaline phosphatase as described (section 2.14). The ligation mix was transformed into host *E. coli* TOP10F' and transformed colonies isolated from LB amp/tet plates followed by minipreps from 10ml LB amp/tet cultures. Restrictional analysis of cloned plasmids identified two clones with opposing orientation, PC3A (β3 sense configuration) and PCa3A (β3 antisense configuration) (fig 5.1, fig 5.2).

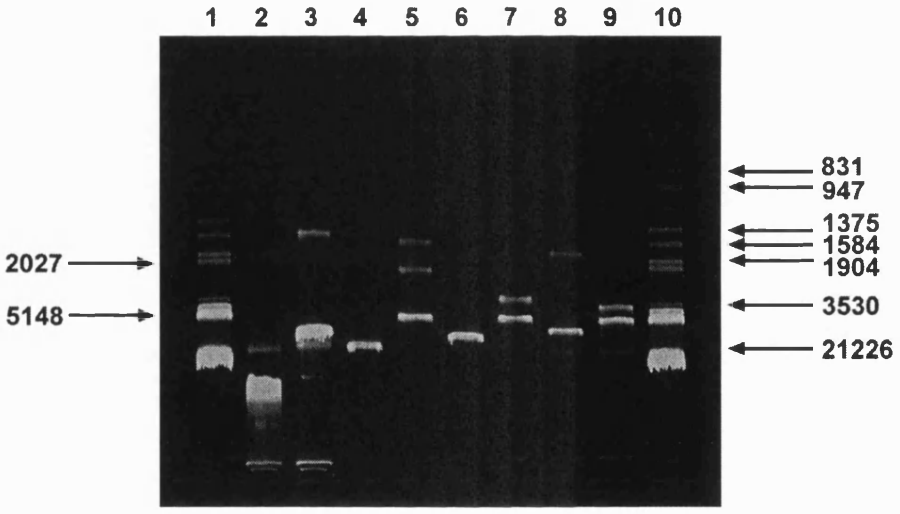

Fig 5.1 1% horizontal TBE agarose gel stained with 0.5μg/ml ethidium bromide showing restrictional analysis of PC3A (sense β3/pcDNA3) plasmid. From left, lanes 1&10 λ *Hind* III/*Eco* RI, lane 2 uncut plasmid, lane 3 *Bam* HI, lane 4 *Bgl* II, lane 5 *Eco* RI, lane 6 *Hind* III, lane 7 *Kpn* I, lane 8 *Not* I, lane 9 *Xba* I.

Figure 5.1 shows that restriction of PC3A with *Xba* I linearised pcDNA3 (5.4kb) and released the entire 3.9kb β3 insert. Restriction of CD3A with *Bgl* II cut the plasmid once, showing that the entire plasmid construct was approximately 9.3kb. Sequence analysis of the human β3 integrin cDNA using the MAP program contained in the GCG Wisconsin package indicated internal *Kpn* I, *Bam* HI and *Eco* RI

restriction sites at 505, 1500 and 2274bp respectively (chapter 2, figure 2.2). Both PC3A and PCa3A were restricted with these enzymes, giving information relating to the orientation of the β3 insert, described below.

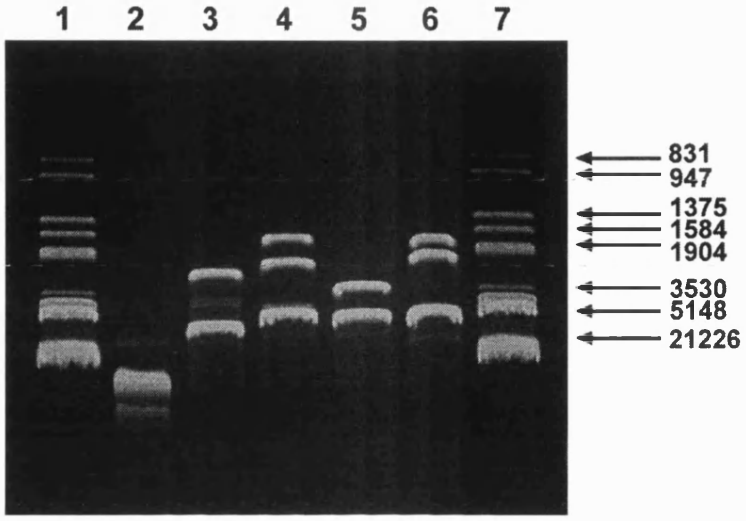

Fig 5.2 1% horizontal TBE agarose gel stained with 0.5μg/ml ethidium bromide showing restrictional analysis of PCa3A (antisense β3/pcDNA3) plasmid. From left, lanes 1&7 λ *Hind* III/*Eco* RI, lane 2 uncut plasmid, lane 3 *Bam* HI, lane 4 *Eco* RI, lane 5 *Kpn* I, lane 6 *Not* I.

Figure 5.2 shows a restriction analysis profile for endonucleases known to cut both pcDNA3 and the β3 insert. Comparison with figure 5.1 shows that restriction of PC3A with *Kpn* I released three bands of ~600bp (faint), ~3300bp and ~5400bp, while *Kpn* I restriction of PCa3A releases two visible bands of ~3300bp and ~5800bp. Since human β3 is known to have a *Kpn* I site at ~505bp, restriction of correctly orientated β3 insert (CD3A) would be expected to release a band of approximately this size (figure 5.1). As three bands are produced on this gel, it can be deduced that another *Kpn* I site must be present at the 3' end of the β3 cDNA insert. Endonuclease restriction with *Bam* HI and *Eco* RI also agreed with this pattern of insert orientation.

1.5.2. Cloning of pcDNA3 with partial antisense β3 inserts

To enable comparative studies for the relationship between antisense insert size and ability for these fragments to affect β3 expression, two smaller 5' fragments of β3 were isolated and cloned in a reverse direction into pcDNA3 using the endonuclease map information gained above. Two β3 fragments were created using double endonuclease restriction digests of 1μg of PC3A with either *Kpn* I/*Xho* I or *Bam* HI/*Xho* I. Subsequent isolation of the correctly sized fragment from a 1% TBE agarose gel was carried out using Geneclean. Approximately 1μg of these β3 fragments were then ligated into pcDNA3 as described, linearised with *Kpn* I/*Xho* I or *Bam* HI/*Xho* I and purified using Geneclean. Ligation mixes were transformed into host *E. coli* TOP10F' and amp/tet resistant clones isolated by miniprep. Restriction mapping of resulting vectors revealed the clones PCKpn3A and PCBam3A shown overleaf (fig 5.3).

Figure 5.3A shows that clone PCKpn3A is linearised when restricted with *Xho* I or *Kpn* I to reveal a single band of approximately 5800bp. Double restriction with *Xho* I/*Kpn* I released a ~5400bp pcDNA3 band and the ~500bp antisensed β3 fragment. Figure 5.3B shows that clone PCBam3A is linearised when restricted with *Xho* I or *Bam* HI to reveal a single band of approximately ~6800bp. Double restriction with *Xho* I/*Bam* HI released a ~5400bp pcDNA3 band and the ~1500bp intermediate sized antisensed β3 fragment. Both clones PCKpn3A and PCBam3A were engineered to include antisensed portions of the 5' end of β3, including the ATG start codon

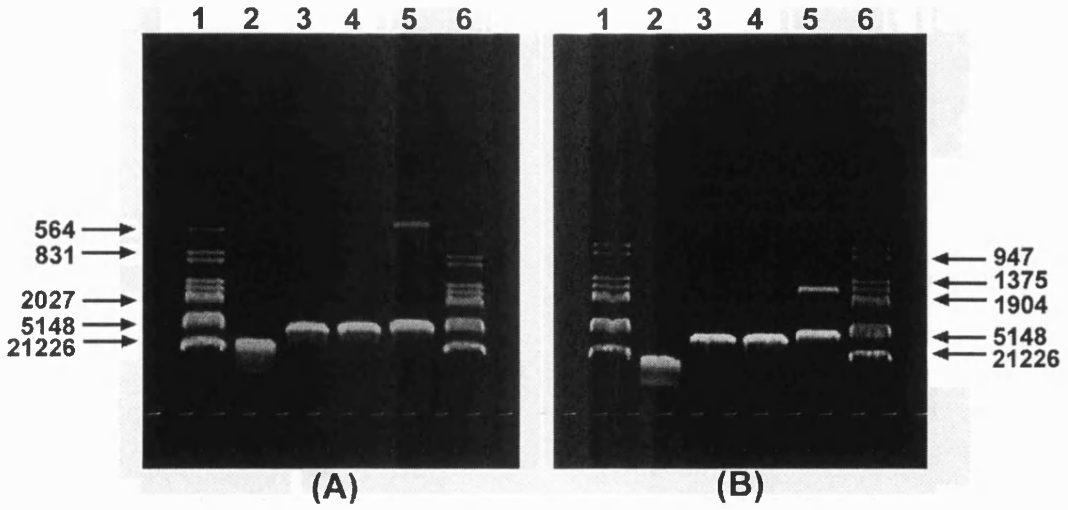

Fig 5.3 1% horizontal TBE agarose gel stained with 0.5µg/ml ethidium bromde showing restrictional mapping of antisense β3 fragment clones. (A) *Kpn* I antisense plasmid, PCKpn3A: lanes 1 & 6 λ *Hind* III/*Eco* RI markers, lane 2 uncut plasmid, lane 3 *Kpn* I, lane 4 *Xho* I, lane 5 double *Kpn* I/*Xho* I . (B) *Bam* HI antisense plasmid PCBam3A: lanes 1 & 6 λ *Hind* III/*Eco*RI markers, lane 2 uncut plasmid, lane 3 *Bam* HI restriction, lane 4 *Xho* I restriction, lane 5 double *Bam* HI/*Xho* I restriction.

5.2. Characterisation of transient expression of antisense β3 vectors

Electroporation is an effective method for the generation of high levels of transient expression of transfected DNA in mammalian cells (see section 6.1). B16a and A375 cells were both used to ascertain the short-term effectiveness of the antisense vectors cloned above, using FACS to determine surface expression of integrins 24-72 hours after electroporation.

5.2.1. Transient expression using B16a cells

Transfection experiments were carried out by electroporation of 20µg of antisense or control pcDNA3 vectors in supercoiled form (using Qiagen Maxipreps) as described in section 2.29 and using the optimised electroporation settings detailed in section 6.1. Surface analysis of β3 expression was then compared using FACS, labeling with mAb Hmβ3 and FITC labeled anti-hamster IgG. Expression of β3 was

measured at 24, 48 and 72 hours. Figure 5.4 illustrates β3 expression of B16a cells 48 hours after electroporation (i.e. the peak of transient expression as ascertained by transfection of cells with reporter vectors expressing β-galactosidase enzyme, section 6.1.3).

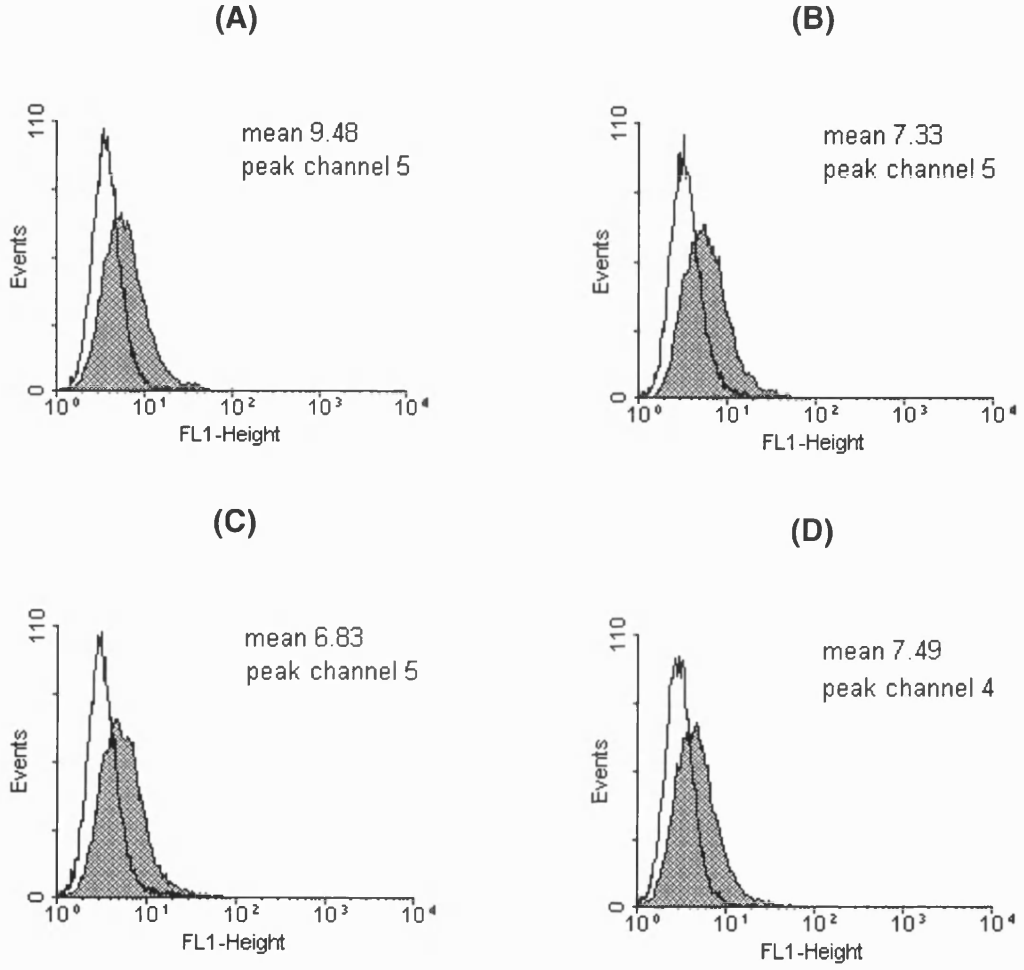

Fig 5.4 FACS analysis profiles showing surface expression of murine β3 integrin subunit from B16a cells 48 hours after transfection with antisense expression vectors, using Hmβ3 mAb and FITC conjugated anti-hamster IgG (shaded area). (A) Control cells transfected with pcDNA3. (B) B16a cells transfected with PCKpn3A plasmid. (C) B16a cells transfected with PCBam3A plasmid. (D) B16a cells transfected with PCa3A plasmid. The non-shaded areas represents non-specific binding of FITC conjugated anti-hamster IgG alone. These scans are representative of three experiments.

Figure 5.4 shows a small decrease in the level of B16a fluorescence by FITC labeled Hmβ3 in cells transfected with antisense β3 constructs. However, all cells

appeared to have reduced levels of murine β3 expression after electroporation. Levels of surface fluorescence of cells at 24 or 72 hour time points post electroporation also failed to show any additional decreases in surface expression of murine β3. Repeats of this assay failed to produce any more significant changes in β3 expression after transfection with antisense β3 constructs on a transient basis.

5.2.2. Transient expression using A375 cells

Transfection studies were carried out with both A375P and A375MM cell lines, examining expression of both human β3 (with mAb Y2/51) and human αv (with mAb P2W7) integrin subunits using FACS. Both antibodies were labeled with a secondary RPE-conjugated goat anti-mouse immunoglobulins as described in section 2.31. Optimisation experiments using electroporation were not carried out with A375 cells. However, using the same optimised electroporation settings as B16a (250μF/300V, see section 6.1) gave similar degrees of cell death (50-60%) which implied a similar level of electroporation efficiency.

Figure 5.5, overleaf shows that antisense DNA treatment of A375MM cells with the vectors constructed and using the electroporation protocol described failed to have a significant affect upon β3 or αv surface expression. Repeats of this experiment at 24 and 72 hours, or with A375P cells also failed to show any significant change in the surface expression of either integrin subunit.

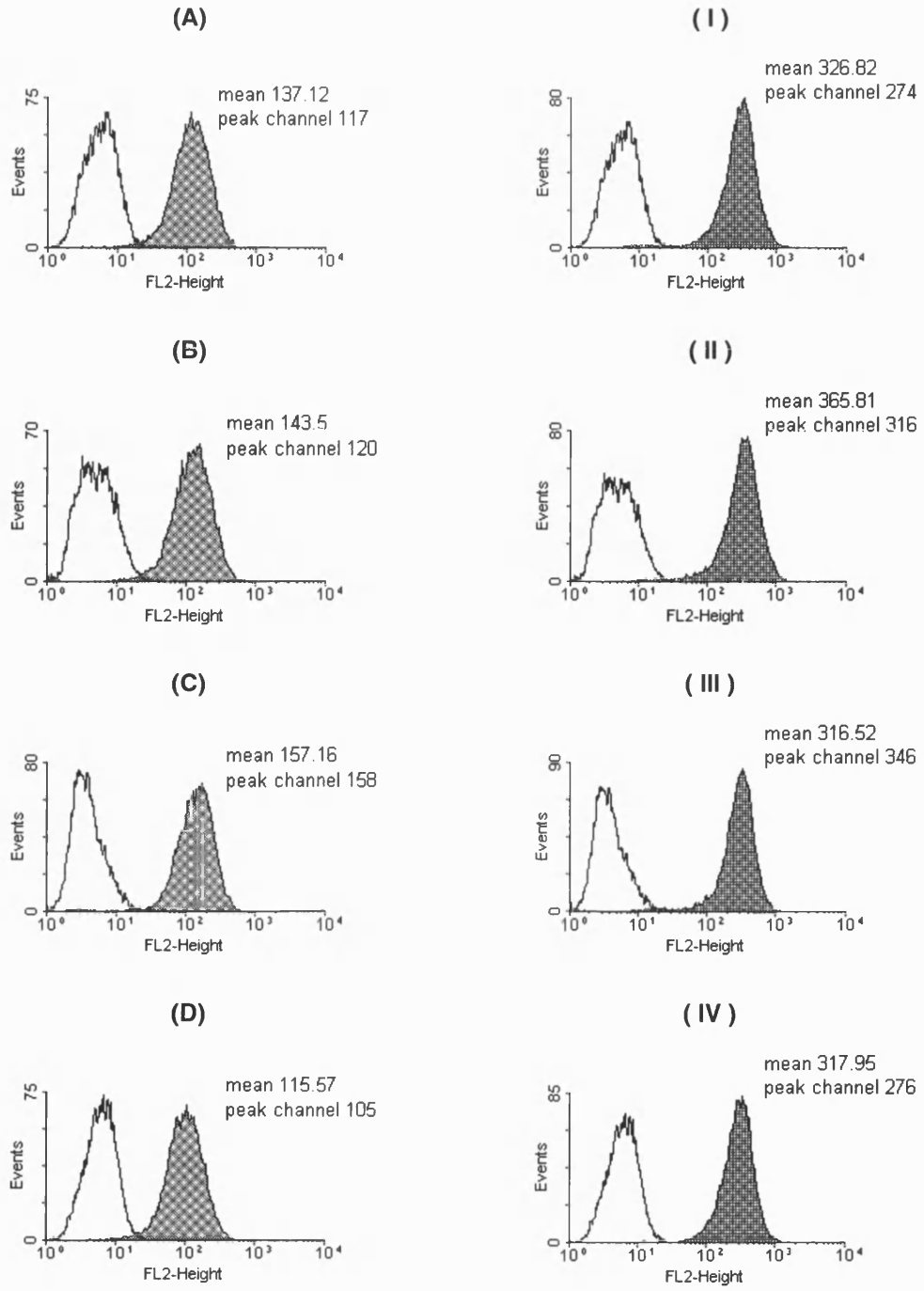

Fig 5.5 FACS analysis profiles showing surface expression of human αv and β3 integrin subunits in A375MM cells 48 hours after transfection with antisense expression vectors. (A-D) β3 expression as measured by FACS using mAb Y2/51 and RPE conjugated anti-mouse IgG1 (light shaded area). (I-IV) αv expression as measured using mAb P2W7 and RPE conjugated anti-mouse IgG1 (dark shaded area). In order from top: PCDNA3 control transfected cells, PCKpn3A transfected cells, PCBam3A transfected cells, PCa3A transfected cells. The unshaded area represents non-specific fluorescence of cells treated with mouse IgG1 negative control. These scans are representative of three experiments.

5.3. Stable transformation of B16a cells with β3 antisense constructs

Transfection of HBE B16a cells and isolation of G418 resistant polyclonal populations was carried out as described in section 2.29 with optimised electroporation settings. The HBE B16a cell line was electroporated with 20μg of plasmid linearised with *Bgl* II, and purified by phenol/chloroform precipitation of proteins (section 2.9). Transfected cells were treated with 1.5 mg/ml G418, added to MEM media 48 hours after electroporation. Resistant clones were ready for sub-culturing into 25cm^2 flasks after a 2-3 week period. Polyclonal populations consisted of approximately 10-30 separate clones, with two populations generated per standard electroporation of 1x10^7 cells. Polyclonal populations were subsequently grown in 1.5 mg/ml G418 and these cells were not used for studies after more than 10 passages from the isolation of original G418 resistant colonies.

5.3.1. FACS analysis of polyclonal stable transfectants

Standard FACS analysis was carried out as detailed, using murine β3 mAb Hmβ3 and anti hamster FITC IgG to detect surface β3 expression. Surface expression was measured as soon as polyclonal populations could be transferred to 75cm^2 tissue culture flasks. Cells were harvested from semi-confluent flasks, grown in the presence of 1.5 mg/ml G418.

Figure 5.6, overleaf indicates an apparent decrease in the mean fluorescence intensity of 44% to 49% of control pcDNA3 treated cell fluorescence. Repeats of these experiments with a second set of polyclonal populations showed a similar trend in downregulation, although the intensity of fluorescence from PCKpn3A cells often approached that of control pcDNA3 cells. The experiments detailed below aim to further clarify the effect of integrated antisense vectors upon integrin expression.

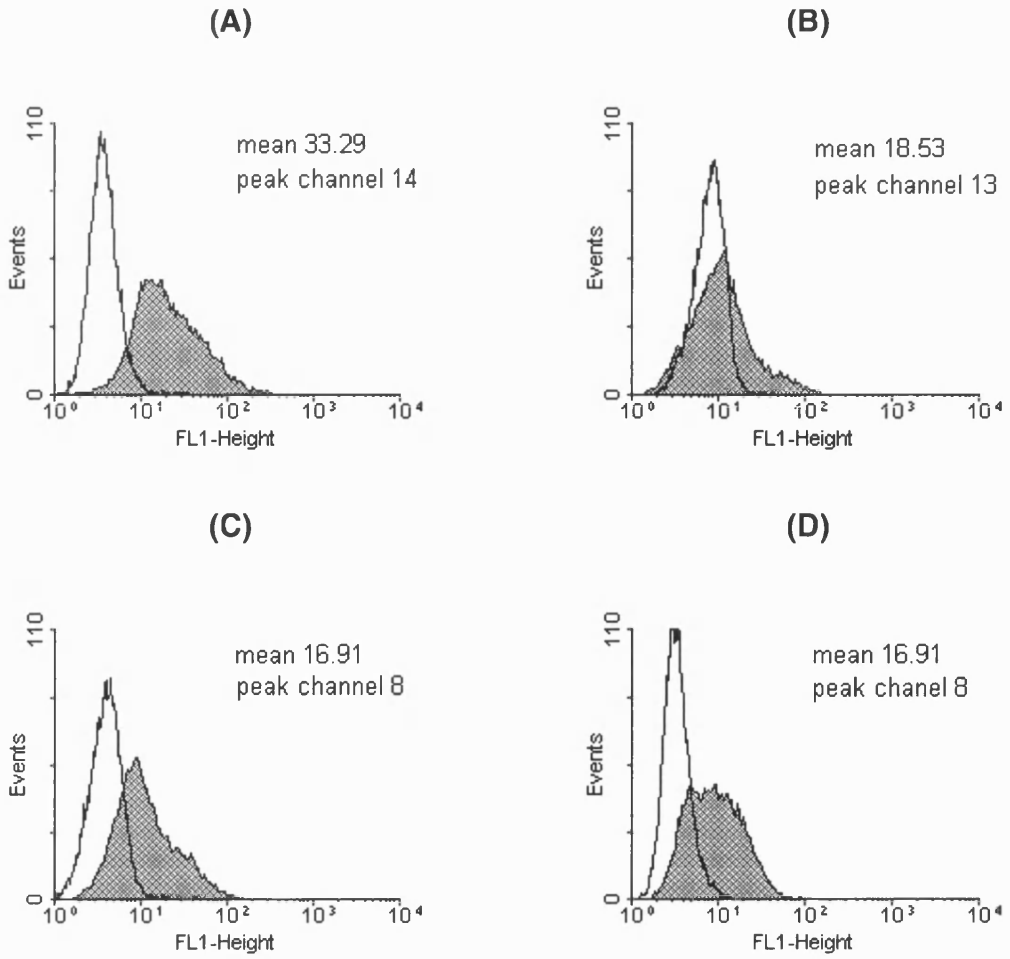

Fig 5.6 FACS analysis profiles showing surface expression of murine β3 integrin subunit from G418 stable polyclonal populations of B16a cells, detected using antibody Hmβ3 and FITC conjugated anti-hamster IgG (shaded area). (A) Control cells transfected with pcDNA3. (B) B16a cells transfected with PCKpn3A plasmid. (C) B16a cells transfected with PCBam3A plasmid. (D) B16a cells transfected with PCa3A plasmid. The non-shaded area of each profile represents non-specific binding of FITC conjugated anti-hamster IgG alone. These scans are representative of three experiments.

5.3.2. Western blotting of total protein extracts from stable transfectants for β3 integrin

Total protein lysate preparations were extracted from G418 resistant B16a cells and subsequent Western blotting was carried out as described in section 2.32. Semi-dry transfer of proteins to nitrocellulose membranes was carried out, using diluted Ponceau S to verify equal loading of proteins across samples. After transfer,

membranes were blocked with 10ml blocking buffer overnight before labeling murine β3 using 0.5μg/ml mAb Hmβ3. Antibody was detected using cross-reaction of antibody with a 1/10 000 dilution of horseradish peroxidase conjugated mouse immunoglobulins. After high stringency washing, blots were developed in ECL for 1 minute as described.

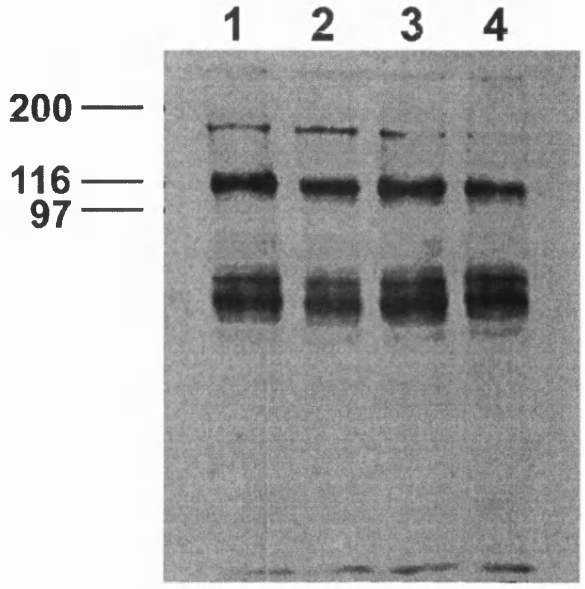

Sample	Mean OD	% Control pcDNA3 transfected cells
pcDNA3	0.859	-
PCKpn3A transfected cells	0.813	94.6%
PCBam3A transfected cells	0.878	102.2%
PCa3A transfected cells	0.807	93.95%

Fig 5.7 Western blot of total cell proteins isolated from polyclonal populations of B16a cells, probed for murine β3 protein using 0.5μg/ml Hmβ3 and a 1:10000 dilution of horseradish peroxidase conjugated goat anti-mouse IgG under reducing conditions. From left, lane 1 pcDNA3 transfected B16a cells, lane 2 PCKpn3A transfected cells, lane 3 PCBam3A transfected cells, lane 4 PCa3A transfected cells. Densitometry of β3 bands was carried out using a Bio-Rad densitometer and Molecular Analyst software (Bio-Rad).

Human β3 integrin subunits are known to hybridise at 105-110 kDa under reducing conditions. Figure 5.7 indicates that cross-reaction between Hmβ3 and

mouse immunoglobulins has isolated a band of approximately the correct size as the predicted murine β3 subunit. Densitometry of these bands revealed a potential decrease of up to 6.05% of band intensity in comparison to control pcDNA3 transfected cells. This level of reduction is small and for PC3A transfected cells (lane 4) could well be due to uneven edge effects of the SDS-PAGE gel. Accurate analysis of any statistics was not possible as this experiment was carried out once. The other bands shown on figure 5.7 are possibly non-specific hybridisation of detecting antibodies, or fragmented/polymerised β3 subunits.

5.3.3. Proliferation of stable transfectants

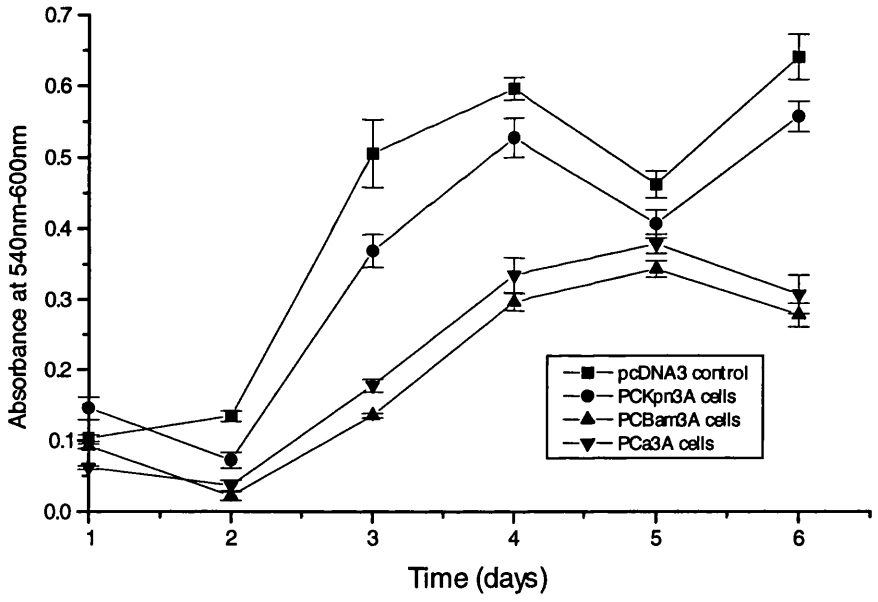

Fig 5.8 MTT assay of B16a cell number over time indicating the rates of proliferation of antisense treated polyclonal B16a populations in the presence of 1.5 mg/ml G418, seeded at a density of $2x10^3$ cells per 96 well-plate. Data points represent mean absorbance ± standard deviation of the mean (n=8). Difference in cell number is statistically significant to a level of $p<0.001$ (with 14 degrees of freedom) for PCBam3A and PCa3A cells from day 2 onwards. PCKpn3A cells are significantly different from control to a level of $p<0.05$ from day 3 onwards Proliferation data shown is representative of six experiments, seeding cells at different densities between $1x10^3$ to $1x10^4$ cells per well.

Sorting of B16a cells using FACS on the basis of β3 expression produced cell lines with highly divergent spreading and proliferation rates (section 4.3, 4.4). Proliferation of polyclonal G418 resistant B16a cells was examined using a standard MTT proliferation assay (section 2.28). All cell lines were seeded from semi-confluent flasks into 96 well-plates at a density of $1x10^3$ to $1x10^4$ cells per well. Assays were carried out over a 6 day period in the presence of 1.5mg/ml G418 (fig 5.8).

Figure 5.8 indicates that transfection of B16a cells with larger antisense β3 constructs (PCBam3A and PCa3A cells) did appear to have a significant effect upon cell proliferation rates. Parallel assays carried out with higher seeding densities of cells also showed a similar trend of growth. The data displayed above shows growth from a starting number of $2x10^3$ cells/well as this gave a good sigmoidal growth curve without premature confluency of wells. B16a polyclonal cells transfected with the larger antisense constructs (BamHI antisense, PCBam3A and total antisense, PCa3A fragments) appeared to not only proliferate at a slower rate than control cells, but also saturate the 96 well-plates at a lower density (much like LBE cells as shown in figure 4.13).

5.4 Discussion

The data presented above describes the generation of a number of antisense β3 expression vectors and their electroporation into human and murine melanoma cells. Analysis of the degree of inhibition of β3 synthesis and surface expression due to

these antisense vectors has lead to conflicting data of their efficacy and efficiency which are discussed below.

Transient expression studies using B16a cells (fig. 5.5), showed little sign of any significant antisense affect. Cells transfected in these studies showed a decrease in the expression of β3 subunits after electroporation, probably due to short-term recovery from the adverse effects of electroporation and introduction of high concentrations of exogenous DNA. B16a cells did not show high levels of surface β3 expression (using FACS), even when sorted to produce the HBE cell line. Therefore, the identification of significant levels of integrin downregulation was difficult using a transient expression system.

Further studies using transient expression of antisense vectors were carried out using the A375 cell lines described in section 4.5. Fluorescence intensities corresponding to both αv and β3 integrin subunits were much higher in this system. Additionally, as A375 is a human melanoma cell line, β3 integrin expressed in these cells carries 100% homology to the antisense vectors constructed, eliminating the problem caused by incomplete antisense homology to murine β3.

Expression of the αv subunit by A375 cells was examined to identify potential secondary effects of antisense β3 on α subunit expression. A number of reports have indicated that functional integrin heterodimer association occurs within the endoplasmic reticulum (ER) before secretion to the cell membrane. From studies of αIIbβ3, absence of a complementary integrin subunit results in retention of monomers in the ER (O'Toole *et al.,* 1989) and their eventual degradation (Kolodziej *et al.,* 1991). Therefore downregulation of complementary β3 integrin subunits (in the

absence of an excess of other complementary β subunits) could possibly result in a simultaneous αv downregulation.

In practice, no significant downregulation of either αv or β3 integrin subunit was observed at 24, 48 or 72 hours with either A375P or A375MM cell lines. Figure 5.5 indicates a typical expression profile of antisense transfected A375MM cells after 48 hours. This lack of significant effect in both A375 and B16a cells could possibly have been due to a time delay between antisense vector expression and observed changes in surface expression of integrins. The transient nature of gene expression in the majority of cells after electroporation results in cells being under an antisense influence for only limited periods. It is conceivable that a significant effect may have been present within another time window than the ones chosen. If for instance, the half-life of integrin receptors is longer than 72 hours, then little antisense reduction of β3 surface levels would be observed over the time course chosen. Some evidence against this theory was presented by Lallier and Bronner-Fraser, (1993) who used phosphorothioate oligonucleotides directed against α1 and β1 integrins in neural crest cells. These antisense oligonucleotides were seen to exhibit a maximal antisense effect 4-6 hours after administration. If the half-life of integrins is beyond 72 hours, transient reduction of their expression would be difficult to observe using the constructs tested. This would be due to a reduction of transient vector expression after 72 hours and eventual dilution of the plasmid-transfected cell population by daughter cells.

Another more likely explanation for the lack of antisense effect is that the level of transient expression of these antisense inserts was not large enough to have a discernible effect. Expression studies at optimum electroporation settings using the

control marker plasmid, pRSV*lac*Z showed high levels of β-galactosidase activity in B16a cells (as studied in section 6.1). However, this should not be regarded as a guarantee of a high level of expression of a different insert, driven by a different promoter.

Studies of β3 expression were also carried out using B16a cells transfected with antisense vectors and then selected for integration of transfected DNA by treatment with G418. Results presented in figure 5.6 indicate that the polyclonal populations examined appeared to exhibit a downregulation of β3 expression, which was more effective with larger antisense fragments. It must be noted however, that the absolute degree of this reduction is difficult to ascertain using FACS due to variation in the level of surface expression observed when measuring cell fluorescence, and the small degree of differences in cell fluorescence between some samples. Additionally, data presented in section 4.4 suggests that downregulation of β3 decreased proliferation rate of β16a cells *in vitro*. A possible consequence of this could be to decrease the proportion of cells expressing low levels of β3 in a polyclonal population, through rapid proliferation of unaffected cells. The studies conducted here using polyclonal populations were chosen to represent the effect of these antisense constructs upon a population of cells, simulating the activity that might be anticipated following treatment of a tumour *in vivo*. A potential method to more accurately ascertain antisense effects upon surface expression would be to study the effect of antisense constructs upon individual cells by isolation of colonies of cells after antibiotic selection using ring cloning. However, using this technique, care must be

taken to separate antisense activity against β3 expression against natural variation between cells from a polyclonal population.

Data obtained from immunoblotting (Western blotting) of total cell proteins with Hmβ3 antibody supported the view that the level of downregulation in these cells was limited. Figure 5.8 clearly indicates a prominent band with a molecular weight of approximately 110 kDa for each sample loaded, in agreement with β3 bands identified in B16a cells by Chen et al. (1992). No significant difference in the intensity of this band was identifiable in any of the immunoblots carried out for the different polyclonal populations generated. The significance of the other bands are not known, although are possibly due to non-specific hybridisation by Hmβ3 or hybridisation to dimers or polymers of β3.

Contradictory data was obtained when the proliferation of polyclonal populations was examined. All B16a antisense cell-lines grew at a slower rate on tissue culture plastic in the presence of G418 antibiotic than cells transfected with expression vector alone. Antisense insert size appeared to be inversely correlated with proliferation rate of B16a cells. This reduction in proliferation rate appears to mirror the observed proliferation data seen after sorting cells for a reduced β3 expression with FACS. The clear suggestion therefore is that in both experiments, reduction of β3 integrins in B16a cells reduces their proliferation rate.

It is possible that this reduction in proliferation, and observed differences in surface β3 expression are a consequence of non-specific antisense events. These could be directed against other β integrins, due to the large areas of homology between β integrin subunits or other unpredictable non-specific events. The incidence of these

non-specific events would be expected to increase with increasing antisense mRNA length. These arguments could be countered by performing further studies using these transfectants. Proliferation assays of transfected cells upon selected ECM matrices may help to deduce the specific nature of this downregulation. FACS analysis of the surface expression of other integrin subunits on transfected B16a cells may help to deduce non-specific inhibition of other endogenous integrin subunits. Also, using polyclonal cell populations transfected with other antisense integrin sequences with little homology to β3 as secondary controls, may give an insight into non-specific antisense effects. This type of experiment, however is potentially difficult to implement due to the high homology between integrin β subunits, and would be labour-intensive. These experiments were not conceivable within the timescale of this project, and given the low level of influence of the antisense β3 treatment on B16 and A375 cells, would be difficult to justify.

Chapter 6: Competitive inhibition of β3 integrins by transfection of cells with inactive β3 subunits

The aim of this chapter is to ascertain the efficiency and efficacy of using transfection of mutated β3 to competitively inhibit expression of functional β3 integrin heterodimers in melanoma cells. As discussed in section 3.5, failure to obtain an entire murine β3 cDNA has lead to an alternative plan of transfection of an inactive mutant of human β3 subunits into the B16a cell line.

This chapter includes transfection efficiency data to ascertain the effectiveness of the electroporation protocol used (section 2.29) in both B16a cells and the COS7 cells described below. It also includes details for the verification of a functional mutation in the clone CD3A D119A by nucleotide sequencing and its cloning, as well as that of the αv clone, VnRα into the expression vector pcDNA3. Transfection experiments have been carried out in a control expression system using the COS7 cell line, an SV40 transformed simian cell line containing the large T antigen (Gluzman 1981). This system replicates the vector and thereby amplifies the expression of any transfected gene when the vector includes the SV40 origin of replication. pcDNA3 includes this sequence which should lead to a positive control for the activity of integrin expression constructs on a transient basis.

Other transfection assays with inactive β3 subunits were carried out using B16a cells, and FACS analysis was used to verify the specificity of antibodies for the human β3 and αv subunits when expressed on the surface of murine B16a cells.

Efficiency of this expression was ascertained on a transient basis, and by isolation of stable polyclonal B16a populations using G418 as described.

6.1. Optimisation of electroporation of mammalian cells

Before any expression studies were carried out, a number of assays were studied in order to ascertain the efficiency of the transfection protocol used (as described in section 2.29). These assays included the use of FITC labeled dextran with FACS to quantify the degree of cell uptake of material after electroporation, the use of propidium iodide with FACS to ascertain the degree of cell death after electroporation and transfection of a reporter plasmid into cells to ascertain efficiency of gene expression after electroporation. Data obtained in this section also had direct implications upon the electroporation conditions used for antisense transfections, as detailed in chapter 5.

6.1.1. Determination of B16a cell uptake and viability after electroporation using FACS

B16a cells were electroporated with 0.5mg FITC/dextran as described in section 2.29.1. Studies were carried out using a number of electroporation voltage settings, ranging from 100-400V, with an associated capacitance range of 125-250μF. The extent of cell permeabilisation that these conditions caused was ascertained by measuring FITC-dextran uptake by cells, as quantified by FACS analysis of cell fluorescence in the FL-1 emission range.

Figure 6.1 shows that the degree of cell fluorescence increases considerably when using the higher capacitance setting of 250μF and higher voltage. Cell uptake of

dextran at the lower capacitance setting (125μF) was relatively small at all voltage settings.

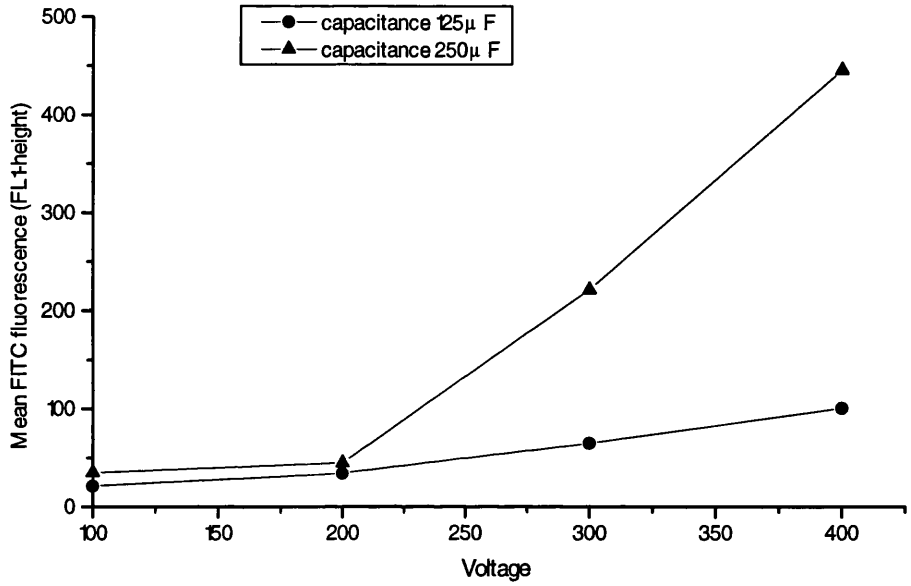

Fig 6.1 Graph showing mean FL-1 fluorescence obtained from FACS analysis after electroporation of $1x10^6$ B16a cells with of 0.5mg FITC labeled dextran as a function of electroporation settings. Fluorescence of cells was measured 4 hours post electroporation. This experiment was performed once.

Figure 6.2, overleaf, indicates that increased B16a uptake of FITC-dextran is closely mirrored by increased cell death, particularly at higher electroporation settings. Data shown in figure 6.2 does not give an entirely representative view of cell viability as propidium iodide does not identify cells fragmented by high voltage electroporation. The longer-term viability of B16a cells after electroporation was actually lower than the data above suggests, with approximately 20% B16a cells surviving 24 hours after a 250μF/400V electroporation. All subsequent electroporation experiments with B16a cells (including those detailed in chapter 5)

were carried out at 250μF/300V, corresponding to a reasonable FITC dextran uptake (mean FL-1 height 206.88) and approximately 50-60% long-term viability.

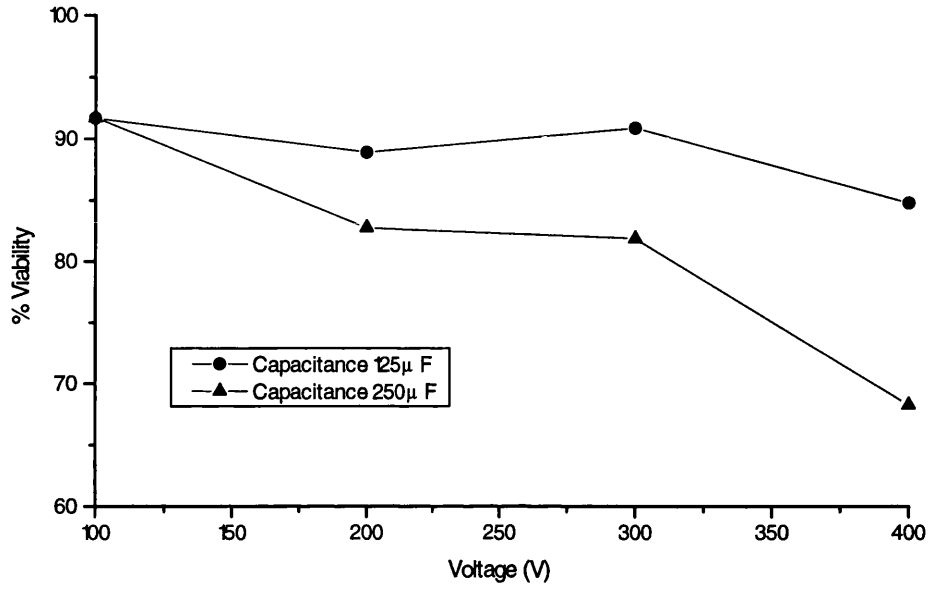

Fig 6.2 Graph showing viability of B16a cells obtained from FACS analysis after electroporation of $1x10^6$ B16a cells with of 0.5mg FITC labeled dextran as a function of electroporation settings. Degree of cell death was measured using FACS after addition of 100ng/ml propidium iodide and calculation of the proportion of the dead cells which had taken up PI, as measured by increased FL-2 fluorescence. This experiment was carried out once.

6.1.2. Determination of COS7 cell uptake and viability after electroporation using FACS

Efficiency of COS7 cell electroporation was estimated by carrying out a similar FITC-dextran electroporation procedure as described above. Figures 6.3 and 6.4 give an indication of cell uptake and cell viability at each electroporation setting.

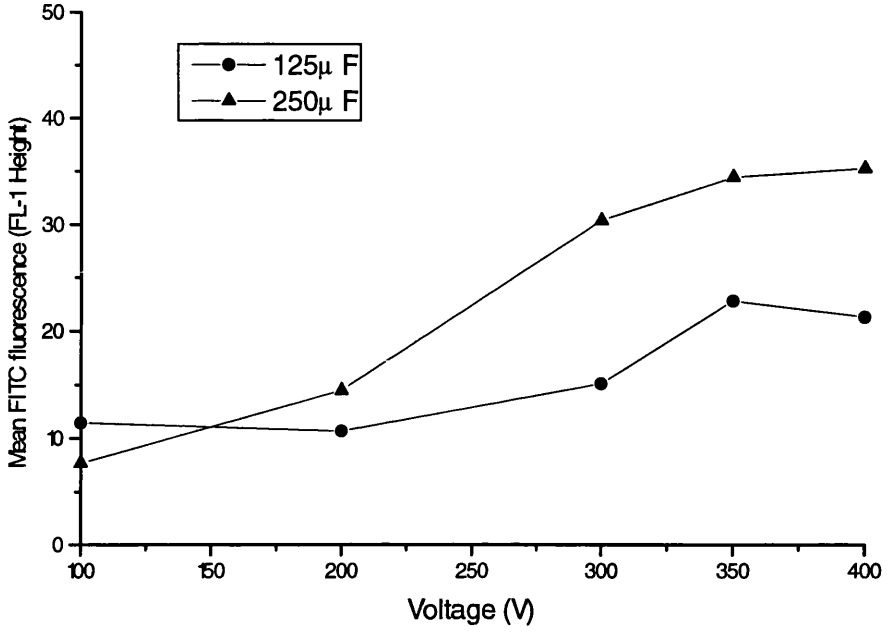

Fig 6.3 Graph showing mean FL-1 fluorescence obtained from FACS analysis after electroporation of $1x10^6$ COS7 cells with of 0.5mg FITC labeled dextran as a function of electroporation settings. Fluorescence of cells was measured 4 hours post electroporation. This experiment was carried out once

Figures 6.3 and 6.4 overleaf, show a similar picture of cell uptake and cell death using COS7 cells as seen with B16a cells. However, the degree of FITC-dextran fluorescence using COS7 cells is considerably lower than the corresponding cell fluorescence of B16a cells. Cell viability of COS7 cells after electroporation appears more erratic than B16a cells, although the trend of decreasing survival with increasing voltage and capacitance appear similar. The erratic nature of COS7 cell viability after transfection with FITC-dextran could possibly be due to poorly suspended cells in clumps protecting cells from electroporation. COS7 cells were seen to have a much higher long-term survival rate with ~50% of cells surviving 24 hours after a 250μF/400V electroporation.

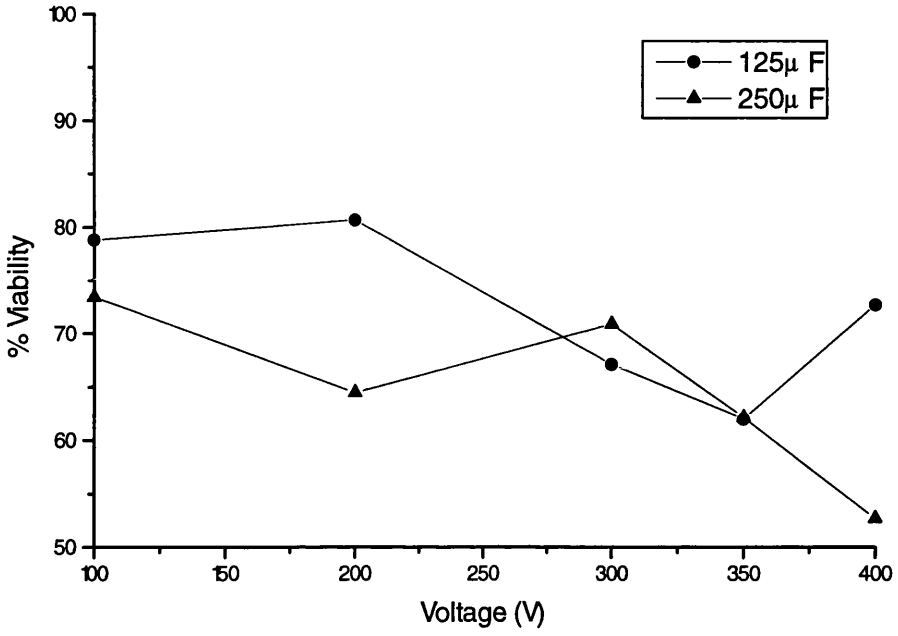

Fig 6.4 Graph showing viability of COS7 cells obtained from FACS analysis after electroporation of $1x10^6$ B16a cells with of 0.5mg FITC labeled dextran as a function of electroporation settings. Degree of cell death was measured using FACS after addition of 100ng/ml propidium iodide and calculation of the proportion of the dead cells which had taken up PI, as measured by increased FL-2 fluorescence. This experiment was carried out once.

6.1.3. determination of electroporation efficiency using β galactosidase expression

A secondary method utilised to ascertain the efficiency of electroporation settings was transfection the reporter vector, pRSV*lacZ* expressing the β-galactosidase enzyme as described in section 2.29.3. Both B16a cells and control COS7 cells were used in this assay, with optimised electroporation settings obtained through FITC-dextran electroporation.

Figures 6.5 and 6.6 overleaf, show that the degree of β-galactosidase expression is roughly the same in both cell types. Maximal expression was seen at 48 hours using either cell line, with maximal expression equating to approximately 50-

60% blue cells. Few cells were seen to carry β-galactosidase activity 24 hours after electroporation, presumably due to the time delay between electroporation and cellular recovery. The intensity of colour seen after treatment of COS7 cells was notably greater than that seen with B16a cells.

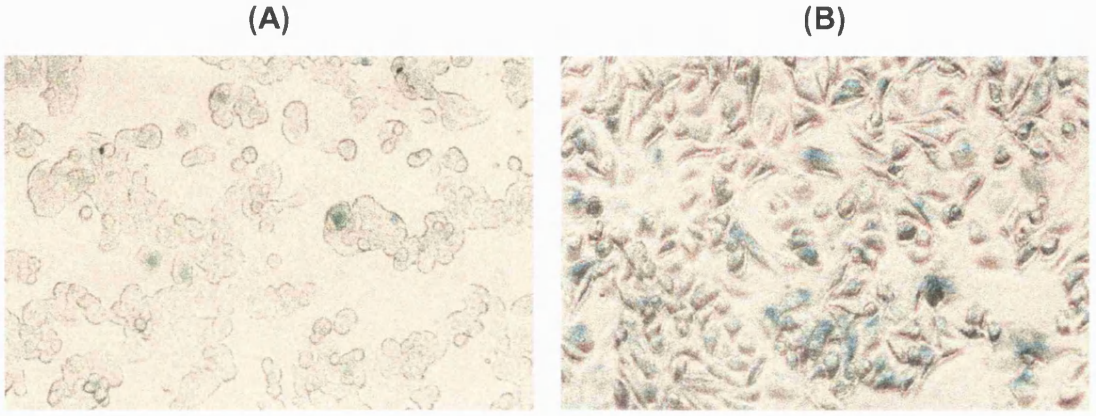

Fig 6.5 Photographs showing B16a cells, fixed and treated with X-Gal solution overnight after electroporation with 20μg pRSV*lac*Z at 250μF/300V. (A) 24 hours post-transfection. (B) 48 hours post transfection. Cells are shown at magnification x300. Cells positive for β-galactosidase activity appear blue after X-Gal treatment.

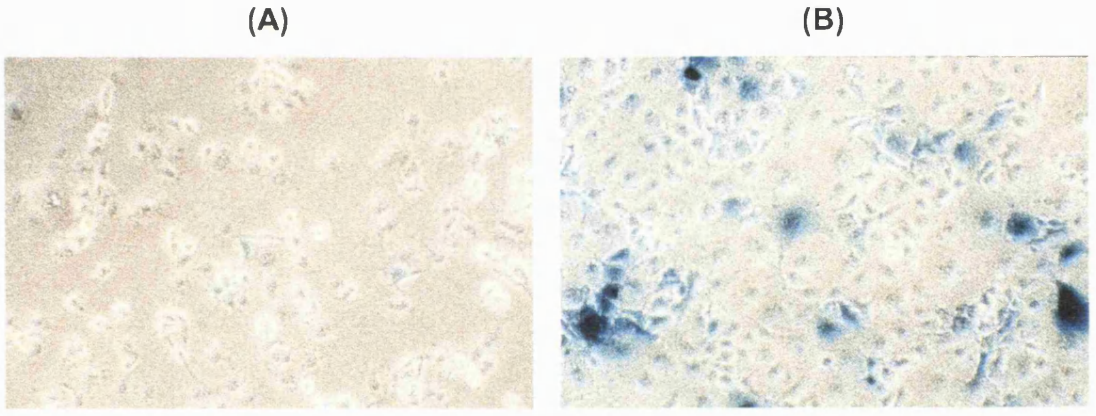

Fig 6.6 Photographs showing COS7 cells, fixed and treated with X-Gal solution overnight after electroporation with 20μg pRSVlacZ at 250μF/400V. (A) 24 hours post-transfection. (B) 48 hours post transfection. Cells are shown at magnification x300. Cells positive for β-galactosidase activity appear blue after X-Gal treatment.

6.2. Verification of mutation of CD3A D119A by nucleotide sequencing

Nucleotide sequencing of the ligand-binding domain (D109-E171, section 1.2.3.) of human β3 clones CD3A and CD3A D119A was carried out using the dideoxy chain-termination method described in section 2.15. Double stranded templates were generated from minipreps of MC1061/P3 cells containing the plasmids of interest, (section 2.15.2) and 1μg of each template was used in an annealing reaction to an oligonucleotide primer designed for homology with a cDNA sequence downstream (3') of the ligand binding domain:

LBS1- 5'-AAGCCAATCCGCAGGTTAC-3'

This 19-mer is homologous to the 3' sense strand of human β3 at positions 556-537 of the cDNA and has a GC content of approximately 50%.

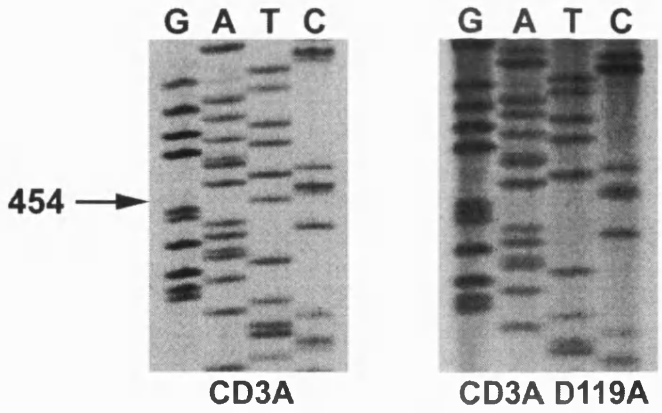

Fig 6.7 Nucleotide sequencing of the ligand binding domain of human β3 cDNA clones CD3A and CD3A D119A. The arrow indicates the position of a T→ G mutation.

Figure 6.7 displays portions of the two sequencing gels obtained using the oligonucleotide primer described. The arrow at position 454 indicates a point mutation in the sequence of clone CD3A D119A from T→G resulting in a codon

change from alanine to aspartic acid at A^{119}. Similar mutations of this position giving an $A^{119} \rightarrow Y^{119}$ substitution (Loftus *et al.*, 1990) have been shown to result in a loss of ligand recognition. The replacement of a non-polar alanine with a highly charged acidic aspartic acid residue will therefore function by a similar mechanism to that described where substitution at this point is with a polar tyrosine group.

6.3. Cloning of integrin subunits into pcDNA3

Clone CD3A D119A was ligated into pcDNA3 in an identical manner to that used for clone CD3A described in section 5.1. Briefly, *Xba* I restriction of CD3A D119A released a ~3.9Kb cDNA insert which was cloned into pcDNA3 restricted with *Xba* I and dephosphorylated using alkaline phosphatase. Orientation of the subsequent pcDNA3 clone, PC3A D119A was verified by restriction mapping, identical to that carried out in section 5.1.

Clone VnRα contains a ~4kb cDNA fragment inserted into the *Eco* RI site of pBluescript SK. Lyophilised vector was reconstituted into 20µl sterile water and a 1µl aliquot of this solution was transformed into host *E. coli* XL1-Blue MRF' as described in section 2.5. Vectors were isolated by miniprep and orientation verified by restrictional analysis. The entire cDNA insert was directionally cloned into pcDNA3 by double endonuclease restriction of 1µg VnRα with *Not* I and *Kpn* I. This freed a ~4kb cDNA insert which was removed from a 1% horizontal agarose gel using Geneclean and ligated into 1µg pcDNA3 restricted with *Not* I / *Kpn* I and similarly gel-purified with Geneclean. The ligated clone, PCVnRα was verified by restriction mapping.

6.4. Transient expression of integrin subunits

Transient expression studies were carried out using both B16a and control COS7 cell lines at optimal electroporation settings as described in section 6.1. Initial expression studies were carried out using the COS7 cell line in order to verify activity of the pcDNA3 expression constructs cloned in sections 5.1 and 6.2. Control transfections were carried out using β3 integrin constructs PC3A and PC3A D119A and the effect of dual transfection with a complimentary αv subunit using PCVnRα was also studied.

6.4.1. Transient expression in COS7 cells

Transfections were carried out using 20μg of supercoiled pcDNA3, PC3A, PC3A D119A or PCVnRα plasmids, obtained by maxiprep, in a standard transfection protocol under optimal electroporation conditions (see section 6.1). Each transfection was carried out using the contents of one semi-confluent 175cm^2 tissue culture flask and cells were analysed by FACS 24-72 hours after transfection. Antibodies used for this analysis were the same as those used for detection of human subunits on A375 cells (section 4.5). Therefore, β3 detection was carried out using mouse anti-human β3 IgG1, Y2/51 and RPE conjugated F(ab')$_2$ fragment of goat anti-mouse IgG. Detection of surface αv was carried out using mouse anti-human αv IgG1, P2W7 with the same RPE secondary antibody. Fluorescence was measured in the FL-2 range of light emission.

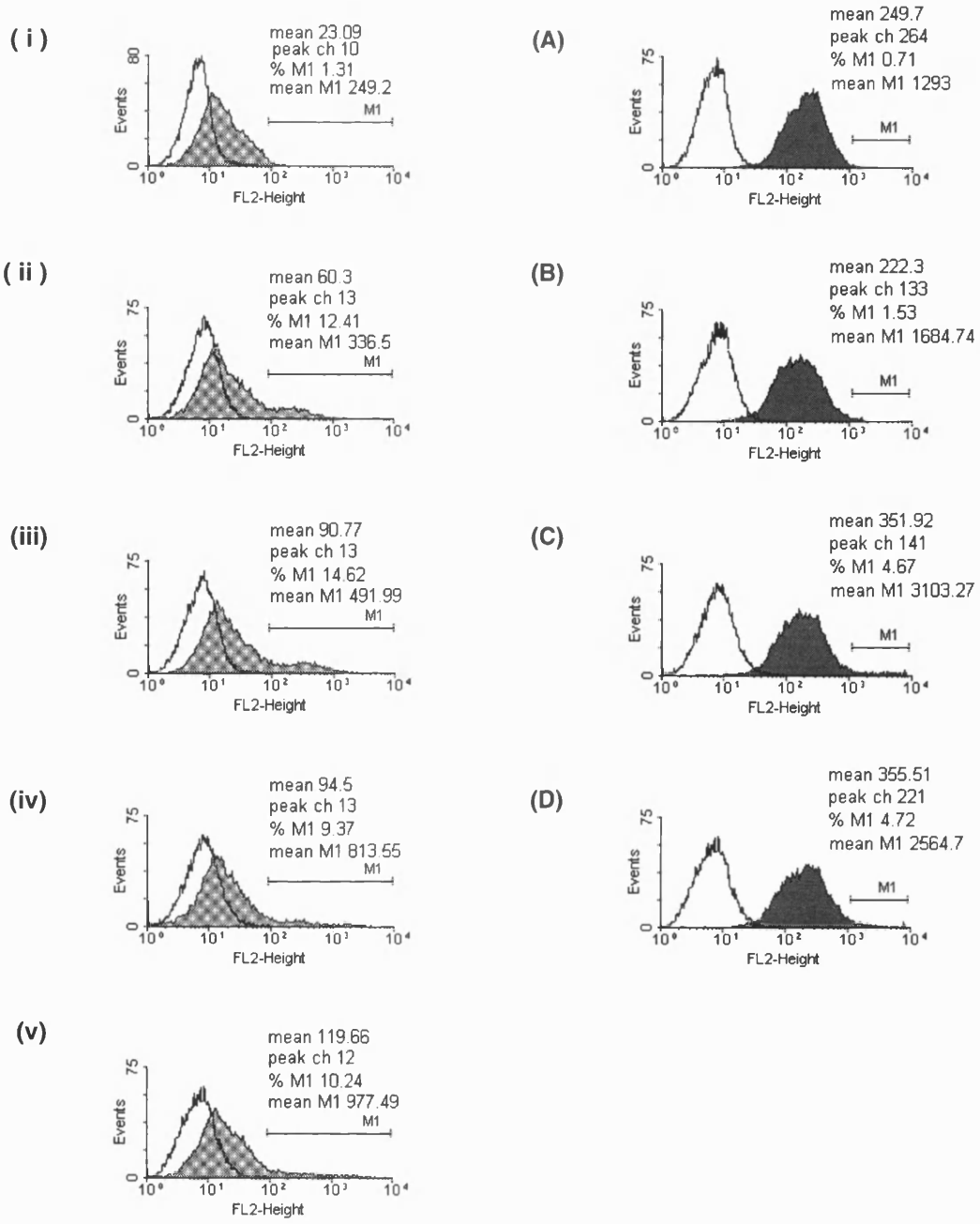

Fig 6.8 Surface expression of integrin subunits detected by FACS analysis of COS7 cells 48 hours post-electroporation with integrin expression constructs. (i-v) Surface expression of human β3 detected using Y2/51 and RPE conjugated goat anti-mouse IgG (light shaded area). (i) pcDNA3 transfection, (ii) PC3A transfection, (iii) PC3A D119A transfection, (iv) dual PCVnRα/PC3A transfection, (v) dual PCVnRα/PC3A D119A transfection. (A-D) Surface expression of human αv detected using P2W7 and PE conjugated goat anti-mouse IgG (dark shaded area). (A) pcDNA3 transfection, (B) PCVnRα transfection, (C) dual PCVnRα/PC3A transfection, (D) dual PCVnRα/PC3A D119A transfection. The unshaded area represents non-specific fluorescence of cells treated with mouse IgG1 negative control. These scans are representative of three repeats.

Figure 6.8 indicates an apparent reaction of both monoclonal antibodies with αv and β3 integrin subunits in control COS7 cells. As COS7 cells are derived from a primate cell-line, cross-reactivity with native integrin subunits would be expected, however, the large level of fluorescence obtained when using Y2/51 indicates the possibility of additional non specific surface-antibody interactions (although control IgG1 does not cross-react). Despite this endogenous level of cell fluorescence, increases in integrin expression were still observed after transfection with all integrin constructs, as indicated by the percent of highly fluorescent cells (as denoted by % M1 above). Use of the marker region M1 helps to illustrate the effect of dual transfection of α and β integrin subunits. Although the proportion of highly fluorescent cells after these transfections was similar to that of single subunit electroporation (or even lower for β3 detection), the mean fluorescence of these positive cells is apparently greater. Expression in these studies was maximal 48-72 hours after electroporation, although only the data for expression at 48 hours is shown in figure 6.1. Data collected for expression at 24 and 72 hours after electroporation, and a repeat of this transfection all showed a similar pattern of integrin expression

6.4.2. Transient expression in B16a cells

Electroporation of B16a cells was carried out in a similar fashion to that described above in section 6.3.1 using optimal transfection settings obtained in section 6.1. Cells were transfected using 20μg of supercoiled vectors pcDNA3, PC3A, PC3A D119A or PCVnRα, generated by maxiprep. Electroporation was carried out using wild-type B16a cells from semi-confluent 175cm^2 flasks. FACS analysis of cells was carried out using the standard analysis protocol at 24-72 hour time points with antibodies specific for the human integrin subunits as described above (section 6.3.1).

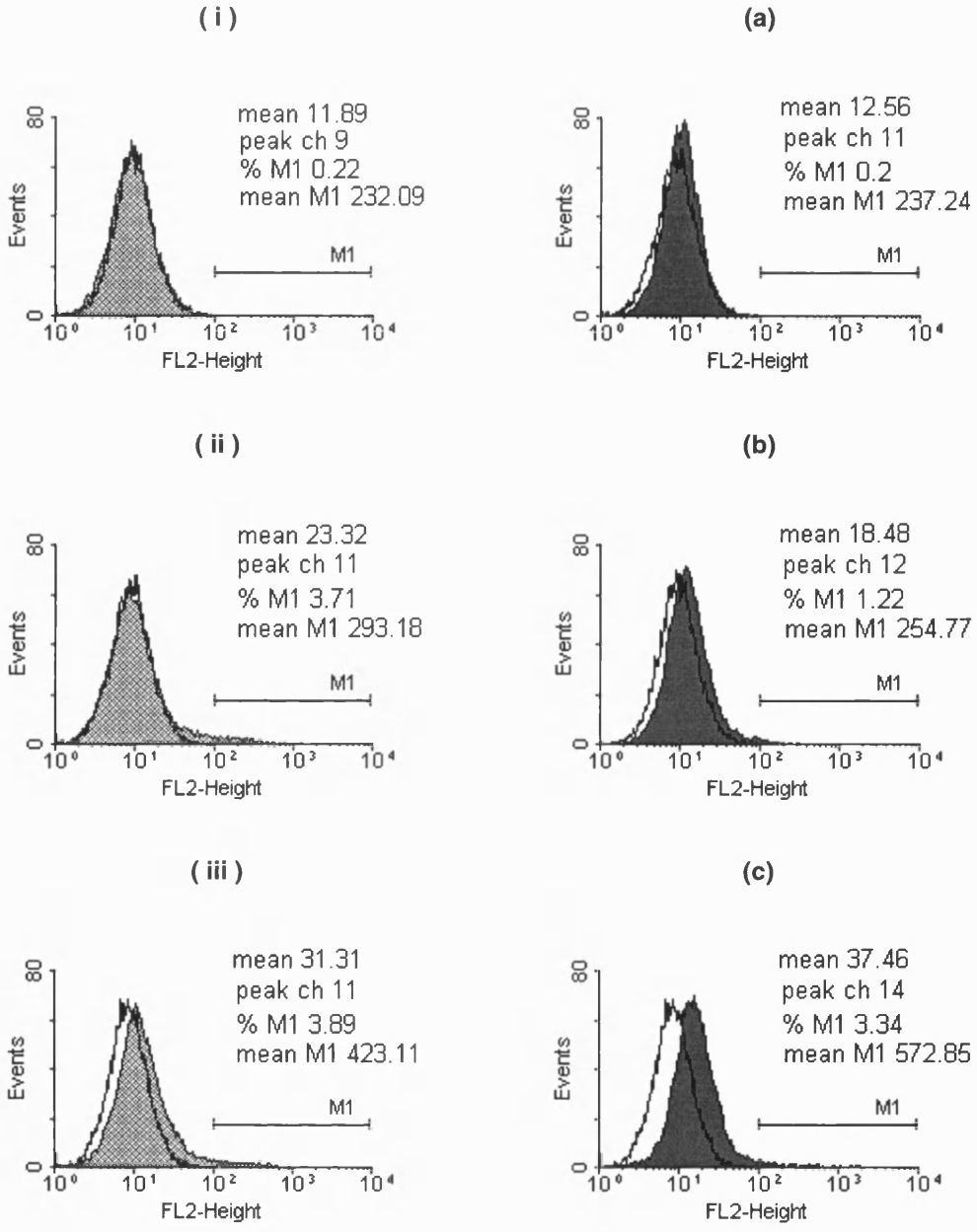

Fig 6.9 FACS analysis of human integrin αvβ3 subunits expressed on the surface of B16a cells 48 hours after electroporation. (i-iii) FACS analysis of human β3 expression using Y2/51 and RPE conjugated goat anti-mouse IgG (light shaded area). (a-c) FACS analysis of human αv expression using P2W7 and RPE conjugated goat anti-mouse IgG (dark shaded area. (i)(a) Cells transfected with control pcDNA3, (ii) PC3A D119A transfection, (b) PCVnRα transfected cells, (iii)(c) dual PCVnRα/CD3A D119A transfection. The unshaded area represents non-specific fluorescence of cells treated with mouse IgG1 negative control and RPE conjugated goat anti-mouse IgG. These scans are representative of three repeats.

Figure 6.3 shows a typical FACS profile obtained from B16a cells transfected with mutant β3 integrin construct PC3A D119A 48 hours after electroporation.

Figure 6.9 illustrates that anti-human mAb Y2/51 and P2W7 did not cross-react with any surface antigens from murine B16a cells. Single subunit transfection gave an increase in cell fluorescence in approximately 5% of the cells analysed. Dual transfection with both subunits resulted in a more noticeable shift in cell fluorescence with approximately 20% of the cells analysed showing increased fluorescence (slightly more for αv scans). Very few cells in figure 6.3 could be seen to have large increases in cell fluorescence with only ~1-4% of cells having a fluorescence greater than one log scale from mean cell fluorescence in single or dual transfections (as denoted by % M1). Unlike transfection of COS7 control cells, dual transfection of B16a cells with αv and β3 did cause a greater proportion of cells to react to both Y2/51 and P2W7, with a shift in intensity of the entire fluorescence profile.

Antibody P2W7 gave non-specific background fluorescence at dilutions less than 1:500 (<10μg/ml), although this was minimised at 1:500 dilution. Level of expression was not altered 72 hours after electroporation and repeats of this transfection showed a consistent pattern of cell fluorescence, as did expression when transfected with functional integrin vector PC3A.

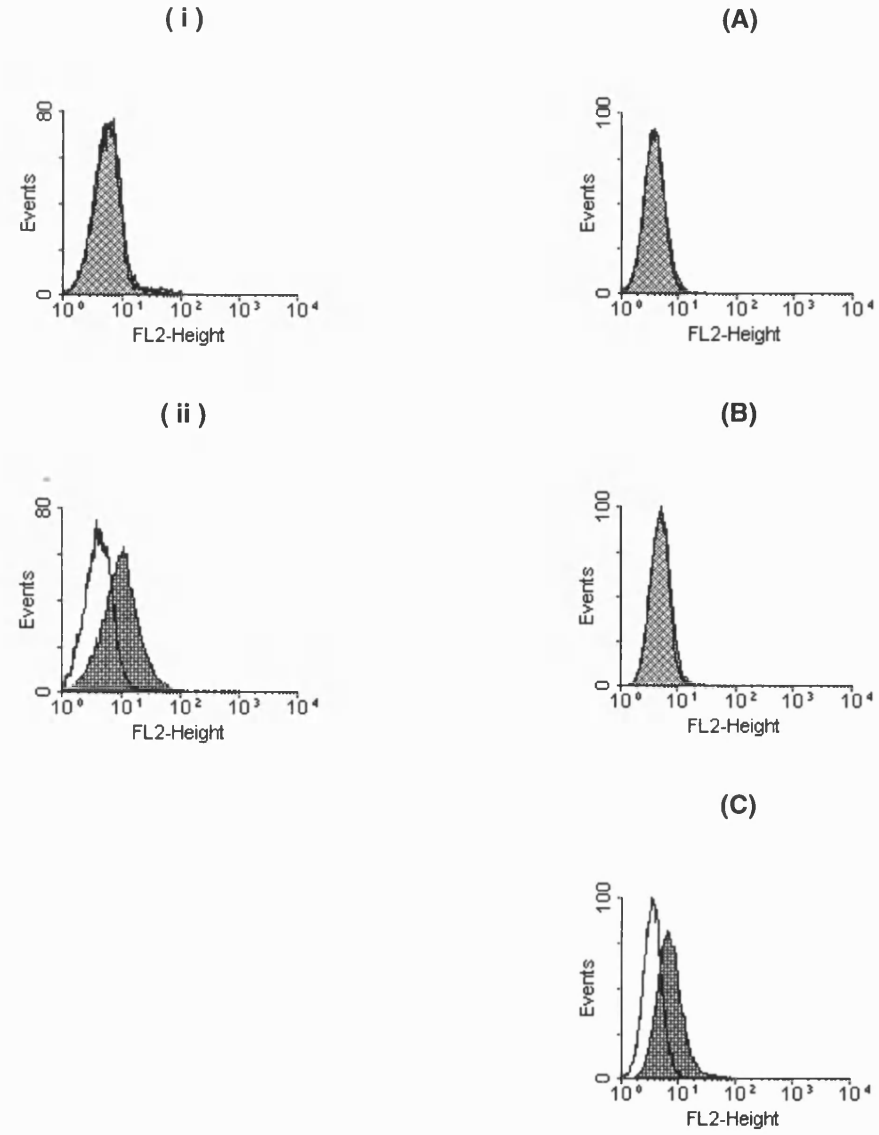

Fig 6.10 FACS analysis of Polyclonal populations of B16a cells transfected with linearised plasmid constructs and isolated by treatment with 1.5mg/ml G418. Detection of integrin subunits is by mAb Y2/51 (for human β3, light shaded area) or P2W7 (for αv, dark shaded area) and RPE conjugated goat anti-mouse IgG (i) human β3 expression in B16a cells transfected with control pcDNA3. (ii) human αv expression in cells transfected with control pcDNA3. (A) human β3 expression in cells transfected with PC3A. (B) human β3 expression in cells transfected with PC3A D119A. (C) Human αv expression in cells transfected with PCVnRα. The unshaded area represents non-specific fluorescence of cells treated with mouse IgG1 negative control and RPE conjugated goat anti-mouse IgG. These scans are representative of four repeats using separately transfected B16a samples.

6.5. Stable expression of integrin subunits using B16a cells

B16a cells were electroporated with pcDNA3, PC3A, PC3A D119A or PCVnRα and subsequently treated with G418 to obtain resistant polyclonal populations as described in section 2.29.3. All plasmids for electroporation were linearised with restriction endonuclease *Bgl* II, except VnRα which was restricted with *Pvu* I as described. Cells were electroporated with 20μg linearised vector and transfected cells were treated with 1.5mg/ml G418 in MEM 48 hours after electroporation. Similarly to antisense vectors, clones were ready for subculturing into 25cm^2 flasks after a 2-3 week period. FACS analysis for human integrin subunits was carried out two passages from subculturing of clones, harvesting cells from semi-confluent 75cm^2 flasks. Standard FACS labeling assays were used with the anti-human IgG1 monoclonal antibodies described in section 2.31.1.

Figure 6.10 (previous page) indicates the degree of non-specific fluorescence given by antibody P2W7 when used in concentrations higher than 1:500. The assay shown in figure 6.4 was carried out with a labeling concentration of 1:100 P2W7 (20μg/ml). The degree of fluorescence of control pcDNA3 transfected cells was of the same intensity indicating its non-specific nature. A second set of independently isolated polyclonal populations also failed to react with Y2/51 or P2W7 antibodies using the same range of transfections as above.

6.5.1. Detection of intracellular integrins using FACS

In order to check whether human integrin subunits transfected into B16a cells were being expressed at mRNA level and translated into active integrin subunits, but not transported to the surface of the murine cells, FACS analysis was carried out using permeabilised B16a transfectants as described in section 2.31.3. Polyclonal PC3A and

PC3A D119A B16a cell lines were fixed with paraformaldehyde and made permeable with methanol as described, measuring fluorescence at each stage of the permeabilising process using mAb Y2/51 and RPE conjugated $F(ab')_2$ fragment of goat anti-mouse IgG as described.

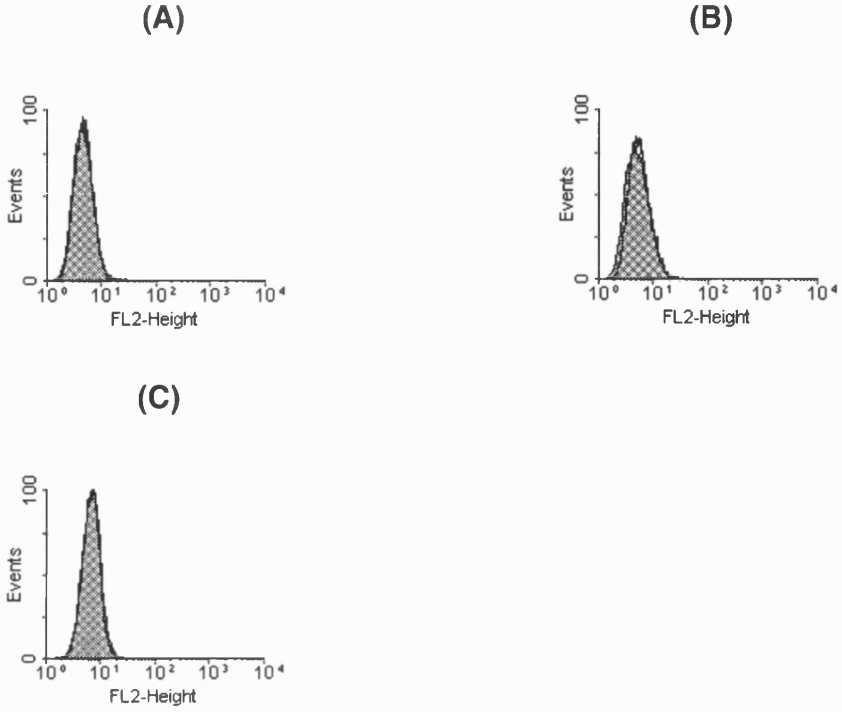

Fig 6.11 Effect of cell permeabilisation with methanol upon FACS analysis of mutated human β_3 integrin subunit in PC3A D119A transfected, G418 stable polyclonal populations of B16a cells using mAb Y2/51 and RPE conjugated $F(ab')_2$ fragment of goat anti-mouse IgG (shaded region). (A) Control PC3A D119A transfected B16a cells. (B) PC3A D119A transfected cells fixed with 0.25% paraformaldehyde before FACS analysis. (C) FACS analysis of paraformaldehyde fixed B16a cells permeabilised with 70% methanol for 60 minutes at 4°C. The unshaded area represents non-specific fluorescence of cells treated with mouse IgG1 negative control and RPE conjugated goat anti-mouse IgG. These scans are representative of two repeats.

Figure 6.11 indicates that neither fixing or permeabilisation of the membranes of fixed cells gave any changes in the fluorescence of PC3A D119A transfected cells. Further experiments carried out using this technique with other polyclonal populations transfected with PC3A also revealed that there were no sequestered β

integrin subunits in the antibiotic resistant cells isolated. No permeabilisation assays were carried out for PCVnRα transfected cells

6.6. Discussion

The data presented in section 6.1 clearly shows that electroporation is an efficient method for the introduction of DNA into mammalian cells. Expression of the reporter vector pRSV*lac*Z was visible in approximately 50-60% of B16a or COS7 cell populations 48 hours after transfection. However, some conflicting data was obtained in that the intensity of FL-1 fluorescence measured after COS7 cell electroporation (figure 6.3) was considerably lower than that seen in B16a cells (fig 6.1). The degree of COS7 cell fluorescence also appeared to reach a maximum at higher electroporation settings. Therefore, it appears that COS7 cells are much more resistant to electroporation than B16a cells, having increased survival rates at higher electroporation settings, and lower degree of FITC-dextran uptake. Studies with the reporter plasmid pRSV*lac*Z, however, indicated similar rates of transfection efficiency to B16a cells. One possible explanation for this similarity is that the COS7 cells were amplifying expression of the gene by replicating the vector as a result of their transformation with the SV40 large T antigen, so that all cells which received vector tested positive. This also explained the higher intensity of colour in COS7 cells tested with X-Gal. COS7 cells, as expected produced a high level of expression and were therefore a useful control for expression of integrin sequences.

It can be clearly seen that the mutated sequence obtained from Dr J C Loftus did indeed contain an inactivating point mutation within the ligand binding region of CD3A at position A^{119}. Additionally, the cloned human β3 and αv pcDNA3

constructs were functional and expressed transiently in both control COS7 and B16a cells after electroporation. Evidence suggests that integrin subunits without a corresponding second subunit will not form a heterodimer and will not be secreted to the cell surface (O'Toole *et al.,* 1989, Kolodziej *et al.,* 1991) . Therefore, the detection of human αv and β3 subunits on the surface of B16a cells indicated that transfected subunits formed heterodimers with corresponding native integrin subunits. Increased expression of both integrin subunits was observed when cells were co-transfected with both αv and β3 integrin subunits simultaneously. This occurred in both B16a and COS7 cells, presumably as excess available complimentary subunits were available for heterodimer formation.

The drawback with the transfection data shown, with respect to practical gene therapy, was the level of transient surface expression. COS7 control cells showed a higher proportion of positive cells after electroporation, as would be expected due to their RSV transformed nature allowing replication of pcDNA3 and consequent enhancement of expression. However, the level of this expression was still low (discernible levels in only ~10% of cells) and the efficiency of detection of positive cells, using either antibody (particularly mAb P2W7 for human αv) was difficult to ascertain due to cross reaction and/or non-specificity between native COS7 integrins. B16a cells routinely expressed approximately 1-2% highly positive cells after electroporation with either a single, or both, α and β integrin constructs. However, co-transfection of both B16a and COS7 cells resulted in higher overall fluorescence after binding of specific antibodies for either subunit. However, co-transfection is not of practical value for gene therapy of melanoma where the strategy is concerned with competitive inhibition of functional β3 subunits.

The low numbers of positive cells which exhibited transient expression after electroporation may be due to a number of factors. Firstly, efficient transcription sometimes requires the presence of some 5' untranslated intronic information. Sequencing of this region of the cDNA's used was not carried out but restrictional analysis of both PCVnRα and PC3A plasmids suggests that some 5' untranslated information was included (cDNA size of human β3 is 2366 bases while human αv is 3146 bases). As yet there is no evidence for any such requirement of integrins for insertion of 5' information before efficient transcription.

The resistance of cells to accept integrins by selection with an antibiotic marker suggests that cells are possibly reluctant to express further integrin subunits introduced by electroporation. The small degree of increase seen on dual transfection of cells with both α and β subunits suggests that other inhibitory pathways may be in place other than simply a lack of available subunits for the formation of expressed heterodimers.

As suggested above, no B16a cells isolated by G418 treatment after transfection expressed human integrin subunits extracellularly or intracellularly. A number of conversations with other workers in the field of integrin transfection (primarily Dr John Marshall, ICRF, London) have indicated similar difficulties in obtaining clones by transfection of foreign integrin subunits and antibiotic selection. Some success has been obtained by the use of FACS to sort transiently expressing integrin populations during antibiotic selection for resistant cells (sorting cells every few days). This evidence suggests that unless treated cells are sorted frequently for transfected integrin expression during the antibiotic isolation process, positive cells are either diluted out or expression is lost. Time limitations prevented a repeat of

transfection studies with the above protocol. Also of some significance to the low range of expression may be the type of expression vector used. Other vector systems are available that use different mechanisms for gene expression, such as viral based systems (integrating retrovirus-based or adenovirus-based) or episomal replicating mammalian expression vectors based on the Epstein Barr Virus (EBV). It would be particularly interesting to examine expression after retroviral transformation, and compare its efficiency with the plasmid transfections carried out here.

The initial aim of this chapter was to investigate the competitive inhibition of active β3 heterodimers by transfection with inactive β3 mutants. Using the expression vectors and electroporation conditions described above, it is clear that the amount of transfected integrin expressed on the surface of B16a cells (and even COS7 cells) is insufficient to cause discernible differences in cell behaviour. Therefore, no further characterisation of cells was carried out in either transfection system.

Chapter 7: Concluding Discussion

Characterisation of β3 integrin expression using B16a cells as a prospective model target for gene therapy of malignant melanoma unearthed a number of interesting observations. The integrin-specific sorting using FACS, which was used to isolate the cell lines LBE and HBE, resulted in populations of cells which were distinctly different from B16a cells isolated from solid tumours by centrifugal elutriation (Onada *et al.*, 1988; Honn et al., 1992; Chang *et al.*, 1992). Populations isolated on the this basis in these studies not only differed in expression of αIIbβ3 but also exhibited notable differences in platelet aggregation, adhesion to substrates and *in vivo* tumorigenicity, the degree of which correlated with integrin expression.

Cells isolated by FACS in this study lacked these differences in static adhesion profiles while exhibiting significantly different proliferation and spreading rates. The papers cited above reported differences in the adhesion of sub-populations of B16a cells to both murine pulmonary endothelial cells (CD3) and surfaces coated with fibronectin (~4.27μg/cm^2). Antibodies against αIIbβ3 reduced this level of adhesion (but only in cells expressing high levels of receptor). Antibodies against the α5 subunit failed to reduce adhesion to fibronectin, implying that they were not significant in the adhesion to fibronectin. No mention of differences in proliferation rates is made in any of the above papers and discussion with Prof Ken Honn (Wayne State University, Detroit) confirmed that no proliferation differences were noted in these subpopulations.

In the assays described in section 4.2.2, B16a cells expressing different levels of β3 did not exhibit different adhesion profiles to either fibronectin or fibrinogen. This suggests that other adhesion molecules are involved in the mediation of adherence to these substrates. Further assays would be needed, however, using a wider range of ECM substrates and blocking antibodies against α3β1 and α5β1 before the similarity of adhesion seen here can be definitely assigned to other integrins.

Similar FACS based cell isolation studies have been carried out by Cheresh and Spiro (1987), using a human melanoma cell line, M21, and the integrin αv subunit as a selection marker. Using an antibody specific for the human αv subunit, a sort of the top and bottom 0.05% of M21 cells was carried out. Bottom sorts of these cells were repeated four times until a cell line expressing no αv subunit was obtained (termed M21-L cells). Cells isolated using this procedure had no difference in growth rates, or rates of protein synthesis, but did differ dramatically in their ability to bind to ECM proteins. FACS and immunoprecipitation studies additionally showed that the complementary β3 subunit was not detected on the surface of M21-L cells, but was translated and expressed intracellularly on a short term basis. This lack of β3 expression in the absence of complementary α subunits correlates with that seen for αIIbβ3 heterodimer surface expression (O'Toole *et al.,* 1989; Kolodziej *et al.,* 1991).

The study by Cheresh and Spiro provides an interesting comparison with the work carried out here. B16a cell lines selected by FACS did not differ in their ability to attach to selected ECM substrates (expressing RGD or KQAGDV motifs), however, rates of growth and spreading were considerably altered. Studies by Cheresh and Spiro, using RGD affinity columns with M21-L cells showed that their ability to bind

this motif was totally lost after cell sorting, suggesting that no other RGD integrins were present in the M21-L cell line. This would help to simplify characterisation of αvβ3 activity in this cell line and help to explain differences in static adhesion.

Further data has been reported by Wayner *et al* (1991), using two cell lines, M21 human melanoma (as described above) and H2981 lung carcinoma cells. Both cell lines were found to express αvβ3 and αvβ5 and required blocking of both receptors with specific antibodies before differences in static vitronectin adhesion could be observed. However, although both receptors recognised the same ligand, distribution studies revealed that only αvβ3 localised at sites of focal contact when plated on vitronectin. The presence of αvβ3 was therefore necessary for cell spreading upon vitronectin, even though both integrins contributed to cell affinity for this substrate. It could be possible that a similar system is at play in B16a cells, where at least three integrins expressed on the B16a surface (αIIbβ3, α5β1 and α3β1) can recognise the RGD motif, but only αIIbβ3 will form focal adhesion sites and stimulate spreading on RGD substrates.

Changes in the proliferation of sorted B16a cells observed in the present study is not a phenomenon reported in similar studies carried out in human melanoma cell lines (A375 and M21) expressing integrin αvβ3. It is clear that αIIbβ3, although mirroring αvβ3 activity in a number of tumour cell assays, has potentially different influences upon cellular signalling in the B16a system. The information described here, is indicative of the specific function of αIIbβ3 on the surface of B16a cells, beyond its activity as an adhesion receptor. FACS analysis suggests that although the expression of this heterodimer is often low - particularly in wild-type cells, other

assays carried out on sorted cells imply that its influence upon cell behaviour is considerable.

Another possible explanation for the changes observed in proliferation, other than the direct influence of αIIβ3 mediated signalling pathways is possible with reference to a number of papers concerning the "classic fibronectin receptor" α5β1. Elevated levels of α5β1 have been associated with the suppression of a transformed phenotype in Chinese hamster ovary (CHO) cells (Giancotti and Ruoslahti 1990). Transfection of this receptor into transformed CHO cells resulted in an increase in fibronectin synthesis, and reduction in migration, growth in soft agar and saturation density. The transformed cells were also non-tumorigenic after subcutaneous injection into nude mice. Therefore, the presence of α5β1 in these cells stabilises their phenotype. Another interesting report (Blystone *et al.*, 1994) suggests that the αvβ3 integrin may regulate the adhesive and phagocytic functions of α5β1 when this receptor is transfected into human erythroleukaemia (K562) cells. Ligation of αvβ3 was seen to inhibit α5β1 mediated phagocytosis (of fibronectin coated beads) by an unknown signalling pathway. Taken together, these reports suggest that αIIbβ3 and α5β1 (or possibly α3β1) could be functioning in a non-independent fashion. Therefore, downregulation of αIIbβ3 may remove the influence of this integrin upon an α5β1 mediated phenotype similar to that suggested by Giancotti and Ruoslahti. It must be noted, however, that the α5β1 integrin has also been associated with enhancing the proliferative response to fibronectin of serum starved human melanoma cell lines (Mortarini *et al.*, 1992), which perhaps suggests that these combinatory

relationships between integrins, and the effect of α5β1 upon proliferation are cell-type specific.

Down-regulation of β3 integrin heterodimers expressed on the surface of melanoma cell-lines proved to be a difficult objective to achieve reproducibly. Many studies have used antisense integrin constructs to reduce integrin expression by target cells, primarily using stable transfectants which were isolated using antibiotic resistance as individual cell clones, which were then examined for an antisense effect (Keely *et al.,* 1995; Riikonen *et al.,* 1995a, 1995b; Koivisto *et al.,* 1994; described in section 1.5.2). A primary aim of this project was to investigate the effectiveness and efficiency of using antisense gene therapy against the expression of target β3 integrin heterodimers. Particular interest was focused upon reduction of β3 expression on a global, polyclonal basis. The basis for this aim is that use of any antisense integrin construct *in vivo* will not only need to be targeted to specific cells (such as melanoma cells), but also have a discernible effect on the majority of target cells. As the use of antibiotic markers is not possible *in vivo*, this vector based delivery system would need to express significant levels of antisense integrin message in the majority of cells on a transient basis. The studies conducted here did not result in an antisense effect upon β3 expression on a transient basis, using the transfection protocols described. Other techniques using different gene delivery strategies such retroviral or even replication competent viral delivery would carry the potential of an integration (or stable production) of antisense genes.

As a model for this potential, cells isolated using the G418 antibiotic resistance marker gave indications of an antisense affect when the cells were stably transfected. Melanoma cells appeared to exhibit downregulation of β3, particularly using FACS

and proliferation assays, although these effects could also have been explained by non-specific events as a result of the large size of antisense inserts. Conflicting data, primarily using Western blotting for total β3 expression also draws this phenomenon into doubt.

In conclusion, using the gene expression system detailed here, antisense therapy of β3 integrins does not give a reliably significant large-scale therapeutic reduction of integrin expression. However, it remains that β3 integrins are a valid target for gene and drug therapy and that antisense treatment of this target using alternative transfection and expression techniques may well provide more acceptable downregulation of expression. The use of ligand mimetics such as superfibronectin (Morla *et al.,* 1994) are likely to produce a shorter term alternative for the treatment of integrin-related phenomena such as prevention of metastasis, angiogenesis (Brooks *et al.,* 1994), haemostatic events (Smith *et al.,* 1995) or bacterial endocytosis (Vannhieu *et al.,* 1996).

Another potential field for rapidly growing clinical interest is the use of ligand mimetics to target cells for the delivery of genes or peptides. Recent work presented by Wickham *et al.* (1995) suggests a potential use for engineering of the adenovirus penton base to target gene delivery to specific integrins. Endocytosis mediated by these integrins may well provide a valuable tool for the targeting of drugs to specific tissues.

The validity of using inactive mutants of β3 integrins to competitively inhibit endogenous integrins of melanoma cells was not rigorously tested during this study due to problems involved with the efficiency of integrin transfection. Using a similar tactic, LaFlamme *et al.* (1994) have successfully used chimeras of integrin

cytoplasmic domains to inhibit the spreading and migration of human fibroblasts. Rather than the use of complete integrin subunits they ligated integrin cytoplasmic domains to the extracellular and transmembrane domains of interleukin-2 (IL-2). This study indicated much higher levels of chimera expression after electroporation, and the authors postulated that the inhibition of endogenous integrin activity was dominant rather than competitive. This is due to the observation that β intracellular domains, expressed in the absence of α intracellular domains bind to intracellular components with the same affinity as ligand-occupied integrins (LaFlamme *et al.,* 1992), disrupting focal contact activity. Similar studies by Lukashev *et al.* (1994) have also noted similar trans-dominant inhibitory effects using β1 cytoplasmic and extracellular domains ligated to a murine CD4 extracellular domain..

Using the system suggested in chapter 6, inhibition of integrins would be on a more competitive basis than that shown by LaFlamme *et al.,* with inhibition arising from competition between endogenous and mutated β3 subunits for accompanying α subunits. This suggests that inhibition of integrins by transfection of inactive subunits will function as long as transfection efficiencies are sufficiently high. The use of integrin chimeras in this system would appear to be preferable as chimeras appear to carry integrin subunit specificity , but with a more efficient dominant-negative activity.

7.1. Further work

Initial studies using HBE and LBE B16a cells suggests an interesting role for αIIbβ3 in the alteration of tumour cell proliferation. It may provide a valuable model for the examination of the signalling events associated with integrin-mediated

stimulation of proliferation. Further studies in this area would be needed to dissect the individual roles of all B16a integrins, and the influence of substrate type upon this phenomenon. Experiments would therefore concentrate on proliferation of sorted and wild type B16a cells upon surfaces coated with various ECM ligands. Additionally, studies of the rate of protein synthesis in these studies (using [^{3}H]leucine incorporation, as utilised by Cheresh and Spiro, 1987) will also elucidate complimentary information of cellular activity. Treatment of cells with blocking antibodies, inhibitory to integrin function (for αIIbβ3, α3β1 or α5β1) could be used. Such assays may reveal information concerning the significance of these individual integrins in proliferation, and their role in any potential feedback between integrins as mentioned above. For instance, treatment of LBE cells with anti α5β1 antibodies will give information concerning its role in control of B16a growth and the observed phenotype of LBE cells.

Parallel studies in a cell line expressing the other β3 integrin, αvβ3 may help to differentiate between events mediated by each integrin. Therefore, similar studies could be carried out using the A375 cell line and sorting for populations on the basis of β3 expression. A375 cells isolated on the basis of *in vivo* metastatic ability (which exhibit higher αvβ3 expression) do not appear to exhibit differences in *in vitro* proliferation and it would be interesting to study whether this relationship holds for cells isolated purely on the basis of αvβ3 expression. Antibody treatment against other expressed integrins, and studies of proliferative response to ECM substrates would also mirror experiments carried out in B16a cells.

Alternatively, transfection of αv subunits into LBE cells would be interesting as this would give clear information concerning homology between αIIbβ3 and αvβ3 activities. A similar experiment along these lines would be possible with transfection of LBE A375 cells with αIIb subunits. Examination of the proliferation of other cell lines transfected with αIIbβ3 may provide information as to whether this phenomenon is specific to this cell-line

Differences observed in B16a cell spreading upon fibronectin could be examined by labelling of B16a cells with fluorescent antibodies to specific integrin subunits while attached to ECM substrates. Confocal microscopy of these samples would reveal cellular distribution patterns from which individual roles of integrins in focal adhesion formation will be revealed. It would be interesting to see if these integrin distribution patterns paralleled those seen by Wayner *et al.* (1991) as discussed above.

The inconsistency of downregulation of β3 integrins by the transfection protocol used may well be a product of the inefficiency of the delivery system used to express sufficient levels of antisense DNA (although transfection data gained from β-galactosidase expression would perhaps suggest otherwise). Alternatively, it may be a product of the type of expression vector selected for these studies. Parallel experiments using alternative gene delivery techniques would help to rule out these suggestions. Such studies could include transfection of HBE B16a cells with the pcDNA3 constructs using cationic liposomes such as DOTAP (Boehringer-Mannheim), known to give high levels of transient expression. Other experiments could concentrate upon the delivery of the antisense β3 inserts within alternative

expression vectors, such as the episomal mammalian expression vectors based on the Epstein Barr virus, or adenoviral delivery and expression systems. Alternatively, use of retroviruses may be a valuable delivery technique for the generation of stable antisense transfectants.

Specificity of antisense downregulation would also be an interesting area for further work, to clarify the potential non-specific inhibition of integrin expression caused by the longer antisense β3 inserts. This could include examination of non-specific integrin downregulation by measuring surface expression of α5β1 and α3β1 integrins in B16a cells before and after antisense transfection with β3 integrin constructs using specific antibodies and FACS. Antisense downregulation of B16a proliferation will also need to be compared to that seen in LBE B16a cells more comprehensively in order to determine if specific β3 downregulation is the actual cause for this phenomenon. Studies could involve similar ECM and inhibitory antibody proliferation assays to those described above, with comparison to assays carried out on cells selected for low β3 expression.

The inhibition of integrins by the transfection of other subunits, or chimeras of other subunits still remains an interesting area for melanoma gene therapy. However, the use of chimeras of integrin subunits for dominant inhibition of integrin function, such as those described by La Flamme *et al.* (1994) may produce a more efficient inactivation of integrins. It may be possible to take this principle a step further by the use of peptides homologous to the functional groups of complementary transmembrane and cytoplasmic domains of integrins to produce a molecule capable of prevention of integrin heterodimer formation, specific to integrin subunit-type. Further elucidation of the mechanisms for integrin links with signalling pathways may

also uncover cytoplasmic interactions where homologous molecules may effectively block integrin mediated signal transduction.

References and Appendices

Agrez M., Chen A., Cone R.I., Pytela R. and Sheppard D. (1994) The αvβ6 integrin promotes proliferation of colon carcinoma cells through a unique region of the β6 cytoplasmic domain. J. Cell Biol. 127: 547-556

Akiyama S.K., Yamada S.S., Yamada K.M. and LaFlamme S.E. (1994) Transmembrane signal transduction by integrin cytoplasmic domains expressed in single-subunit chimeras. J. Biol. Chem. 269: 15961-15964

Akhtar S., Kole R. and Juliano R.L. (1991) Stability of antisense DNA oligonucleotide analogues in cellular extracts and sera. Life Sci. 49: 1793-1801

Albelda S.M., Mette S.A., Elder D.E., Stewart R., Damjanovich L., Herlyn M. and Buck C.A. (1990) Integrin distribution in malignant melanoma: association of the beta 3 subunit with tumor progression. Cancer Res. 50: 6757-6764

Andreason G.L. and Evans G.A. (1989) Optimization of electroporation for transfection of mammalian cell lines. Analyt. Biochem. 180 (2): 269-75

Arnould R., Dubois J., Abikhalil F., Libert A., Ghanem G., Atassi G., Hanocq M. and Lejeune F.J. (1990) Comparison of two cytotoxicity assays - tetrazolium derivative reduction (MTT) and tritiated thymidine uptake on three malignant mouse cell lines using chemotherapeutic agents and investigational drugs. Anticancer Res. 10: 145-154

Bajt M.L., Ginsberg M.H., Frelinger A.L. Berndt M.C. and Loftus J.C. (1992) A spontaneous mutation of integrin αIIbβ3 (platelet glycoprotein IIb-IIIa) helps define a ligand binding site. J. Biol. Chem. 267 (6): 3789-3794

Bajt M.L. and Loftus J.C. (1994) Mutation of a ligand-binding domain of beta(3) integrin - integral role of oxygenated residues in alpha(IIb)beta(3) (GPIIb-IIIa) receptor function. J. Biol. Chem. 269 (33): 20913-20919

Balch C.M., Soong S-J., Shaw H.M. and Milton G.W. (1985a) An analysis of prognostic factors in 4000 patients with cutaneous melanoma. In: Cutaneous

melanoma: clinical management and treatment results worldwide. J.B. Lippincott, Philadelphia, Pa: 321-352

Balch C.M., Soong S-J. and Shaw H.M. (1985b) A comparison of worldwide melanoma data. In: Cutaneous melanoma: clinical management and treatment results worldwide. J.B. Lippincott, Philadelphia, Pa: 507-518

Bastida E., Ordinas A., Escolar G. and Jamieson G.A. (1984) Tissue factor in microvesicles shed from U87MG human gliobastoma cells induces coagulation, platelet-aggregation, and thrombogenesis. Blood 64 (1): 177-184

Bennett C.F., Chiang M.Y., Chan H., Shoemaker J.E. and Mirabelli C.K. (1992) Cationic lipids enhance cellular uptake and activity of phosphorothioate antisence oligonucleotides. (1992) Molec. Pharmacol. 41: 1023-1033

Berlin C., Berg E.L., Briskin M.J., Andrew D.P. Kilshaw P.J., Holzmann B, Weissman I.L., Hamann A. and Butcher E.C. (1993) α4β7 integrin mediates lymphocyte binding to the mucosal vascular addressin MAdCAM-1. Cell 74: 185-195

Birnboim H.C. and Doly J. (1979) A rapid alkaline extraction procedure for screening recombinant plasmid DNA. Nucleic Acids Res. 7 (6): 1513-1523

Blystone S.D., Graham I.L., Lindberg F.P. and Brown E.J. (1994) Integrin αvβ3 differentially regulates adhesive and phagocytic functions of the fibronectin receptor α5β1. J. Cell Biol. 127 (4): 1129-1137

Boukerche H., Berthier-Vergnes O., Bailly M., Doré J.F., Leung L.L.K. and McGregor J.L. (1989) A monoclonal antibody (LYP18) directed against the blood platelet glycoprotein IIb/IIIa complex inhibits human melanoma growth *in vivo.* Blood 74: 909-912

Boukerche H., Benchaibi M., Berthier-Vergnes O., Lizard G., Bailly M., Bailly M. and McGregor J.L. (1994) Two human melanoma cell-line variants with enhanced *in vivo* tumor growth and metastatic capacity do not express the β3 integrin subunit. Eur. J. Biochem. 220: 485-491

Bratty J., Chartrand P., Ferbeyre G. and Cedergren R. (1993) The hammerhead RNA domain, a model ribozyme. Biochem. Biophys. Acta 1216 (3): 345-359

Breslow A. (1970) Thickness, cross-sectional areas and depth of invasion in the prognosis of cutaneous melanoma. Ann. Surg. 172: 902-908

Brooks P.C., Clark R.A.F. and Cheresh D.A. (1994a) Requirement of vascular integrin αvβ3 for angiogenesis. Science 264: 569-571

Brooks P.C., Montgomery A.M.P., Rosenfeld M., Reisfeld R.A., Tianhua H., Klier G. and Cheresh D.A. (1994b) Integrin αvβ3 antagonists promote tumour regression by inducing apoptosis of angiogenic blood vessels. Cell 79: 1157-1164

Brooks P.C., Strömblad S., Klemke R., Visscher D., Sarker F.H. and Cheresh D.A. (1995) Antiintegrin αvβ3 blocks human breast cancer growth and angiogenesis in human skin. J. Clin. Invest. 96: 1815-1822

Buyon J.P., Slade S.G., Reibman J., Abramson S.B., Philips M.R., Weissmann G. and Winchester R. (1990) Constitutive and induced phosphorylation of the alpha-chains and beta-chains of the CD11/CD18 leukocyte integrin family - relationship to adhesion-dependent functions. J. Immunol. 144: 191-197

Calvete J.J., Henschen A. and Gonzales-Rodriguez J. (1991) Asignment of disulphide bonds in human platelet GPIIIa. A disulphide pattern for the beta-subunits of the integrin family. Biochem. J. 274: 63-71

Carrell N.A., Fitzgerald L.A., Steiner B., Erickson H.P. and Phillips D.R. (1985) Structure of human-platelet membrane glycoprotein-IIb and glycoprotein-IIIa as determined by electron-microscopy. J. Biol. Chem. 260 (3): 1743-1749

Cech T.R. and Bass B.L. (1986) Biological catalysis by RNA. Annu. Rev. Biochem. 55: 599-629

Chang Y.S., Chen Y.Q., Timar J., Nielsen K.K., Grossi I.M., Fitzgerald L.A., Diglio C.A. and Honn K.V. (1992) Increased expression of αIIbβ3 in subpopulations of murine melanoma cells with high lung colonising ability. Int. J. Cancer 51: 445-451

Chen Q., Kinch M.S., Lin T.H., Burridge K. and Juliano R.L. (1994a) Integrin-mediated cell adhesion activates mitogen-activated protein kinases. J. Biol. Chem. 269: 26602-26605

Chen W.T. and Singer S.J. (1982) Immunoelectron microscopic studies of the sites of cell-substratum and cell-cell contacts in cultured fibroblasts. J. Cell Bio.95 (1): 205-222

Chen Y.P., Djaffar I., Pidard D., Steiner B., Cieutat A.M., Caen J.P. and Rosa J.P. (1992a) Ser-752-Pro mutation in the cytoplasmic domain of integrin β3 subunit and defective activation of platelet integrin αIIbβ3 (glycoprotein IIb-IIIa) in a variant of Glanzmann thrombasthenia. Proc. Natl. Acad. Sci. USA. 89: 10169-10173

Chen Y.Q., Gao X., Timar J., Tang D., Grossi I.M., Chelladurai M., Kunicki T.J., Fligiel S.E.G., Taylor J.D. and Honn K.V. (1992b) Identification of the αIIbβ3 integrin in murine tumour cells. J. Biol. Chem. 267: 17314-17320

Chen Y., O'Toole T.E., Shipley T., Forsyth J., Laflamme S.E., Yamada K.M., Shattil S.J. and Ginsberg M.H. Inside-out signal-transduction inhibited by isolated integrin cytoplasmic domains. (1994b). J. Biol. Chem. 269: 18307-18310

Cheresh D.A. and Spiro R.C. (1987) Biosynthetic and functional properties of an RGD-directed receptor involved in human melanoma cell attachment to vitronectin, fibronectin and von willebrand factor. J. Biol. Chem. 262 (36): 17703-17711

Cheresh D.A., Berliner S.A., Vicente V. and Ruggeri Z.M. (1989) Recognition of distinct adhesive sites on fibrinogen by related integrins on platelets and endothelial-cells. Cell, 58 (5): 945-953

Chu G., Hayakawa H. and Berg P. (1987) Electroporation for the efficient transfection of mammalian-cells with DNA. Nucleic Acids Res. 15 (3): 1311-1326

Cieutat A.M., Rosa J.P., Letourneur F., Poncz M. and Rifat S. (1993) A comparative analysis of cDNA-derived sequences for rat and mouse β3 integrins (GPIIIA) with their human counterpart. Biochem. Biophys. Res. Comm. 193 (2): 771-778.

Clark E.A. and Brugge J.S. (1995) Integrins and signal transduction pathways: the road taken. Science 268: 233-239

Clark W.H., From L., Bernadino E.A. and Mihm M.C. (1969) The histogenesis and biological behaviour of primary human malignant melanomas of the skin. Cancer Res. 29: 705-726

Clark W.H.J., Elder D.E., Guerry D.I., Epstein M.N., Greene M.H. and Van Horn M. (1984) A study of tumor progression: the precursor lesions of superficial spreading and nodular melanoma. Human Pathol. 15: 1147-1165

Clark W.H.J., Elder D.E., and Van Horn M. (1986) The biological forms of malignant melanoma. Human Pathol. 17: 443-450

Coburn J., Leong J.M. and Erban J.K. (1993) Integrin αIIbβ3 mediates binding of the lyme disease agent *borrelia burgdorferi* to human platelets. Proc. Natl. Acad. Sci. USA. 90: 7059-7063

Cohen H.J., Cox E., Manton K. and Woodbury M. (1987) Malignant melanoma in the elderly. J. Clin. Oncol. 5: 100-106

Crowe D.T., Chiu H., Fong S. and Weissman I.L. (1994) Regulation of the avidity of integrin alpha(4)beta(7) by the beta(7) cytoplasmic domain. J. Biol. Chem. 269: 14411-14418

Dahlback K., Lofberg H., Alumets J. and Dahlback B. (1989) Imunohistochemical demonstration of age-related deposition of vitronectin (S-protein of complement) and terminal complement complex on dermal elastic fibres. J. Invest. Dermatol. 92 (5): 727-733

Danen E.H.J., Ten Berge P.J.M., Van Muijen G.N.P., Van't Hof-Grootenboer A.E., Bröcker A.B. and Ruiter D.J. (1994) Emergence of α5β1 fibronectin- and αvβ3 vitronectin-receptor expression in melanocytic tumor progression. Histopathology 24: 249-256

Danen E.H.J., Jansen C.F.J., Van Kraats A., Cornelissen I.M.H.A., Ruiter D.J. and Van Muijen G.N.P. (1995) Alpha-v integrins in human melanoma: gain of

αvβ3 and loss of αvβ5 are related to tumor progression in situ but not to metastatic capacity of cell lines in nude mice. Int. J. Cancer 61 (4): 491-496

Davis G.E. (1992) Affinity of integrins for damaged extracellular-matrix - alpha-v-beta-3 binds to denatured collagen type-I through RGD sites. Biochem. Biophys. Res. Commun. 182 (3): 1025-1031

Dedhar S., Rennie P.S., Shago M., Hagesteijn C.Y.L., Yang H.L., Filmus J., Hawley R.G., Bruchovsky N., Cheng H., Matusik R.J. and Giguere V. (1994) Inhibition of nuclear hormone-receptor activity by calreticulin. Nature 367 (6462): 480-483

Delcommenne M. and Streuli C.H. (1995) Control of integrin expression by extracellular matrix. J. Biol. Chem. 270 (5): 26794-26801

Dower W.J., Miller J.F. and Ragsdale C.W. (1988) High efficiency transformation of *E. coli* by high voltage electroporation. Nucleic Acids Research. 16 (13): 6127-6145

D'Souza S.E., Ginsberg M.H., Burke T.A., Lam S.C. and Plow E.F. (1988) Localisation of an Arg-Gly-Asp recognition site within an integrin adhesion receptor. Science 242: 91-93

D'Souza S.E., Ginsberg M.H., Matsueda G.R. and Plow E.F. (1991) A discrete sequence in a platelet integrin is involved in ligand recognition. Nature 350: 66-68

D'Souza S.E., Haas T.A., Piotrowicz R.S., Byersward V., McGrath D.E., Soule H.R., Cierniewski C., Plow E.F. and Smith J.W. (1994) Ligand and cation-binding are dual functions of a discrete segment of the integrin beta(3) subunit - cation displacement is involved in ligand-binding. Cell 79 (4): 659-667

Dustin M.L. and Springer T.A. (1989) T-cell receptor cross-linking transiently stimulates adhesiveness through LFA-1. Nature 341: 619-624

Du X., Plow E.F., Frelinger A.L., O'Toole T.E., Loftus J.C. and Ginsberg M.H. (1991) Ligands "activate" integrin αIIbβ3 (platelet GPIIb-IIIa). Cell 65: 409-416

Elices M.J. and Hemler M.E. (1989) The human integrin VLA-2 is a collagen receptor on some cells and a collagen/laminin receptor on others. Proc. Natl. Acad. Sci. USA. 86: 9906-9910

Felding-Habermann B., Habermann R., Saldívar E. and Ruggeri Z.M. (1996) Role of β3 integrins in melanoma cell adhesion to activated platelets under flow. J. Biol. Chem 271(10): 5892-5900

Filardo E.J., Brooks P.C., Deming S.L., Damsky C. and Cheresh D.A. (1995) Requirement of the NPXY motif in the integrin subunit cytoplasmic tail for melanoma cell migration *in vitro* and *in vivo*. J. Cell. Biol. 130: 441-450

Fitzgerald L.A. and Phillips D.R. (1985) Calcium regulation of the platelet membrane glycoprotein-IIb-IIIa complex. J. Biol. Chem. 260: 11366-11374

Fitzgerald L.A., Steiner B., Rall S.C., Lo S.S. and Phillips D.R. (1987) Protein-sequence of endothelial glycoprotein-IIIa derived from a cDNA clone - identity with a platelet glycoprotein IIIa and similarity to integrin. J. Biol. Chem. 262 (9): 3936-3939

Gailit J. and Ruoslahti E. (1988) Regulation of the fibronectin receptor affinity by divalent cations. J. Biol. Chem. 263: 12927-12933

Gehlsen K.R., Argraves W.S., Piersbacher M.D. and Ruoslahti E. (1988) Inhibition of *in vitro* tumour cell invasion by Arg-Gly-Asp containing synthetic peptides. J. Cell Biol. 106: 925-930

Giancotti F.G., Tarone G., Knudsen K., Damsky C. and Comoglio P.M. (1985) Cleavage of a 135kd cell surface glycoprotein correlates with loss of fibroblast adhesion to fibronectin. Exp. Cell Res. 156: 182-190

Giancotti F.G. and Ruoslahti E. (1990) Elevated levels of the α5β1 fibronectin receptor suppress the transformed phenotype of chinese hamster ovary cells. Cell 60: 849-859

Ginsberg M.H., Forsyth J., Lightsey A., Chediak J. and Plow E.F. (1983) Reduced surface expression and binding of fibronectin by thrombin-stimulated thrombasthenic platelets. J. Clin. Invest. 71: 619-624

Gluzman Y. (1981) SV40-transformed simian cells support the replication of early SV40 mutants. Cell 23 (1): 175-182

Goldman L.I., Elder D., Clark W.H., Mastrangelo M.J. and Stennett J. (1986) Assessment of survival rates with metastatic malignant melanomas. Surg. Gynecology and Obstetrics. 162 (3): 199-203

Gould R.J., Polokoff M.A., Friedman P.A., Huang T.F., Holt J.C., Cook J.J. and Niewiarowski S. (1990) Disintegrins: a family of integrin inhibitory proteins from viper venoms. Proc. Soc. Exp. Biol. Med. 195: 168-171

Graf J., Iwamoto Y., Sasaki M., Martin G.R., Kleinman H.K., Robey F.A. and Yamada Y. (1987) Identification of an amino-acid sequence in laminin mediating cell attachment, chemotaxis, and receptor-binding. Cell 48 (6): 989-996

Graziadel L. (1991) Introduction of unlabeled proteins into living cells by electroporation and isolation of viable protein-loaded cells using dextran-FITC as a marker for protein uptake. Analyt. Biochem. 194 (1): 198-203

Greene M.H., Clark W.H., Tucker M.A., Elder D.E., Kraemer K.H., Guerry D., Witmer W.K., Thompson J., Matozzo I and Fraser M.C. (1985) Acquired precursors of cutaneous malignant-melanoma - the familial dysplastic nevus syndrome. New Eng. J. Med. 312 (2): 91-97

Grignini G. and Jamieson G.A. (1988) Platelets in tumor-metastasis - generation of adenosine-diphosphate by tumor-cells is specific but unrelated to metastatic potential. Blood 71 (4): 844-849

Gulino D., Boudignon C., Zhang L., Concord E., Rabiet M.J. and Marguerie G. (1992) Calcium-binding properties of the platelet glycoprotein Iib ligand-interacting domain. J.Biol. Chem. 267: 1001-1007

Hannigan G.E., Leung-Hagesteijn C., Fitz-Gibon L., Coppolino M.G., Radeva G., Filmus J., Bell J.C. and Dedhar S. (1996) Regulation of cell adhesion and anchorage-dependent growth by a new β1-integrin-linked protein kinase. Nature 379: 91-96

Hart I.R., Goode N.T., Wilson R.E. (1989) Molecular aspects of the metastatic cascade. Biochem. Biophys. Acta 989: 65-84

Hélène C. and Toulme J.J. (1990) Specific regulation of gene expression by antisense, sense and antigene nucleic acids. Biochem. Biophys. Acta 1049: 99-125

Hemler M.E. (1990) VLA proteins in the integrin family: Structures, functions, and their role on leukocytes. Annu. Rev. Immunol. 8: 365-400

Herlyn M., Rodeck U., Mancianti M.L., Cardillo F.M., Lang A., Ross A.H., Jambrosic J. and Koprowski H. (1987) Expression of melanoma-associated antigens in rapidly dividing human melanocytes in culture. Cancer Res. 47 (12): 3057-3061

Hibbs M.L., Jakes S., Stacker S.A., Wallace R.W. and Springer T.A. (1991) The cytoplasmic domain of the integrin lymphocyte function-associated antigen-1 beta-subunit-sites required for binding to intercellular-adhesion molecule-1 and the phorbol ester stimulated phosphorylation site. J. Exp. Med. 174: 1227-1238

Holden H.T. (1973) Quantitative methods for measuring cell growth and death. Tissue Culture Methods and Applications. NY Academic Press: 408-412

Holly E.A., Kelly J.W., Shpall S.N. and Chiu S.H. (1987) Number of melanocytic nevi as a major risk factor for malignant-melanoma. J. Am. Acad. Derm. 17 (3): 459-468

Honn K.V., Chen Y.Q., Timar J., Onada J.M., Hatfield J.S., Fligiel S.E.G., Steinert B.W., Diglio C.A., Grossi I.M., Nelson K.K. and Taylor J.D. (1992) αIIbβ3 integrin expression and function in subpopulations of murine tumors. Exp. Cell Res. 201: 23-32

Honn K.V., Tang D.G. and Chen Y.Q. (1992) Platelets and cancer metastasis - more than an epiphenomenon. Semin. Thromb. Haemostasis 18 (4): 392-415

Hopp T.P. and Woods K.R. (1981) Prediction of antigenic determinants from amino acid sequences. Proc. Natl. Acad. Sci. USA. 78 (6): 3824-3828.

Huang T.F., Holt J.C., Lukasiewicz H. and Niewiarowski S. (1987) Trigramin - A low-molecular weight peptide inhibiting fibrinogen interaction with platelet receptors expressed on glycoprotein-IIB-IIIA complex. J. Biol. Chem. 262: 16157-16153

Hughes P.E., Diaz-Gonzalez F., Leong L., Wu C., McDonald J.A., Shattil S.J. and Ginsberg M.H. (1996) Breaking the integrin hinge. J. Biol. Chem. 271(12): 6571-6574

Humphries M.J., Olden K. and Yamada K.M. (1986) A synthetic peptide from fibronectin inhibits experimental metastasis of murine melanoma cells. Science 233: 467-470

Humphries M.J., Yamada K.M. and Olden K. (1988) Investigation of the biological effects of anti-cell adhesive synthetic peptides that inhibit experimental metastasis of B16-F10 murine melanoma cells. J. Clin. Invest. 81: 782-790

Hynes R.O. (1992) Integrins: Versatility, Modulation, and Signaling in Cell Adhesion. Cell 69: 11-25

Ish-Horowitz D. and Burke J.F. (1981) Rapid and efficient cosmid cloning. Nucleic Acids Res. 9 (13): 2989-2998

Iwamoto Y., Robey F.A., Graf J., Sasaki M., Kleinman H.K., Yamada Y. and Martin G.R. (1987) YIGSR, a synthetic laminin pentapeptide, inhibits experimental metastasis formation. Science 238 (4830): 1132-1134

Jimbow K., Salopek T.G., Dixon W.T., Searles G.E. and Yamada K. (1991) The epidermal melanin unit in the pathophysiology of malignant melanoma. Am. J. Dermatol. 13: 179-188

Juliano R.L. (1987) Membrane-receptors for extracellular-matrix macromolecules relationship to cell-adhesion and tumor-metastasis. Biochim. Biophys. Acta. 907 (3): 261-278

Juliano R.L. and Varner J.A. (1993) Adhesion molecules in cancer: the role of integrins. Curr. Opin. Cell Biol. 5: 812-818

Kashani-Sabet M., Funato T., Florenes V.A., Fodstad O. and Scanlon K.J. (1994) Suppression of the neoplastic phenotype *in vivo* by an anti-*ras* ribozyme. Cancer Research 54 (5): 900-902

Kassner P.D., Kawaguchi S. and Hemler M.E. (1994) Minimum alpha-chain cytoplasmic tail sequence needed to support integrin-mediated adhesion. J. Biol. Chem. 269 (31): 19859-19867

Keely P.J., Fong A.M., Zutter M.M. and Santoro S.A. (1995) Alteration of collagen-dependant adhesion, motility, and morphogenesis by the expression of antisense α2 integrin mRNA in mammary cells. J. Cell Science 108: 595-607

Koivisto L., Heino J., Häkkinen L and Larjava H. (1994) The size of the intracellular β1-integrin precursor pool regulates maturation of β1-integrin subunit and associated α-subunits. 300: 771-779

Kirchhôfer D., Languino L.R., Ruoslahti E. and Pierschbacher M.D. (1990) Alpha2 beta1 integrins from different cell types show different binding specificities. J. Biol. Chem. 265: 615-618

Kolodziej M.A., Vilaire G., Rifat S., Poncz M. and Bennett J.S. (1991) Effect of deletion of glycoprotein-IIB exon 28 on the expression of the platelet glycoprotein-IIB glycoprotein-IIIA complex. Blood 78 (9): 2344-2353

Kornberg L.J., Earp H.S., Turner C.E., Procktop C.J. and Juliano R.L. (1991) Signal transduction by integrins: increased protein tyrosine phosphorylation caused by integrin clustering. Proc. Natl. Acad. Sci. USA. 88: 8392-8396

Kramer R.H., Vu M.P., Cheng Y.F. and Ramos D.M. (1991) Integrin expression in malignant melanoma. Cancer Metast. Rev. 10: 49-59

Laflamme S.E., Thomas L.A., Yamada S.S. and Yamada K.M. (1994) Single subunit chimeric integrins as mimics and inhibitors of endogenous integrin functions in receptor localization, cell spreading and migration, and matrix assembly. J. Cell Biol. 126 (5): 1287-1298

Lallier T. and Bronner-Fraser M. (1993) Inhibition of neural crest cell attachment by integrin antisense oligonucleotides. Science 259: 692-695

Lam S.C.T. (1992) Isolation and characterization of a chymotryptic fragment of platelet glycoprotein-IIb-IIIa retaining arg-gly-asp binding-activity. J. Biol. Chem. 267: 5649-5655

Lanza F., Stierlé A., Fournier D., Morales M., André G., Nurden A.T. and Cazenave J.P. (1992) A new variant of Glanzmann's thrombasthenia (Strasbourg I): platelets with functionally defective glycoprotein IIb-IIIa complexes and a glycoprotein IIIa 214Arg-214Trp mutation. J. Clin. Invest. 89: 1995-2004

Leahy D.J., Hendrickson W.A., Aukhill I. and Erickson H.P. (1992) Structure of a fibronectin type III domain from tenascin phased by MAD analysis of the selenomethyl protein. Science 258: 87-991

Lee, J.-O., Rieu P., Arnaout M.A. and Liddington R. (1995a) Crystal structure of the A-domain from the α sub-unit of integrin CR3 (CD11b/CD18). Cell 80: 631-638

Lee, J.-O., Bankston L., Arnaout M.A. and Liddington R. (1995b) Two conformations of the integrin A-domain: a pathway for activation? Current Opinion in Cell Structure 3: 1333-1340

Leonetti J.P., Degols G., Clarenc J.P., Mechti N. and Lebleu B. (1993) Cell delivery and mechanism of action of anti-sense oligonucleotides. Prog. Nucleic Acid Res. Mol. Biol. 44: 143-166

Loftus J.C., O'Toole T.E., Plow E.F., Glass A., Frelinger A.L.III and Ginsberg M.H. (1990) A β3 integrin mutation abolishes ligand binding and alters divalent cation-dependant conformation. Science 249: 915-918

Loftus J.C., Halloran C.E., Ginsberg M.H., Feigen L.P., Zablocki J.A. and Smith J.W. (1996) The amino-terminal one-third of αIIb defines the ligand recognition specificity of the integrin αIIbβ3. J. Biol. Chem. 271(4): 2033-2039

Longenecker G.L., Beyers B.J., Bowen R.J. and King T. (1989) Human rhabdosarcoma cell-induced aggregation of blood-platelets. Cancer Res. 49 (1): 16-19

Lugtenberg B., Meijers J., Peters R., Van der Hoek P. and Van Alphen L. (1975) Electrophoretic resolution of the major outer membrane protein of *E. coli* K12 into four bands. FEBS Lett. 58: 254-258

Lukashev M.E., Sheppard D. and Pytela R. (1994) Disruption of integrin function and induction of tyrosine phosphorylation by the autonomously expressed β1 integrin cytoplasmic domain. J. Biol. Chem. 269: 18311-18314

MacGregor G.R., Nolan G.P., Fiering S., Roederer M. and Herzenberg L.A. (1991) Use of E. coli *lac*Z (β-galactosidase) as a reporter gene. Methods Mol. Biol. 7: 217-235

Maher L.J.III, Wold B. and Dervan P.B. (1989) Inhibition of DNA binding proteins by oligonucleotide-directed triple helix formation. Science 245: 725-730

Main A.L., Harvey T.S., Baron M., Boyd J. and Campbell I.D. (1992) The three-dimensional structure of the tenth type III module of fibronectin: an insight into RGD-mediated interactions. Cell 71: 671-678

Maitra R.K., Li G.Y., xiao W., dong B.H., torrence P.F. and Silverman R.H. (1995) Catalytic cleavage of an RNA target by 2-5A antisense and RNAse-L. J. Biol. Chem. 270: 15071-15075

Marks R. (1988) Role of childhood in the development of skin-cancer. Australian Paed. Jn. 24 (6): 337-338

Marlin S.D. and Springer T.A. (1987) Purified intercellular-adhesion molecule-1 (ICAM-1) is a ligand for lymphocyte function-associated antigen-1 (LFA-1). Cell 51: 813-819

Marx J. (1993) Cell-death studies yield cancer clues. Science 259: 760-761

Masumoto A. and Hemler M.E. (1993) Multiple activation states of VLA-4. J. Biol. Chem. 268: 228-234

Matsukura M.K., Shinozuka K., Zon H., Mitsuya H., Reitz M., Cohen J.S. and Broder S. (1987) Phosphorothioate analogs of oligodeoxynucleotides - inhibitors of replication and cytopathic effects of human immunodeficiency virus. Proc. Natl. Acad. Sci. USA. 84: 7706-7710

McGregor B., McGregor J.L., Weiss L.M., Wood G.S., Hu C.H., Boukerche H. and Warnke R.A. (1989) Presence of cytoadhesins (IIb-IIIa-like glycoproteins) on human metastatic melanomas but not on benign melanocytes. J. Am. Clin. Pathol. 92: 495-499

Merrill J.T., Slade S.G., Weissmann G., Winchester R. and Buyon J.P. (1990) Two pathways of CD11b/CD18-mediated neutrophil aggregation with different involvement of protein-kinase C-dependent phosphorylation. J. Immunol. 145: 2608-2615

Michishita M., Videm V. and Arnaout M.A. (1993) A novel divalent cation-binding site in the A domain of the β2 integrin CR3 (CD11b/CD18) is essential for ligand binding. Cell 72: 857-867

Miyamoto S., Akiyama S.K. and Yamada K.M. (1995a) Synergistic roles for receptor occupancy and aggregation in integrin transmembrane function. Science (Wash. DC) 267: 883-885

Miyamoto S., Teramoto H., Coso O.A., Gutkind J.S., Burbelo P.D., Akiyama S.K. and Yamada K.M. (1995b) Integrin function: molecular hierarchies of cytoskeletal and signaling molecules. J. Cell Biol. 131: 791-805

Montgomery A.M.P., Reisfeld R.A. and Cheresh D.A. (1994) Integrin αvβ3 rescues melanoma cells from apoptosis in three-dimensional dermal collagen. Proc. Natl. Acad. Sci. USA. 91: 8856-8860

Morla A., Zhang Z. and Ruoslahti E. (1994) Superfibronectin is a functionally distinct form of fibronectin. Nature 367: 193-196

Moser H.E. and Dervan P.B. (1987) Sequence-specific cleavage of double helical DNA by triple helix formation. Science 238: 645-650

Mosher D.F. (1993) Assembly of fibronectin into extracellular matrix. Curr. Opin. in Struc. Biol. 3: 214-222

Mosmann T. (1983) Rapid colorimetric assay for cellular growth and survival: application to proliferation and cytotoxicity assays. Jn. Immunological Methods 65: 55-63

Natali P.G., Nicotra M.R., Cavaliere R., Giannarelli D. and Bigotti A. (1991) Tumor progression in human malignant melanoma is associated with changes in α6β1 laminin receptor. Int. J. Cancer 49: 168-172

Natali P.G., Nicotra M.R., Bartolazzi A., Cavaliere R. and Bigotti A. (1993) Integrin expression in cutaneous malignant melanoma: association of the α3β1 heterodimer with tumour progression. Int. J. Cancer 54: 68-72

Nermut M.V., Green N.M., Eason P., Yamada S.S. and Yamada K.M. (1988) Electron-microscopy and structural model of human fibronectin receptor. EMBO J. 7(13): 4093-4099

Neumann E., Schaeferridder M., Wang Y. and Hofschneider P.H. (1982) Gene-transfer into mouse lyoma cells by electroporation in high electric-fields. EMBO J. 1(7): 841-845

Nicolson G.L. (1988) Cancer metastasis: tumour cell and host organ properties important in metastasis to specific secondary sites. Biochem. Biophys. Acta. 948: 175-224

Nip J., Shibata H., Loskutoff D.J., Cheresh D.A. and Brodt P. (1992) Human melanoma cells derived from lymphatic metastases use integrin αvβ3 to adhere to lymph node vitronectin. J. Clin. Invest. 90: 1406-1413

Nip J., Rabbani S.A., Shibata H.R. and Brodt P. (1995) Coordinated expression of the vitronectin receptor and the urokinase-type plasminogen activator receptor in metastatic melanoma cells. J. Clin. Invest. 95: 2096-2103

Obara M., Kang M.S. and Yamada K.M. (1988) Site-directed mutagenesis of the cell-binding domain of human fibronectin: separable, synergistic sites mediate adhesive function. Cell 53: 649-657

O'Toole T.E., Loftus J.C., Plow E.F., Glass A., Harper J.R. and Ginsberg M.H. (1989) Efficient surface expression of platelet GPIIb-IIIa requires both subunits. Blood 74: 14-18

O'Toole T.E., Katagiri Y., Faull R.J., Peter K., Tamura R., Quaranta V., Loftus J.C., Shattil S.J and Ginsburg M.H. (1994) Integrin cytoplasmic domains mediate inside-out signal transduction. J. Cell Biol. 124: 1047-1059

Peerschke E.I., Zucker M.B., Grant R.A., Egan J.J. and Johnson M.M. (1980) Blood 55: 841-847

Pelletier A.J., Kunicki T. and Quaranta V. (1996) Activation if the integrin αvβ3 involves a discrete cation-binding site that regulates conformation. J. Biol. Chem. 271 (3): 1364-1370

Phillips D.R., Charo I.F., Parise L.V. and Fitzgerald L.A. (1988) The platelet membrane glycoprotein-IIB-IIIA complex. Blood 71 (4): 831-843

Pierschbacher M.D. and Ruoslahti E. (1984) Cell attachment activity of fibronectin can be duplicated by small synthetic fragments of the molecule. Nature 309: 30-33

Plantefaber L.C. and Hynes R.O. (1989) Changes in integrin receptors on oncogenically transformed cells. Cell 56: 281-290

Plow E.F., Ginsberg M.H. and Marguerie G.A. (1986) in Biochemistry of Platelets. Phillips D.R. and Shuman M.A. eds. Academic Press, Orlando, FL: 225-256

Pollice A.A., McCoy J.P., Shackney S.E., Smith C.A., Agarwal J., Burholt D.R., Janocko L.E., Hornicek F.J., Singh S.G. and Hartsock R.J. (1992) Sequential paraformaldehyde and methanol fixation for simultaneous flow cytometric analysis of DNA, cell-surface proteins, and intracellular proteins. Cytometry 13: 432-444

Pytela R., Pierschbacher M.D. and Ruoslahti E. (1985) Identification and isolation of a 140kd cell surface glycoprotein with properties expected of a fibronectin receptor. Cell 40: 191-198

Qian F., Vaux D.L. and Weissman I.L. (1994) Expression of the integrin alpha-4 beta-1 on melanoma cells can inhibit the invasive stage of metastasis formation. Cell 77 (3): 335-347

Reynolds M.A., Arnold L.J., Almazan M.T., Beck T.A., Hogrefe R.I., Metzler M.D., Stoughton S.R., Tseng B.Y., Trapane T.L., Ts'O P.O.P. and Woolf T.D. (1994) Triple-strand-forming methylphosphonate oligodeoxynucleotides targeted to mRNA efficiently block protein synthesis. Proc. Natl. Acad. Sci. USA. 91: 12433-12437

Rigel D.S. (1992) Epidemiology and prognostic factors in malignant melanoma. Ann. Plast. Surg. 28: 7-8

Riikonen T., Koivisto L., Vihinen P. and Heino J. (1995a) Transforming growth factor-β regulates collagen gel contraction by increasing α2β1 integrin expression in osteogenic cells. J. Biol. Chem. 270: 376-382

Riikonen T., Westermarck J., Koivisto L., Broberg A., Kähäri V.M. and Heino J. (1995b) Integrin α2β1 is a positive regulator of collagenase (MMP-1) and collagen α1(I) gene expression. J. Biol. Chem. 270: 13548-13552

Rojiani M.V., Finlay B.B., Gray V. and Dedhar S. (1991) In vitro interaction of a polypeptide homologous to human-Ro/SS-A-antigen (calreticulin) with a highly conserved amino-acid-sequence in the cytoplasmic domain of integrin alpha-subunits. Biochemistry 30(41): 9859-9866

Roskelley C.D., Desprez P.Y. and Bissell M.J. (1994) Extracellular matrix-dependant tissue-specific gene expression in mammary epithelial cells requires both physical and biochemical signal transduction. Proc. Natl. Acad. Sci. USA. 91: 12378-12382

Ruoslahti E. and Reed J.C. (1994) Anchorage dependence, integrins, and apoptosis. Cell 77: 477-478

Ruggeri Z.M. (1993) von Willebrand factor and fibrinogen. Curr. Opin. in Cell Biol. 5: 989-906

Saelman E.U.M., Keely P.J. and Santoro S.A. (1995) Loss of MDCK cell α2β1 integrin expression results in reduced cyst formation, failure of hepatocyte growth factor/scatter factor-induced branching morphogenesis, and increased apoptosis. J. Cell Science 108: 3531-3540.

Saiki I., Murata J., Iida J., Nishi N., Sugimura K. and Azuma I. (1989) The inhibition of murine lung metastasis by synthetic polypeptides [poly(arg-gly-asp) and poly(tyr-ile-gly-ser-arg)] with a core sequence of cell adhesion molecules. Br. J. Cancer 59: 194-197

Saiki R.K., Gelfland D.H., Stoffel S., Scharf S.J., Higuchi R., Horn G.T., Mullis K.B. and Erlich H.A. (1988) Primer-directed enzymatic amplification of DNA with a thermostable DNA polymerase. Science 239: 487-491

Sambrook J., Fritsch E.F. and Manniatis T. (1989) Molecular cloning. A laboratory manual. Cold Spring Harbor. New York: Cold Spring Harbor Laboratory Press.

Sanders L.C., Felding-Habermann B., Mueller B.M. and Cheresh D.A. (1992) Role of αv integrins and vitronectin in human melanoma cell growth. Cold Spring Harbor Symposia on Quantitative Biology 57: 233-240

Sanger F., Nicklen S. and Coulson A.R. (1977) DNA sequencing with chain terminating inhibitors. Proc. Natl. Acad. Sci. USA. 74: 5463-5467

Sasaki D.T., Dumas S.E. and Engleman E.G. (1987) Discrimination of viable and non-viable cells using propidium iodide in two color immunofluorescence. Cytometry, 8: 413-420

Sastry S.K. and Horwitz A.F. (1993) Integrin cytoplasmic domains: mediators of cytoskeletal linkages and extra- and intracellular initiated transmembrane signaling. Curr. Opin. Cell. Biol. 5: 819-

Schadendorf D., Gawlik C., Haney U., Ostmeier H., Suter L. and Czarnetzki B.M. (1993) Tumor progression and metastatic behaviour *in-vivo* correlates with integrin expression on melanocytic tumors. J. Pathol. 170 (4): 429-434

Schaller M.D., Borgman C.A., Cobb B.C., Reynolds A.B. and Parsons J.T. (1992) $pp125^{FAK}$, a structurally distinctive protein-tyrosine kinase associated with focal adhesions. Proc. Natl. Acad. Sci. USA. 89: 5192-5196

Schlaepfer D.D., Hanks S.K., Hunter T. and van der Geer P. (1994) Integrin-mediated signal transduction linked to Ras pathway by GRB2 binding to focal adhesion kinase. Nature 372: 786-791

Schwartz M.A. and Lechene C. (1992) Adhesion is required for protein kinase C-dependent activation of the Na+/H+ antiporter by platelet derived growth factor. Proc. Natl. Acad. Sci. USA. 89:6138-6141

Schwartz M.A., Brown E.J. and Fazeli B. (1993) A 50kDa integrin-associated protein is required for integrin-related calcium entry in endothelial cells. J. Biol. Chem. 268: 19931-19934

Seftor R.E.B., Seftor E.A., Gehlsen K.R., Stetler Stevenson W.G., Brown P.D., Ruoslahti E. and Hendrix M.J. (1992) Role of the $\alpha v\beta 3$ integrin in human melanoma cell invasion. Proc. Natl. Acad. Sci. USA. 89: 1557-1561

Seftor R.E.B., Seftor E.A., Stetler-Stevenson W.G. and Hendrix M.J.C. (1993) The 72 kDa type IV collagenase is modulated via differential expression of $\alpha v\beta 3$ and $\alpha 5\beta 1$ integrins during human melanoma cell invasion. Cancer Res. 53: 3411-3415

Shattil S.J., Hoxie J.A., Cunningham M. and Brass L.F. (1985) Changes in the platelet membrane glycoprotein IIb-IIIa complex during platelet activation. J. Biol. Chem. 260: 11107-11114

Shattil S.J. and Brugge J.S. (1991) Protein tyrosine phosphorylation and the adhesive function of platelets. Curr. Opin. Cell Biol. 3: 869-879

Shaw H.M., McGovern V.J. and Milton G.W. (1980) Histological features of tumours and the female superiority in survival from malignant melanoma. Cancer 45: 1604-1608

Si Z.Y. and Hersey P. (1994) Immunohistological examination of the relationship beween metastatic potential and expression of adhesion molecules and selectins on melanoma-cells. Pathology 26 (1): 6-15

Sims P.J., Ginsberg M.H., Plow E.F. and Shattil S.J. (1991) Effect of platelet activation on the conformation of the plasma membrane glycoprotein IIb-IIIa complex. J. Biol. Chem. 266 (12): 7345-7352

Smith C.C., Aurelian L., Reddy M., Miller P.S. and Ts'O P.O.P. (1986) Antiviral effect of an oligo(nucleoside methylphosphonate) complementary to the splice junction of herpes-simplex virus type-1 immediate early pre-messenger RNA-4 and pre-messenger RNA-5. Proc. Natl. Acad. Sci. USA. 83: 2787-2791

Smith J.W. and Cheresh D.A. (1988) The arg-gly-asp binding domain of the vitronectin receptor - photoaffinity cross-linking implicates amino-acid residues-61-203 of the beta-subunit. J. Biol. Chem. 263: 18726-18731

Smith J.W. and Cheresh D.A. (1991) Labeling of integrin-αvβ3 with Co-58(III) - evidence of metal-ion coordination sphere involvement in ligand-binding. J. Biol. Chem. 266: 11429-11432

Smith J.W., Piotrowicz R.S. and Mathis D. (1994) A mechanism for divalent-cation regulation of beta-3-integrins. J. Biol. Chem. 269 (2): 960-967

Smith J.W., Tachias K. and Madison E.L. (1995) Protein loop grafting to construct a variant of tissue-type plasminogen activator that binds platelet integrin αIIbβ3. J. Biol. Chem. 270 (51): 30486-30490

Staatz W.D., Fok K.F., Zutter M.M., Adams S.P., Rodriguez B.A. and Santoro S.A. (1991) Identification of a tetrapeptide recognition sequence for the α2β1 integrin in collagen. J. Biol. Chem. 266 (12): 7363-7367

Stein C.A. and Cheng Y.C. (1993) Antisense oligonucleotides as therapeutic agents - is the bullet really magical. Science 261 (5124): 1004-1012

Streuli C.H. and Bissell M.J. (1990) Expression of extracellular-matrix components is regulated by substratum. J. Cell Biol. 110 (4): 1405-1415

Suzuki S. and Naitoh Y. (1990) Amino acid sequence of a novel integrin β4 subunit and primary expression of the mRNA in epithelial cells. EMBO J. 9: 757-763

Thorn M., Adami H.O., Ringborg U., Bergstrom R. and Krusemo U. (1987) Long-term survival in malignant melanoma with special reference to age and sex as prognostic factors. J. Natl. Cancer Inst. 79 (5): 969-974

Thorn M., Adami H.O., Ringborg U., Bergstrom R. and Krusemo U. (1989) The association between anatomical site and survival in melanoma - an analysis of 12,353 cases from the swedish cancer registry. Eur. J. Cancer Clin. Oncol. 25 (3): 483-491

Tohgo A., Tanaka N.G. and Ogawa H. (1985) Platelet aggregating activities of metastasizing tumor cells. 3. Platelet aggregation as resulting from thrombin generation by tumor-cells. Invasion Metastasis 5 (2): 96-105

Towbin H., Staehelin T. and Gordon J. (1979) Electrophoretic transfer of proteins from polyacrylamide gels to nitrocellulose sheets: procedure and some applications. Proc. Natl. Acad. Sci. USA. 76: 4350-4354

Trikha M., Declerck Y.A., Markland F.S. (1994) Contortrostatin, a snake-venom disintegrin, inhibits beta-1 integrin-mediated human metastatic melanoma cell-adhesion and blocks experimental metastasis. Cancer Research 54 (18): 4993-4998

Tremble P., Damsky C.H. and Werb Z. (1995) Components of the nuclear signaling cascade that regulate collagenase gene expression in response to integrin-derived signals. J. Cell. Biol. 129: 1707-1720

Van Duinen C.M., Van den Broek L.J.C.M., Vermeer B.J., Fleuren G.J. and Bruijn J.A. (1994) The distribution of cellular adhesion molecules in pigmented skin lesions. Cancer 73: 2131-2139

Vannhieu G.T., Krukonis E.S., Reszka A.A., Horwitz A.F. and Isberg R.R. (1996) Mutations in the cytoplasmic domain of the integrin beta(1) chain indicate a role for endocytosis factors in bacterial internalization. J.Biol. Chem. 271(13): 7665-7672

Vuori, K. and Ruoslahti E. (1994) Association of insulin-receptor substrate-1 with integrins. Science 266 (5190): 1576-1578

Wagner R.W. (1994) Gene inhibition using antisense oligodeoxynucleotides. Nature 372: 333-335

Walder R.Y. and Walder J.A. (1988) Role of RNase H in hybrid-arrested translation by antisense oligonucleotides. Proc. Natl. Acad. Sci. USA. 85: 5011-5015

Wayner E.A., Orlando R.A. and Cheresh D.A. (1991) Integrins αvβ3 and αvβ5 contribute to cell attachment to vitronectin but differentially distribute on the cell surface. J. Cell Biol. 113(4): 919-929

Weidner N., Folkman J., Pozza F., Bevilacqua P., Allred E.N., Moore D.H., Meli S. and Gasparini G. (1992) Tumour angiogenesis: a new significant and independant prognostic indicator in early-stage breast carcinoma. J. Natl. Cancer Inst. 84: 1875-1887

Weidner N., Carroll P.R., Flax J., Blumenfield W. and Folkman J. (1993) Tumor angiogenesis correlates with metastasis in invasive prostate carcinoma. Am. J. Pathol. 143: 401-409

Weisel J.W., Nagaswami C., Vilaire G. and Bennett J.S. (1992) Examination of the platelet membrane glycoprotein-IIb-IIIa complex and its interaction with fibrinogen and other ligands by electron-microscopy. J. Biol. Chem. 267(23): 16637-16643

Weiss L. and Greep R.O. (1977) Histology, 4th edition, McGraw-Hill Publication Inc., New York. 595-598

Wickham T.J., Mathias P., Cheresh D.A. and Nemerow G.R. (1993) Integrin-alpha-v-beta-3 and integrin-alpha-v-beta-5 promote adenovirus internalization but not virus attachment. Cell 73(2): 309-319

Wickham T.J., Filardo E.J., Cheresh D.A. and Nemerow G.R. (1994) Integrin alpha-v-beta-5 promotes adenovirus-mediated cell-membrane permeabilisation. J. Cell Biol. 127(1): 257-264

Wickham T.J., Carrion M.E. and Kovesdi I. (1995) Targeting of adenovirus penton base to new receptors through replacement of its RGD motif with other receptor-specific peptide motifs. Gene Therapy. 2(10): 750-756

Williams J.A. (1992) Disintegrins: RGD-containing proteins which inhibit cell/matrix interactions (adhesion) and cell/cell interactions (aggregation) via the integrin receptors. Pathol. Biol. 40: 813-821

Wippler J., Kouns W.C., Schlaeger E.J., Kuhn H., Hadvary P. and Steiner B. (1994) The integrin alpha(IIb)-beta(3), platelet glycoprotein IIb-IIIa, can form a functionally active heterodimer complex without the cysteine-rich repeats of the beta(3) subunit. J. Biol. Chem. 269(12): 8754-8761

Wong T.K. and Neumann E. (1982) Electric-field mediated gene-transfer. Biochem. Biophys. Res. Comm. 107(2): 584-587

Woods A. and Couchman J.R. (1992) Protein kinase C involvement in focal adhesion formation. J. Cell Sci. 101:277-290

Woolf T.M., Melton D.A. and Jennings C.G.B. (1992) Specificity of antisense oligonucleotides *in vivo*. Proc. Natl. Acad. Sci. USA 89: 7305-7309

Yaar M. and Gilcrest B.A. (1991) Human melanocyte growth and differentiation: a decade of new data. J. Invest. Dermatol. 97(4): 611-617

Yamada K.M. (1983) Cell surface interactions with extracellular materials. Ann. Rev. Biochem. 52: 761-799

Ylänne J., Chen Y.L., O'Toole T.E., Loftus J.C., Takada Y. and Ginsberg M.H. (1993) Distinct functions of integrin α and β subunit cytoplasmic domains in cell spreading and formation of focal adhesions. J. Cell Biol. 122: 223-234

Zamecnik P.C. and Stephenson M.L. (1978) Inhibition of Rous sarcoma virus replication and cell transformation by a specific oligodeoxynucleotide. Proc. Natl. Acad. Sci. USA. 75: 280-284

Zhang Z., Vuori K., Wang H-G., Reed J.C. and Ruoslahti E. (1996) Integrin activation by R-ras. Cell 85: 61-69

Appendix A: Amino acids.

Amino acid.	Abbreviation.	Code Letter.	Mass.	Properties (hydrophilicity).
Alanine	Ala	A	89.09	Neutral, (-0.5)
Arginine	Arg	R	174.2	Basic, (3.0)
Asparagine	Asn	N	132.1	Neutral, (0.2)
Aspartic acid	Asp	D	133.1	Acidic, (3.0)
Cysteine	Cys	C	121.12	Neutral, (-1.0)
Glutamic acid	Glu	E	147.13	Acidic, (3.0)
Glutamine	Gln	Q	146.15	Neutral, (0.2)
Glycine	Gly	G	75.07	Neutral, (0.0)
Histidine	His	H	155.16	Basic, (-0.5)
Isoleucine	Ile	I	131.17	Neutral, (-1.8)
Leucine	Leu	L	131.17	Neutral, (-1.8)
Lysine	Lys	K	146.19	Basic, (3.0)
Methionine	Met	M	149.21	Neutral, (-1.3)
Phenylalanine	Phe	F	165.19	Neutral, (-2.5)
Proline	Pro	P	115.13	Neutral, (0.0)
Serine	Ser	S	105.09	Neutral, (0.3)
Threonine	Thr	T	119.12	Neutral, (-0.4)
Tryptophan	Trp	W	204.22	Neutral, (-3.4)
Tyrosine	Tyr	Y	181.19	Neutral, (-2.3)
Valine	Val	V	117.15	Neutral, (-1.5)

Hydrophilicity value according to Hopp and Woods, (1981)

Appendix B: Molecular Weight Markers.

For agarose gel electrophoresis, markers consisted of *Eco*RI/*Hin*dIII-cut lambda DNA (Northumbria Biologicals). The digest consists of DNA fragments of the following sizes (Base pairs):

1:	21226	8:	1584
2:	5148	9:	1375
3:	4973	10:	947
4:	4268	11:	831
5:	3530	12:	564
6:	2027	13:	125
7:	1904		

For PCR and small fragments, low weight electrophoresis markers were used (Promega). These consisted of DNA fragments of the following sizes (base pairs):

1:	1000	4:	300
2:	750	5:	150
3:	500	6:	50

For SDS-PAGE and Western blotting, pre-stained markers (Bio-Rad, broad range) consisted of:

Protein	Molecular Weight
Myosin	208kDa
β-galactosidase	115 kDa
Bovine serum albumin	79.5 kDa
Ovalbumin	49.5 kDa
Carbonic anhydrase	34.8 kDa
Soybean trypsin inhibitor	20.4 kDa
Aprotinin	7.2 kDa

Appendix C: Media and Solutions.

Where appropriate, media and solutions were sterilised by autoclaving for 20 minutes at 15 lbs/sq inch (121°C) on a liquid cycle. Unless specified, all reagents were obtained from Sigma Biochemicals.

Chloroform:isoamyl alcohol: Chloroform mixed with isoamyl alcohol 24:1 (Amresco).

Denaturing solution: 1.5M NaCl, 0.5M NaOH.

Denhardt's solution (100x): 2% Bovine serum albumin (BSA), 2% Ficoll, 2% polyvinylpyrrolidone (PVP).

DNA loading buffer: 0.5% SDS, 25% glycerol, 0.25% bromophenol blue, 0.05M EDTA.

Formaldehyde gel running buffer (5x): 0.1M MOPS (pH 7.0), 40mM sodium acetate, 5mM EDTA.

LB medium (Luria-Bertani Medium): (per litre) 10g Bacto tryptone (Difco), 5g Bacto yeast extract (Difco) and 10g NaCl, pH adjusted to 7.0 with NaOH. LB plates were made from 1 litre of LB medium plus 20g agar (Difco).

Neutralising solution: 1.5M NaCl, Tris HCl pH 7.2, 0.001M EDTA.

NZY Broth: (per litre) 5g NaCl, 2g $MgSO_4$, 5g Bacto yeast extract (Difco) and 10g NZ amine (ICN) pH 7.5. NZY plates were made from 1 litre of NZY broth plus 20g agar (Difco).

PBS: 15mM sodium phosphate, 150mM sodium chloride (pH 7.3).

Phenol/chloroform: Tris Phenol : Chloroform : Isoamyl alcohol 25:24:1 (Amresco).

SM (Phage dilution buffer): (per litre) 5.8g NaCl, 2g $MgSO_4$, 50ml 1M Tris pH 7.5 and 5ml 2% gelatin.

SOC: 2% Bacto Tryptone (Difco), 0.5% Bacto yeast extract (Difco), 10mM NaCl, 2.5mM KCl, 10mM $Mgcl_2$, 10mM $MgSO_4$, 20mM glucose.

Solution I (minipreps): 50mM glucose, 25mM Tris, 10mM EDTA.

Solution II (minipreps): 0.2N NaOH, 1% SDS; freshly prepared asceptically from 10N NaOH and 10% SDS stocks.

Solution III (minipreps): (per 100ml) 60ml 5M potassium acetate, 11.5ml glacial acetic acid, ddH_2O 28.5ml.

SDS-PAGE running buffer (1x): 25mM Tris base, 192mM glycine, 0.1% SDS.

SDS-PAGE blocking buffer: 1%w/v ovalbumin, 0.05% sodium azide, in TBS.

SDS-PAGE loading buffer (5x): 5% SDS, 50% glycerol, 200mM Tris Hcl (pH 6.8), 5% 2-mercaptoethanol, 2% bromophenol blue.

SDS-PAGE solubilisation buffer: 50mM Tris-HCl (pH 7.5), 150mM NaCl, 1% Nonidet P40, 10% glycerol, 5mM EDTA, 1mM sodium vanadate, 1mM sodium molybdate, 10mM sodium fluoride, 40µg/ml PMSF, 0.7µg/ml pepstatin A, 10µg/ml aprotinin, 10µg/ml leupeptin, 10µg/ml soyabean trypsin inhibitor.

SSC (1x): 0.15M NaCl, 0.015M trisodium citrate pH 7.0

TBE (1x): (per litre) 10.8g Tris base, 5.5g boric acid, 0.93g $Na_2EDTA.H_2O$, pH 8.3

TBS: 150mM NaCl, 20mM Tris HCl, pH 7.5.

TBSN: 150mM NaCl, 20mM Tris HCl, pH 7.5, 0.05% NP-40

TE: 10mM Tris-HCl, 1mM EDTA pH 7.0

TE Glucose: 25% $^{w}/_{v}$ glucose, 100mM Tris, 10mM EDTA pH 7.0

TGS (Semi-dry transfer buffer): 39mM glycine, 48 mM Tris base, 0.0375% SDS, 20%(v/v) methanol.

Tumour dispersion solution: (per 100ml) 100mg collagenase type III (Worthington Biochemicals), 7mg DNAse I (Sigma), 10mg soybean trypsin inhibitor (Worthington Biochemicals), 1g fatty acid free bovine albumin (Sigma).

X-Gal solution: 0.2% X-Gal (Melford laboratories), 1mM $MgCl_2$, 150mM NaCl, 3.3mM $K_4Fe(CN)_6$, 3.3mM $K_3Fe(CN)_6$.